

**DESIGN OF A NOVEL H5N1 ELECTROCHEMICAL  
BIOSENSOR**

**A THESIS SUBMITTED TO THE GRADUATE  
SCHOOL OF APPLIED SCIENCES  
OF  
NEAR EAST UNIVERSITY**

**By  
ALEMU ABIBI MEKONEN**

**In Partial Fulfillment of the Requirements for  
the Degree of Master of Science  
in  
Biomedical Engineering**

**NICOSIA, 2019**

**ALEMU ABIBI  
MEKONEN**

**DESIGN OF A NOVEL H5N1 ELECTROCHEMICAL  
BIOSENSOR**

**NEU  
2019**



**DESIGN OF A NOVEL H5N1 ELECTROCHEMICAL  
BIOSENSOR**

**A THESIS SUBMITTED TO THE GRADUATE  
SCHOOL OF APPLIED SCIENCES  
OF  
NEAR EAST UNIVERSITY**

**By  
ALEMU ABIBI MEKONEN**

**In Partial Fulfillment of the Requirements for  
the Degree of Master of Science  
in  
Biomedical Engineering**

**NICOSIA, 2019**

**Alemu Abibi MEKONEN: DESIGN OF A NOVEL H5N1 ELECTROCHEMICAL  
BIOSENSOR**

**Approval of Director of Graduate School of  
Applied Sciences**

**Prof. Dr. Nadire ÇAVUŞ**

**We certify this thesis is satisfactory for the award of the degree of Masters of Science  
in  
Biomedical Engineering**

**Examining Committee in Charge:**

|                                   |   |
|-----------------------------------|---|
| Prof. Dr. Tulin Bodamyali         | Chairperson, Department of Health Sciences'<br>Faculty of Health Sciences, GAU      |
| Assoc. Prof. Dr. Terin Adali      | Supervisor, Department of Biomedical of<br>Engineering, Faculty of Engineering, NEU |
| Assist. Prof. Dr Ayse A. Sariođlu | Co-supervisor, Department of Medical<br>Microbiology, Faculty of Medicine, NEU      |
| Assist. Prof. Dr. Ayse Cagatan    | Committee Member, Department of Health<br>Sciences, Faculty of Health Sciences, GAU |
| Assoc. Prof. Dr. Meryem Guvenir   | Committee Member, Department of Medical<br>Microbiology, Faculty of Medicine, NEU   |
| Assoc. Prof. Dr. Rasime Kalkan    | Committee Member, Department of Medical<br>Genetics, Faculty of Medicine, NEU       |

I hereby declare that all the information in this document has been obtained and presented in accordance with the academic rules and ethical conduct. I also declare that, as required by these rules and conduct, I have fully cited and referenced all materials and results that are not original to this work.

Name, Last name:

Signature:

Date:

## ACKNOWLEDGEMENTS

I would like to express profound acknowledge to my supervisor Assoc. Prof. Dr. Terin Adali for her expertly advice, immense help and invaluable support to supply all necessary chemicals and materials for the experiment to make this work possible. I sincerely thank my co-supervisor Assist. Prof. Dr Ayşe A. Sarioğlu for her consult, support and constructive suggestions for the accomplishment of my thesis.

I would like to thank to the Ethiopia Ministry of Science and Technology “Betre Science” scholarship program sponsored my study through a two-year grant. I take this opportunity to express my gratitude to Near East University Department of Biomedical Engineering academic staffs. During my entire stay in the Northern Cyprus I shall remember the hospitality, culture sharing and make to feel the dormitory service as home.

I thank to Biologist Nadire Kiyak who supported me in all laboratory studies and I also would like to thank to all of my friends consulting and words of encouragements their immense help to successfully finish my thesis.

Last but not least, I would like to thank to God, I will keep on trusting you throughout my life. I would also like to thank my family for their endless love, supports and praying for my success.

**To my parents...**

## ABSTRACT

Influenza viruses are the most important cause of infectious diseases of the upper respiratory tract that cause epidemics, especially in winter, resulting in high mortality and morbidity rate. Influenza viruses are members Orthomyxoviridae families. The viruses have three different types of influenza viruses (influenza C, influenza B and influenza A) according to the antigenic difference of matrix (M) proteins and nucleoprotein (NP). Type A viruses the most common pandemic in humans and poultry and frequently divided based on the surface of glycoproteins structure of neuraminidase (NA and hemagglutinin (HA) as well as viral genome. The antigens and proteins of AIV H5N1 can be detected by commercially available diagnostic devices. Biosensors are able to quantify the physiological and biochemical changes and integrate them into the electrical response with biological components. The aim of this thesis is to design a direct-load transfer-based diagnostic biosensor that can be able to detect HA glycoprotein on the surface of AIV H5N1. The design provides point- of care, rapid, quantitative results with high specify and reliability to be used in diagnosis of H5N1. For this purpose, silk fibroin (SF) film and SF/x-linked film immobilized with AIV H5N1 antibody on the SPE. The layer – by –layer design of SPE indicated that SF film and SF / x-linking film are proposed as good candidates for the detection of H5N1 with the proposed design. CV and CA measurements were obtained by using by PalmSens4 Potentiostat (PalmSensBV, Netherlands) for the detection of H5N1 antigen.

**Keywords:** AIV H5N1; film casting; electrochemical biosensor; silk fibroin; electrode

## ÖZET

İnfluenza virüsleri, özellikle kışın yüksek morbidite ve mortalite ile sonuçlanan epidemilere neden olan üst solunum yollarının bulaşıcı hastalıklarının en önemli etkenlerindedirler. *Orthomyxoviridae* familyasına ait grip virüsleri, nükleoprotein (NP) ve matris (M) proteinlerindeki antijenik farklılıklara göre üç farklı tipe ayrılmaktadır (İnfluenza A, B ve C. İnsanlarda ve kanatlı hayvanlarda en yaygın salgınlara neden olan İnfluenza A virüsleri (kuş gribi virüsleri / AIV), hemagglutinin (HA) ve neuraminidaz (NA) glikoproteinlerinin antijenik yapılarına göre alt tiplere ayrılmaktadır. AIV alt tipi H5N1 insanlar ve hayvanlar için yüksek oranda patojenik, yayılabilir enfeksiyonlara neden olan küresel bir tehdittir. Virüs salgınlara ve pandemiye yol açarak büyük sağlık, sosyal ve ekonomik kayıplara neden olabilir. AIV'nin antijenleri ve proteinleri ticari olarak temin edilebilen tanı kitleri ile tespit edilebilir. Ancak, bu kitlerle tanı nitel olarak konulabilir. Bu nedenle, nicel sonuçlar veren hızlı, güvenilir, bakım noktası tanılama kiti teknolojilerinin geliştirilmesine ihtiyaç duyulmaktadır. Bu tezin amacı AIV H5N1'in tanısında kullanılacak kantitatif ve hızlı sonuçlar veren, özgüllüğü ve güvenilirliği yüksek, sahada analiz yapmaya imkan sağlayacak AIV H5N1 tanı kiti tasarlamaktır. Bu tezin amacı, AIV H5N1'in yüzeyindeki HA glikoproteini tespit edebilen doğrudan yük aktarımına dayalı bir tanı biyosensörü tasarlamaktır. Bu amaçla, AIV H5N1 yüzeyinde bulunan hemagglutinin (HA) glikoproteinini algılayan elektrotlar üzerine ipek fibroin protein ile AIV H5N1 antikoru immobilize edildi. Elektrokimyasal karakterizasyon PalmSens4 Potentiostat (PalmSensBV, Hollanda) cihazı ile siklik voltammetri ve kronoamperometri ölçümleri yapılarak elde edildi.

**Anahtar Kelimeler:** AIV H5N1; elektrokimyasal biyosensör; film kaplama; ipek fibroin; elektrotlar

## TABLE OF CONTENTS

|                                    |      |
|------------------------------------|------|
| <b>ACKNOWLEDGEMENTS</b> .....      | ii   |
| <b>ABSTRACT</b> .....              | iv   |
| <b>ÖZET</b> .....                  | v    |
| <b>TABLE OF CONTENTS</b> .....     | vi   |
| <b>LIST OF TABLES</b> .....        | x    |
| <b>LIST OF FIGURES</b> .....       | xi   |
| <b>LIST OF ABBREVIATIONS</b> ..... | xiii |

### **CHAPTER 1: INTRODUCTION**

|  |   |
|--|---|
| 1.1 Statement of Problem .....         | 3 |
| 1.2 Aim of the Study .....             | 4 |
| 1.3 The Importance of the Thesis ..... | 4 |
| 1.4 General Objective.....             | 5 |
| 1.5 Specific Objective .....           | 5 |
| 1.6 Thesis Outline.....                | 5 |

### **CHAPTER 2: LITERATURE REVIEW**

|  |    |
|--|----|
| 2.1 Influenza Virus .....                                  | 6  |
| 2.2 Avian Influenza A Virus .....                          | 7  |
| 2.2.1 Life cycle.....                                      | 8  |
| 2.2.2 Transmission.....                                    | 9  |
| 2.2.3 Diagnosis and prevention of AIV .....                | 9  |
| 2.2.4 Treatment .....                                      | 10 |
| 2.2.5 Effect of AIV in the world.....                      | 10 |
| 2.3 Overview of Biosensors .....                           | 11 |
| 2.4 Electrochemical Based AIV H5N1 Biosensors.....         | 12 |
| 2.4.1 DNA biosensor (Nucleic acid-modified electrode)..... | 12 |
| 2.4.2 Immune biosensor (Antibody modified electrode).....  | 13 |
| 2.5 Optical Biosensor for Detection of H5N1 .....          | 15 |

|   |    |
|---|----|
| 2.5.1 Surface plasmon resonance biosensor (SPR).....                        | 16 |
| 2.5.2 Fluorescence based biosensor .....                                    | 16 |
| 2.6 Electrochemical Measurements.....                                       | 18 |
| 2.6.1 Cyclic voltammetry (CV) .....   | 18 |
| 2.6.2 Chronoamperometry (CA).....   | 20 |
| 2.7 Biomaterials for Biosensor Design .....                                 | 21 |
| 2.7.1 Polymers for improving sensitivity of electrode.....                  | 21 |
| 2.8 Biorecognition Elements .....   | 22 |
| 2.8.1 Enzyme-based bio recognition elements .....                           | 22 |
| 2.8.2 Antibody-based biorecognition elements .....                          | 23 |
| 2.8.3 Aptamer based biorecognition elements.....                            | 25 |
| 2.8.4 DNA based bio recognition element .....                               | 25 |
| 2.9 Techniques of Bio Receptor Immobilization.....                          | 28 |
| 2.9.1 Entrapment.....   | 28 |
| 2.9.2 Adsorption .....  | 29 |
| 2.9.3 Covalent .....  | 29 |
| 2.9.4 Crosslinking.....   | 29 |
| 2.10 Silk Cocoons.....  | 30 |
| 2.10.1 Silk Properties .....  | 30 |
| 2.11 Reduction and Oxidation Species .....                                  | 31 |
| 2.11.1 Potassium ferricyanide (K <sub>3</sub> [Fe (CN) <sub>6</sub> ])..... | 31 |

**CHAPTER 3: MATERIALS AND METHODS**

|  |    |
|--|----|
| 3.1 Materials.....                         | 33 |
| 3.1.1 Palmsens4 Blv, potentiostat.....     | 33 |
| 3.1.2 Screen printed electrode (SPE) ..... | 34 |
| 3.2 Methods .....                          | 35 |
| 3.2.1 Purification of silk fibroin .....   | 35 |
| 3.2.1.1 Cleaning process.....              | 35 |
| 3.2.1.2 Degumming process.....             | 36 |

|  |    |
|--|----|
| 3.2.1.3 Dissolution process .....  | 37 |
| 3.2.1.4 Dialysis process .....   | 38 |
| 3.2.1 Preparation of phosphate buffer saline solution (PBS).....           | 39 |
| 3.2.2 Preparation of silk fibroin micro particles .....                    | 39 |
| 3.2.3 Connection of the screen-printed electrode .....                     | 41 |
| 3.2.4 Construction of H5N1 biosensor on the screen-printed electrode ..... | 42 |
| 3.2.5 Preparation antibody of H5N1 .....                                   | 44 |
| 3.2.6 Preparation of H5N1 inactivated antigen.....                         | 45 |
| 3.2.7 Method 1: Characterization of CV and CA .....                        | 45 |
| 3.2.8 Method 2: Detection of H5N1 using CV and CA .....                    | 46 |
| 3.2.9 Setup Devices .....  | 47 |
| 3.2.10 Electrochemical measurements.....                                   | 47 |

## **CHAPTER 4: RESULTS AND DISCUSSION**

|   |    |
|---|----|
| 4.1 Cyclic Voltammetry and Chronoamperometry Analysis.....  | 48 |
| 4.1.1 Characterization using platinum as a working electrode .....  | 48 |
| 4.1.2 Characterization using screen printed electrode .....   | 51 |
| 4.1.3 CV analysis of the monoclonal antibody immobilized SF film coated SPE in<br>PBS solution with and without H5N1 antigen..... | 56 |
| 4.1.4 Antibody immobilized SF/x-linked film on SPE.....   | 57 |
| 4.1.5 Unused SPE with 25µl antibody with the PBS solution.....  | 58 |
| 4.1.6 SF film coated SPE and 25µl antibody within the PBS solution.....   | 60 |
| 4.2 Potassium Ferricyanide.....   | 61 |
| 4.3 Antibody- Antigen Concentration.....  | 62 |
| 4.4 Antibody –Antigen Interaction.....  | 63 |
| 4.5 Detection of H5N1 by Screen Printed Electrode .....   | 64 |
| 4.5.1 SPE with immobilized SF film antigen and antibody as a solution .....   | 66 |
| 4.5.2 Measurements of unused SPE in antigen, antibody and PBS solution .....  | 67 |
| 4.5.3 Antibody immobilized SF film coated SPE in antigen and PBS solution.....  | 68 |
| 4.5.4 SPE with immobilized SF/x-linked film antibody and antigen .....  | 69 |

|   |           |
|---|-----------|
| 4.6 Findings .....                        | 71        |
| 4.7 Comparison to the Other Studies ..... | 73        |
| <br><b>CHAPTER 5: CONCLUSION</b>          |           |
| 5.1 Conclusion.....                       | 75        |
| <b>REFERENCE .....</b>                    | <b>76</b> |

## LIST OF TABLES

|  |    |
|--|----|
| <b>Table 2.1:</b> Comparison of different types of influenza A Virus H5N1 biosensors .....               | 26 |
| <b>Table 3.1:</b> Contents of PBS .....  | 39 |
| <b>Table 4.1:</b> Peaks data of CV silk fibroin analysis.....  | 50 |
| <b>Table 4.2:</b> Peaks date of cyclic voltammetry using SPE .....                                       | 55 |
| <b>Table 4.3:</b> Data of Figure 4.5.....  | 58 |
| <b>Table 4.4:</b> CV analysis date SPE with 25 $\mu$ l of antibody within the PBS as a<br>solution ..... | 59 |
| <b>Table 4.5:</b> CV SF film coated SPE and 25 $\mu$ l antibody within a PBS solution.....               | 60 |
| <b>Table 4.6:</b> Peaks data of Figure 4.8 .....   | 62 |
| <b>Table 4.7:</b> Peaks date of CV with SPE SF film antigen and antibody as a solution ....              | 66 |
| <b>Table 4.8:</b> Peaks data of unused SPE in antigen, antibody and PBS as a solution.....               | 67 |
| <b>Table 4.9:</b> Peaks date of CV using silk SF film with SPE.....                                      | 68 |
| <b>Table 4.10:</b> Peaks data CV recorded using SF/x-linked film with SPE .....                          | 69 |
| <b>Table 4.11 :</b> Results of characterization and detection H5N1 antigen using<br>SF/x-linked .....    | 73 |

## LIST OF FIGURES

|   |    |
|---|----|
| <b>Figure 2.1:</b> Structure of avian influenza A virus .....   | 7  |
| <b>Figure 2.2:</b> Life cycle of influenza virus .....  | 8  |
| <b>Figure 2.3:</b> Schematic representation of a biosensor.....   | 11 |
| <b>Figure 2.4 :</b> Immunosensor detection of AIV H5N1 immobilized the viral<br>antibody H5N1 .....   | 14 |
| <b>Figure 2.5:</b> Schematic diagram of biosensor fabrication for the detection of H5N1<br>and H1N1 using antigen dual screen printed electrode .....       | 15 |
| <b>Figure 2.6:</b> Schematic diagram of fluorescence-based biosensor design using<br>MoS <sub>2</sub> -QD and MNPs using electrochemical spectroscopy ..... | 17 |
| <b>Figure 2.7:</b> Schematic diagram of cyclic voltammetry .....  | 18 |
| <b>Figure 2.8:</b> Immunosensor detection of AIV anti-hemagglutinin H5 using CV .....   | 19 |
| <b>Figure 2.9:</b> Schematic diagram of chronoamperometry graph.....  | 20 |
| <b>Figure 2.10:</b> Schematic diagram of glucose biosensor.....   | 23 |
| <b>Figure 2.11:</b> Schematic diagram of antibody-antigen interaction . .....   | 24 |
| <b>Figure 2.12:</b> Schematic immobilization techniques .....   | 29 |
| <b>Figure 2.13:</b> Structure of SF.....  | 31 |
| <b>Figure 3.1:</b> Chemicals and materials .....  | 33 |
| <b>Figure 3.2:</b> Electrochemical instrument PalmSens4 Blv.....  | 34 |
| <b>Figure 3.3:</b> Screen printed electrode.....  | 35 |
| <b>Figure 3.4:</b> Silk cocoons and cutting into pieces.....  | 36 |
| <b>Figure 3.5:</b> Degumming of silk cocoons with 0.1M Na <sub>2</sub> CO <sub>3</sub> solution.....  | 36 |
| <b>Figure 3.6:</b> Purification method of pure SF protein .....   | 38 |
| <b>Figure 3.7:</b> Extraction method of SF micro particles .....  | 40 |
| <b>Figure 3.8:</b> SF micro particles mixing with PBS solution and filter .....   | 41 |
| <b>Figure 3.9:</b> Mounting screen-printed electrode on the cell kit .....  | 42 |
| <b>Figure 3.10:</b> SPE electrodes for the construction of H5N1 biosensor.....  | 43 |
| <b>Figure 3.11:</b> Immobilization of H5N1 on to the SPE.....   | 44 |
| <b>Figure 3.12:</b> Characterization using CV and CA.....   | 45 |
| <b>Figure 3.13:</b> Detection of H5N1 using CV and CA .....   | 46 |

|  |    |
|--|----|
| <b>Figure 3.14:</b> Plam Sens4 and configuration of software PSTrace 5.5 .....                       | 47 |
| <b>Figure 4.1:</b> Characterization of PBS buffer and Sf (3% w/v) solutions with platinum .....      | 50 |
| <b>Figure 4.2:</b> Chronoamperometry analysis of PBS buffer and SF solutions .....                   | 51 |
| <b>Figure 4.3:</b> Cyclic voltammetry characterization .....   | 54 |
| <b>Figure 4.4:</b> Chronoamperometry characterization by using SPE .....                             | 56 |
| <b>Figure 4.5:</b> CV analysis of SPE coated monoclonal antibody immobilized SF film ..              | 57 |
| <b>Figure 4.6:</b> CV voltammograph for unused SPE with 25 $\mu$ l of antibody with.....             | 58 |
| <b>Figure 4.7:</b> CV voltammograph of SF film coated SPE and 25 $\mu$ l antibody within a PBS ..... | 60 |
| <b>Figure 4.8:</b> CV analysis of potassium ferric cyanide .....                                     | 61 |
| <b>Figure 4.9:</b> Antibody –antigen concentration.....  | 63 |
| <b>Figure 4.10:</b> Show the interaction of antigen and antibody before and after the antigen .....  | 64 |
| <b>Figure 4.11:</b> CV voltammograph SPE with SF film antigen and antibody as a solution .....       | 66 |
| <b>Figure 4.12:</b> CV Voltammograph for unused SPE in antigen, antibody and PBS solution .....      | 67 |
| <b>Figure 4.13:</b> CV recorded detection of H5N1 antigen using SF film.....                         | 68 |
| <b>Figure 4.14:</b> CV recorded detection of H5N1 using SF/x-linked film.....                        | 69 |
| <b>Figure 4.15:</b> Chronoamperometry detection of H5N1 using of SF film with SPE .....              | 70 |
| <b>Figure 4.16 :</b> Chronoamprometry detection of H5N1 using SF/x-linked film coated SPE.....       | 70 |

## LIST OF ABBREVIATIONS

|                    |   |
|--------------------|---|
| <b>μA:</b>         | Micro Ampere  |
| <b>A:</b>          | Adenine   |
| <b>AE:</b>         | Auxiliary Electrode   |
| <b>AIV:</b>        | Avian Influenza Virus   |
| <b>Ala:</b>        | Alanine   |
| <b>Au:</b>         | Gold  |
| <b>C:</b>          | Cytosine  |
| <b>CA:</b>         | Chronoamperometry   |
| <b>CdS:</b>        | Cadmium Sulfide   |
| <b>CdTe:</b>       | Cadmium Telluride   |
| <b>CE:</b>         | Counter Electrode   |
| <b>CSPE:</b>       | Carbon-Based Screen-Printed Electrode                           |
| <b>CV:</b>         | Cyclic Voltammetry  |
| <b>DC:</b>         | Direct Current  |
| <b>DNA:</b>        | Deoxyribonucleic Acid   |
| <b>DPV:</b>        | Differential Pulse Voltammetry                                  |
| <b>E:</b>          | Potential   |
| <b>EIS:</b>        | Electrochemical Impedance Spectroscopy                          |
| <b>ELIA:</b>       | Enzyme-Linked Immunosorbent Assay                               |
| <b>EPa:</b>        | Anode Peak Potential  |
| <b>EPc:</b>        | Cathode Peak Potential  |
| <b>G:</b>          | Guanine   |
| <b>G:</b>          | Gram  |
| <b>GCE:</b>        | Glassy Carbon Electrode   |
| <b>Gly:</b>        | Glycine   |
| <b>GO-PAb-BSA:</b> | Graphene Oxide-H5-Polychonal Antibodies-Bovine<br>Serum Albumin |
| <b>H5N1:</b>       | Hemagglutinin 5 Neuraminidase 1                                 |
| <b>HA:</b>         | Hemagglutinin   |

|                         |   |
|-------------------------|---|
| <b>Ipa:</b>             | Anode Peak Current                              |
| <b>IPc:</b>             | Cathode Peak Current                            |
| <b>kPa:</b>             | Kilo Pascal                                     |
| <b>L:</b>               | Litter  |
| <b>LSV:</b>             | Linear Sweep Voltammetry                        |
| <b>M:</b>               | Mole  |
| <b>Mab:</b>             | Monoclonal Antibody                             |
| <b>MB-GO:</b>           | Methylene Blue -Graphene Oxide                  |
| <b>ml:</b>              | Milliliter                                      |
| <b>MmHg:</b>            | Millimeter of Mercury                           |
| <b>MNP:</b>             | Metal Nanoparticles                             |
| <b>MoS<sub>2</sub>:</b> | Molybdenum Disulfide                            |
| <b>MWCNT:</b>           | Multi-Walled Carbon Nanotubes-                  |
| <b>CoPC/PAMAM:</b>      | Cobalt Phthalocyanine–Poly Amidoamine           |
| <b>NA:</b>              | Neuraminidase                                   |
| <b>NP:</b>              | Nucleoprotein                                   |
| <b>PA:</b>              | Polymerase Acidic Protein                       |
| <b>PAb:</b>             | Polyclonal Antibodies                           |
| <b>PB1:</b>             | Polymerase Base Protein1                        |
| <b>PB2:</b>             | Polymerase Base Protein 2                       |
| <b>PCR:</b>             | Polymerase Chain Reaction                       |
| <b>PSR:</b>             | Surface Plasmon Resonance                       |
| <b>QCM:</b>             | Quartz Crystal Microbalance                     |
| <b>QD:</b>              | Quantum Dot                                     |
| <b>RE:</b>              | Reference Electrode                             |
| <b>RNA:</b>             | Ribonucleic Acid                                |
| <b>Rpm:</b>             | Revolution Per Minute                           |
| <b>RT–PCR:</b>          | Reverse Transcriptase Polymerase Chain Reachion |
| <b>S:</b>               | Second  |
| <b>Ser:</b>             | Serine  |
| <b>SF:</b>              | Silk Fibroin                                    |

|                |  |
|----------------|--|
| <b>SFN:</b>    | Silk Fibroin Nanoparticle                  |
| <b>SPE:</b>    | Screen Printed Electrode                   |
| <b>ssDNA:</b>  | Single Stranded Deoxyribonucleic Acid      |
| <b>T:</b>      | Thymine                                    |
| <b>US FDA:</b> | US of America Food and Drug Administration |
| <b>V:</b>      | Voltage                                    |
| <b>vRNA:</b>   | Viral Ribonucleoproteins                   |
| <b>vRNP:</b>   | Viral Ribonucleoproteins                   |
| <b>WE:</b>     | Working Electrode                          |
| <b>WHO:</b>    | World Health Organization                  |



## **CHAPTER 1**

### **INTRODUCTION**

Influenza (flu) is an upper respiratory infection which is caused by influenza viruses (Dziąbowska et al., 2018). Influenza viruses that infect human can be classified into three main groups (Influenza A, B and C) according to the antigenic differences in nucleoprotein (NP) and matrix (M) proteins (Yang et al., 2018). Influenza A viruses which cause the most commonly pandemic in humans and poultry are divided into subtypes based on the antigenic structure of hemagglutinin (H) and neuraminidase (N) glycoproteins (Ho et al., 2009).

Currently Influenza A subtypes H1N1 and H3N2 are more commonly circulating in human population however, especially influenza A subtype H5N1 is a dangerous pathogen that threatens the poultry where there are chickens and turkeys (Moreno et al., 2013). The influenza A virus H5N1 is also known as avian influenza or bird flu. Highly pathogenic avian influenza viruses (HPAIV) (H5 / H7) among the most well-known species H5N1 virus can be transmitted from chicken, turkey and birds to the people and can cause serious diseases and economic crises (Neumann et al., 2009).

World Health Organization (WHO) reported that the mortality rate of infection caused by H5N1 virus is 60% this caused a devastating epidemic and a huge global health, social and economic problem (WHO, 2011). The virus has an envelope protein membrane which consists of viral genome for replication in the host cell and hemagglutinin (HA) glycoprotein for the attachment of sialic acid and endocytosis (administered) the genome of viral interested in the host cells and neuraminidase glycoprotein for the cleavage of sialic acid and release of more virus into the neighbor cell to invade it (Nelson & Guyer, 2012).

A new outbreak of poultry H5N1 was reported in Turkey 2005 in the Igdir, eastern province. Additional outbreaks in human also reported in Turkey 2006 with two case and the virus rapidly control at the same time wild birds also infected (WHO, 2016). An epidemic and outbreak H5N1 were highly pathogenic influenza virus that, had previously observed throughout Asia, with major health and economic repercussions and extended to Eastern

Turkey in the late December 2005 and early January 2006 (Sahin et al., 2006). Cyprus is a country of island and geographic location lack of poultry trade and Cyprus is considered a low risk and negligible of AIV H5N1 virus (Lockhart et al., 2016).

The avian influenza A virus (AIV) can be diagnosed by using conventional laboratory methods and other techniques such as biosensor (Yang et al., 2018). Conventional methods include viral culture-based assay, polymerase chain reaction (PCR)-based assay, serological assay. Early detection of the virus is important for the prevention of pandemics and important outbreaks that can be caused by avian influenza virus. Each of the laboratory methods used in the diagnosis of influenza viruses has unique advantages and disadvantages. Although virus isolation is widely used by cell culture technique, it is disadvantageous that the laboratory and experienced staff need to be used for a long time to obtain the result.

Additionally, the relatively low sensitivity of existing rapid tests that detect antigen limits their use. For these reasons, there is a need for new technologies which provide sensitive, high soluble, low false positive / negative rate, fast, mobile and quantitative results. The biosensors have the advantage of performing a quick and easy analysis, low cost, selectivity, and low limit of determination compared to conventional methods (Wong et al., 2017).

Nowadays, using micro and nanoparticles-based biosensors is the recent approach for early detection of AIV and prevention of infections. Biosensors are devices which combines biological receptors such as antibodies, oligonucleotides (DNA, RNA), aptamers, physical elements including transducer of three electrode, electronics amplifiers, converters and polymers in order to improve the sensitivity and selectivity of electrode for rapid detection of AIV H5N1. Geno sensor, immunosensor, and optical sensor are commonly used biosensors in the detection of AIV (Grieshaber et al., 2006).

Biosensors are devices which are miniaturize, low cost, small sample volume requirement, high speed, easily handle, very sensitive and selective for the detection of pathogen (Grabowska et al., 2014). For the detection of AIV H5N1, different types of biosensors (nanocomposite, antigen-antibody, oligonucleotide sequence and / or aptamers based) which produce signal or chemical changes have been designed.

Lee and his colleagues developed Geno sensor on the glassy carbon electrode modified with MWCNTs-CoPC/PAMAM nanocomposite materials to detect the oxidation of Guanine and designed Geno sensor using ferrocene (FC) attaches to 5' end of hemagglutinin (H) and the methylene blue (MB) that attaches to the neuraminidase (N) (Lee et al., 2018).

Immune sensor has been designed with gold-graphene and CdTe on screen printed electrode (Lee et al. 2018). GO-PAb-BSA biomaterials of nanohybrid on the gold electrode and the fluorescence biosensor has also been designed with CdTe/CdS Qd for the detection of H5N1. The other types of biosensors will also be explained in the biosensors section in detail (Buozis et al., 2018).

Silk is an electrically conductive, biocompatible, low immunogenic, biodegradable and natural protein that supports bio receptors attachment. Silk contains varieties of amino acid residue to immobilize the bio receptors (E.Kavalci and T. Adali, 2014). The bio receptors can be immobilized on the gold electrode, screen printed electrode, carbon electrode, and other electrodes either entrapment, crosslinking, adsorption or covalence techniques. The reaction in which between the bio recognition element and the virus antigen measure using electrochemical impedance spectroscopy, cyclic voltammetry, chronoamperometry and differential pulse voltammetry measurement techniques.

This study focused on designing of immunosensor for the detection of AIV H5N1 biosensor which was based on the formation of antibody-antigen complex on the screen-printed electrode surface. The reaction took place in an electrolyte aqueous solution thus, the movements or accessibility of ions (electrons) from redox centers was achieved towards into the embedded electrode sensing layers. The output of this phenomenon changed the redox center characterization (characteristics) which is the basic of electrochemical biosensor signal generation in the detection of H5N1 using electrochemical measurement techniques of cyclic voltammetry and chronoamperometry.

### **1.1 Statement of Problem**

Globalization has accelerated the transportation system and it allows to materials and human movement from one country to the other country across the world. The interconnection may

have great role for the transmission of emergency and pandemic diseases in particular the AIV H5N1. The AIV H5N1 is highly contagious and infectious disease which is transmitted through contamination of virus from animal to human via versa which causes high health, economic, social and ethnical damages in human beings (Lee et al., 2018).

The AIV infects a million and kills hundred thousand people in each years (Nidzworski et al., 2014). The diagnosis of AIV through the traditional diagnostic methods includes; virus isolation, serology and rt-PCR (Yang et al., 2018). The new approach is to design different types of biosensors such as; electrochemical, optical, impedance, conductance, piezoelectric, cantilever, surface plasmon resonance to detect the AIV H5N1(Dziąbowska et al., 2018).

The traditional diagnostic methods of AIV are expensive, poor in specificity, not appropriate for the field work, low sensitive, require long time procedures, are time consuming, require well qualified laboratory setting and trained staff and need more sample. The biosensors based on detection of AIV are also expensive and some devices are low sensitive, selective, affects with interference and are not effectively used in all environmental conditions at any condition of working environment (such as temperature) for the bio recognition element (Yang et al., 2018).

## **1.2 Aim of the Study**

The objective was to design a novel biosensor to detect the H5N1 virus by immobilizing antibody of H5N1 on the screen printed electrode modified with SF film and SF/x-linked film.

## **1.3 The Importance of the Thesis**

The AIV is the global threat disease which has social and economic damages in poultry and human. To prevent the death of human, poultry and damage of economic related with the contagious and pathogenic diseases of AIV early diagnosis and treatment is required with ultrasensitive, rapid and accurate biosensors. The importance of the thesis is to design a novel AIV biosensor from local available biomaterials of silk fibroin which is rapid, point of care, low cost, friendly use, handheld, sensitive, small volume of sample, and wuantitative results for the diagnosis of AIV H5N1.

#### **1.4 General Objective**

- Design a novel AIV H5N1 biosensor by immobilizing antibody of H5N1 on the SPE modified with silk fibroin.

#### **1.5 Specific Objective**

- Description of avian influenza A virus subtype H5N1 life cycle, diagnosis, transmission and different types AIV H5N1 biosensors.
- Description of bio recognition element, measurement and immobilization techniques of avian influenza A virus subtypes H5N1.
- Explanation of the polymers for improving sensitivity of biosensors and silk fibroin extraction method
- Purification of silk fibroin protein from silk cocoons through the steps of degumming, dissolution and dialysis processes.
- Conduction of silk fibroin film, particles, SF x/linked film and PBS solution characteristics using CV and CA to determine the conductive and sensitivity of the electrode.
- Preparation of the screen-printed electrode to immobilize the antibody of AIV H5N1 with SF film and SF/x-linked film.
- Detection of H5N1 using silk fibroin film, SF/x-linked film and antibody of H5N1.

#### **1.6 Thesis Outline**

Chapter 1 provided a general information, aim, importance, general objective and specific objective of the thesis. In chapter 2, literature reviews on influenza virus, avian influenza virus and its subtypes, different types of AIV biosensors, biomaterials, bio recognition elements, measurement techniques and silk fibroin. Chapter 3 described the materials and methods parts. Chapter 4 described the result and discussion parts. Chapter 5 explained the conclusion part of the thesis.

## CHAPTER 2

### LITERATURE REVIEW

#### 2.1 Influenza Virus

Influenza is a spreadable and infection disease caused by influenza virus. Influenza is highly contagious diseases that attacks nose, throat and lungs and it causes runny nose, chills, fever, sore throat, muscle aches, fatigue and cough. The influenza virus is extremely small and can only be visible through the electron microscope (Fujiyoshi et al., 2012).

The virus is considered as an outbreak, emergency and pandemic disease. This virus affects both human and animals which causes devastating death in the world and also causes economics destruction, high mortality and morbidity mainly in humans, birds and swine. It circulates and transmits to animals and humans. The influenza virus transmits the boundary from one country to the other by the humans, large migratory birds (Regea, 2017).

The influenza virus has high mutation rate and the ability to change the antigenic behavior through antigenic shift and antigenic drift (Grabowska et al., 2014). The influenza virus is a member of enclosed viruses that has a core RNA and proteins. The genetic materials of the virus allows more copies during the invasion of the new host cell. This genetic material enclosures with protein shell which protects the virus as it travels from humans to animals infects (Regea, 2017).

The influenza virus is belonging to member of family *Orthomyxoviridae*, which contains a negative polarity single strand ribonucleic acid (ssRNA) and it is mainly categorized in A (most harmful), B (harmful) and C (less harmful) influenza virus. The virus has its own host specificity, nucleoprotein antigens, numbers of gene segment and clinical manifestation which differs from each other (Krejčová et al., 2014).

The neuraminidase (NA) and hemagglutinin (HA) proteins allow the virus to infect the new cells by merging with the cell's outer membrane sticking out the spikes of protein molecules. The flu virus uses HA spikes like a key to get inside your cells which attaches the sialic acid

with the host cell and NA spikes allow to cut or cleavage the sialic acid for copies of the virus to break away from your infected cells to infect more cells (Yang et al., 2018).

## 2.2 Avian Influenza A Virus

The AIV considered as human influenza classified as H1N1, H1N2,... , the Avian influenza H1N1, H1N8, H5N1, ... etc. and as well as swine influenza H1N1, H1N2, H2N1,... etc. (Lee et al., 2018). The AIV subtype H5N1 causes sickness and infections in both humans and birds. This highly pathogenic avian virus influenza of subtypes is subtype A and is causative of flu which is also known as AIV or bird flu.

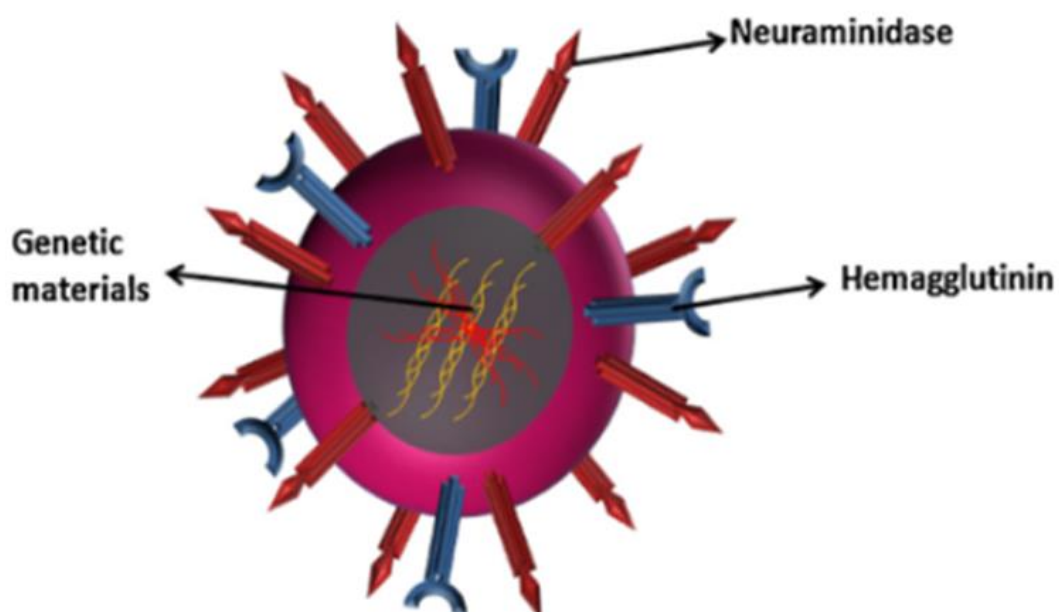


**Figure 2.1:** Structure of avian influenza A virus (Tepeli & Ülkü, 2018)

The AIV has serious antigenic drift occurs since the copies or daughter virus antigenic portions of N and H glycoproteins differ from the parent virus or easily exchangeable and the antigenic shift occur when two virus with different origin (one from animal and one from human) affect one cell the daughter virus emerge through the combination those two influenza viruses (Peiris et al., 2007).

This assortment consequences in the emerging of extremely mortal avian influenza viruses (AIV) such as the H7N9 and H5N1 that can be transmitted from birds to human (Yang et al., 2018).

The influenza A virus on the base of basis of antigenicity classified into 16 hemagglutinin (H) subtypes includes: H1, H2,..., H16 and 9 neuraminidase (N) subtypes includes: N1, N2,..., N9 (Neumann et al., 2009).

### 2.2.1 Life cycle

AIV have an enveloped protein membrane and it contains a negative sense single strand segmented ribonucleic acid (RNA) that enables the virus invade and replicate. The virus has eight segments for encoding the viral genome includes hemagglutinin and it's large in numbers of protein which accounts 80%, neuraminidase which make up of 17% (Samji, 2008).

The viral ribonucleoproteins (RNP) made from the single stranded negative RNAs and cover around the nucleoprotein (NP) and consist of three polymerase proteins, polymerase base protein1(PB1), polymerase base protein 2 (PB2) and polymerase acidic protein (PA) which make up the viral RNA polymerase complex. The life cycle of influenza virus A have stages to invade and replicate in the host cell which includes attach the hemagglutinin into the host cell of sialic acid, endocytosis of viral ribonucleoproteins (vRNP) into the nucleus of host cell, viral genome transcription and replication in the host cell, assembly, budding and release at the host cell was shown in Figure 2.2 (Nelson & Guyer, 2012).

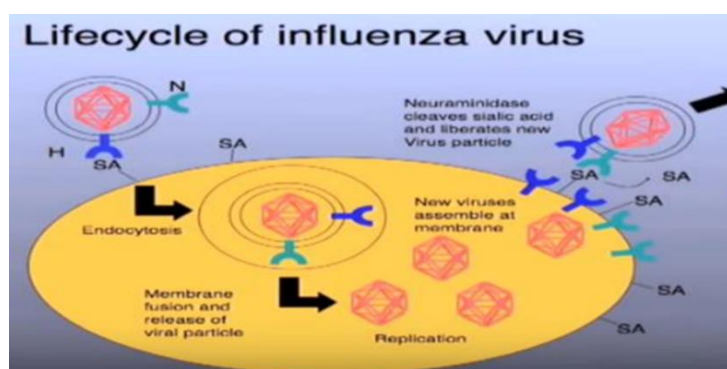


**Figure 2.2:** Life cycle of influenza virus (iBology, 2019)

### **2.2.2 Transmission**

The influenza virus affects the upper respiratory organs, muscle, nose, throat, and the lungs and it affects all ages among youth, elders and children. It shows symptoms in the infected individual average 9 or 10 days and death occurs due to respiratory failure. The influenza virus more rampant and frequently appears during cold months of the year (Diseas- et al., 2013).

The influenza virus selectively destroys and attacks the upper body of respiratory tract, trachea and the tiny hair which is found in the respirator tracks (ciliated epithelial) cells. Influenza virus transmits with contact of contaminated objects, through infected individual sneeze, cough and with aerosol from infected person (Regea, 2017).

### **2.2.3 Diagnosis and prevention of AIV**

The AIV is highly contagious and pathogenic infectious disease that causes infection from mild to severe diseases in poultry and also to human (Zhu et al., 2009). The AIV is highly infectious diseases and causes social, economic, ethnical and health problems to the society (Lee et al., 2018).

Diagnosis and prevention of influenza virus is required to have a healthy community and to prevent deaths, spread and damage associated with AIV. The development of analytical laboratory medical devices which allows a rapid detection with ultrasensitive and selective for the diagnosis of the AIV are needed (Lee et al., 2018).

The diagnosis of influenza virus can be done by viral culture-based assay, polymerase chain reaction (PCR)-based assay, serological assay, rapid diagnostic kits and biosensors (Yang et al., 2018). The devices will explain in more details in chapter two background and literature reviews parts. The first detection of H5N1 was in 1997 in China and WHO has recorded 844 confirmed cases since 2003 and among of those cases, the mortality rate was 60% which involved 449 deaths (WHO, 2011). The influenza virus A H5N1 has high mortality rate and in order to control the outbreaks, rapid diagnosis and prevention the spread from country to country are important (Wong et al., 2017).

#### **2.2.4 Treatment**

Treatment of influenza virus conducts after diagnosis of the virus which discovered in the patient body through laboratory devices, handheld biosensors and rapid kits by the trained physicians. Adamantanes drugs are common drugs which consist of two drugs class called Amantadine and Rimantadine. Both of these drugs play a role in blockings viral un coating and preventing acidification of the internal virus which is needed for viral encoding. This drugs are also used as prophylaxis against influenza for patients that have been exposed to the virus (Peiris et al., 2007). There are several problems with these drugs which is only used for the influenza A treatment and has no effective in the treatment of the influenza B (Klimov et al., 2007).

Amantadine can cause a side effect in adverse central nervous system (CNS) confusion and anxiety as well as anticholinergic effect, dry mouth and urinary retention which can be especially problematic in the elderly. Rimantadine appears to have less CNS effects these drugs are also teratogenic so cannot be used in a pregnant female (Goloubeva et al., 2002) The second drug is neuraminidase inhibitors which the most frequently used class of antivirals against influenza drugs. This drug includes Oseltamivir and Zanamivir and were used for preventing release of the new virus in the host cell because inhibition of neuraminidase enzyme blocks the cleave of sialic acid to prevent the release of a new virus from the infected cells thus limiting the severity of infection (Reece, 2010).

#### **2.2.5 Effect of AIV in the world**

Influenza has been a major global health problem and one of the first documented pandemics of influenza was the famous pandemic of 1918 which wiped out enormous portion of the population over 70 million deaths have been attributed to this particular flu pandemic which by the way is more deaths than were associated with World War one and World War two combined so this was a major killer back in 1900s (WHO, 2011).

The influenza A virus cause every year 65 million illness, 30 million medical visit, 200,000 hospitalization, 25,000 death and \$3-5 billion in economic losses. The influenza virus H1N1 Spanish in 1918 , H2N1 Asian flu in 1957 and H3N1 Hong Kong flu 1968 occurs (Steinhoff, 2007).

### 2.3 Overview of Biosensors

Lyons and Clark are the first biosensor inventors in the 1960s (Yoo & Lee, 2010). Biosensor is a device combining bio recognition element includes nucleic acids, tissue, cell receptors, microorganisms, organelles, antibodies, enzymes, proteins) with physio-chemical integrated three electrodes system (Cernavodeanu, 2001) that are capable to detect a chemical, physical or biological property of a specific substance and an electronic transducer consists of signal processing, amplifying, recording and display the result in readable format shown on Figure 2.3 (Cavallini, 2015).

Biosensors which are designed with various types are DNA biosensors, enzyme based biosensors, thermal biosensors, piezoelectric biosensors, immune sensor, optical biosensors, amptamer biosensor and etc.(Mehrotra, 2016).

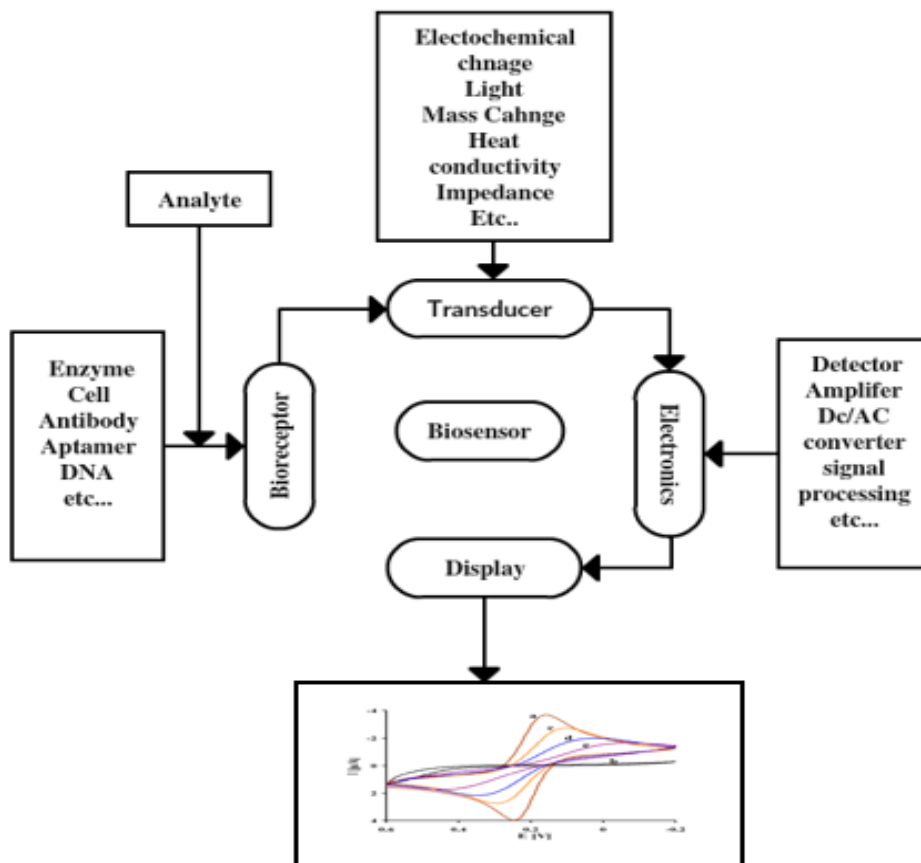


**Figure 2.3:** Schematic representation of a biosensor

## **2.4 Electrochemical Based AIV H5N1 Biosensors**

The electrochemical biosensors are used for converting biological sample information into electrical signal. The sensor designed with bio receptors to the specific analyte determine concentration in for the biological sample in the clinical, biological, research center and biotechnological application (Grieshaber et al., 2006).

The electrochemical biosensor measurements mainly classified in two broad classes; one in potentiometry techniques which measures potential between working electrode and reference electrode with constant current and amperometry techniques is measured a current between the counter and working electrode with constant potential (W.Wang, et al., 2010). The electrochemical based influenza A virus H5N1 biosensors are used for the detection of influenza A virus H5N1 to prevent massive death and controlling the transmission from on country to the other due to their sensitivity, selectivity and economically affordable than the conventional detection method.

The design of electrochemical based influenza virus A H5N1 has considered varies factors including the detecting targets, selection of types electrode, the immobilization techniques, method of electrochemical detection, materials for the immobilization of antigen and the transducers (Yang et al., 2018). Based on the targets here with explain some of electrochemical based influenza virus A H5N1 biosensor.

### **2.4.1 DNA biosensor (Nucleic acid-modified electrode)**

DNA influenza virus A H5N1 biosensor is a reliable and suitable analytical device and newly emerged designed for the detection AIV H5N1. The sensor used DNA as the bio recognition element to detect the AIV H5N1. This device is miniaturize, low cost, small sample volume requirement, high speed, easily handle, friendly use, very sensitive and selective for the detection of pathogen (Grabowska et al., 2014).

The biological active element on the DNA biosensor specific oligonucleotide sequences single strand DNA (ssDNA) used for the identification viral genome of complementary ssDNA during hybridization process. In the Geno sensor, varies method to immobilize the

DNA oligonucleotides sequences and used different biomaterials for the stability and enhancement the sensitivity of the electrode (Grabowska et al., 2014).

Immobilized DNA on glassy carbon electrode (GCE) modified with multiwall carbon nanotube (MWCNT), cobalt, phthalocyanine (PC) and poly (amidoamine) (PAMA) which abbreviated (MWCNTs-CoPC/PAMAM) biomaterials are used to detect H5N1 and the nanocomposite materials are used to improve sensitivity of the electrode. The Geno sensor detects the H5N1 using hybridization process. The detection of H5N1 using DNA probe at oxidation of guanine when hybridization occurs and mismatches base sequence between probe ssDNA and the complementary ssDNA of the viral genome (Lee et al., 2018).

The Geno sensor also is designed using ferrocene and methylene blue immobilize onto gold electrode with the two oligonucleotide probes hemagglutinin and neuraminidase. The two modified probes; ferrocene (FC) attaches to 5' end of hemagglutinin H (5'-FC-ATT TGG AGC TAT AGC AGG TT-SH-3') is complementary DNA (cDNA) part of hemagglutinin H5 the influenza A virus H5N1 and the methylene blue (MB) attaches to the neuraminidase N (5'-MB-AAT GGG ACT GTC AAA GAC AG-SH-3') is complementary DNA (cDNA) part of neuraminidase N1 the influenza A virus H5N1 (Grabowska et al., 2013).

The Genosensor of H5N1 is also designed with modified glassy carbon electrode with avidin biotin conjugation and the biotinylated probe single strand (ssDNA) 5'-biotin-ATG AGT CTT CTA ACC GAG GTC GAA-3'. The hybridization of the probe ssDNA (probe DNA (5'-biotin-ATG AGT CTT CTA ACC GAG GTC GAA-3') and the complementary ssDNA (target DNA (5'-TTC GAC CTC GGT TAG AAG ACT CAT-3') of the viral genome the current value is evaluated using cyclic voltammetry (Krejčová et al., 2014).

#### **2.4.2 Immune biosensor (Antibody modified electrode)**

Immunosensor or immune biosensor is one of the analytical devices to measure and detect antigen or antibody concentration of the influenza virus A H5N1 based on the interaction between the antibodies – antigen and it provides the signal from the interaction to determine the virus in the sample. This method is highly sensitive, selective and low cost than the convectional detection methods of the influenza virus A H5N1 (Wang & Tang, 2008)

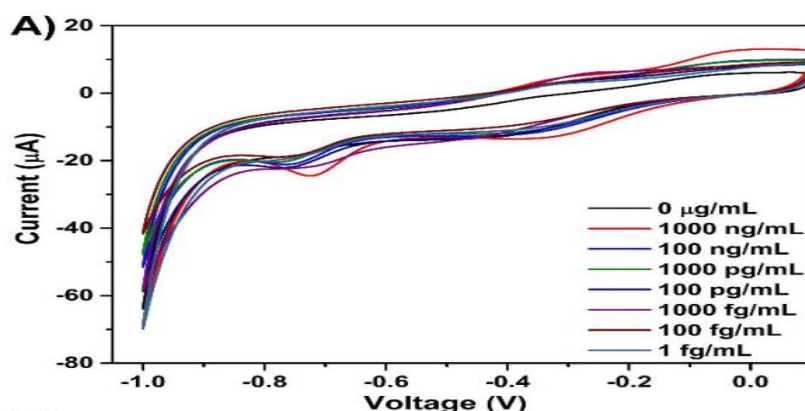


**Figure 2.4 :** Immunosensor detection of AIV H5N1 immobilized the viral antibody H5N1

In Figure 2.4, the screen printed electrode modified with gold-graphene nanocomposites through N-(3-dimethylaminopropyl)-N'-ethylcarbodiimide (EDC) and N-hydroxysuccinimide (NHS), and Cadmium telluride (CdTe) quantum dots have been recorded with a cyclic voltammetry scan range of 0.1 V to -1 V with a scan rate of 0.01 V/s and the antibody H5N1 concentration range from 0 µg/mL to 1 fg/mL. 5mM of K<sub>4</sub>[Fe(CN)<sub>6</sub>] and K<sub>3</sub>[Fe(CN)<sub>6</sub>] in 1X PBS (pH 7.4) was used as the electrolyte solution. Two peaks of negative characteristics were found in the CV profiles/graph, one at -0.35V and the second at -0.75V, corresponding to the CdTe bioconjugate reporters. It was found that the characteristic peaks at -0.75V was more noticeable, and thus was used to obtain the currentantigen concentration data (Buoziš et al., 2018).

The antigen and antibody reaction measure immobilized the viral antibody on screen printed electrode with modified nanocomposite materials of gold-graphene and quantum dot electrochemical CdTe and through N-(3-dimethylaminopropyl)-N'-ethylcarbodiimide and N21 hydroxysuccinimide chemistry. The signal produced from the reaction was measured and detected with cyclic voltammetry (CV) to validate the detection of influenza virus A H5N1. The magnitude of signal produced during the reaction of CdTe (Cadmium telluride) mechanism is proportional to the concentration antigen that present in the sample (Buoziš et al., 2018).

The electrochemical immunosensor (Immune biosensor) has been designed with nanohybrid materials with graphene oxide, H5-polychonal antibody and bovine serum albumin. The graphene oxide used for carried the H5-polychonal antibodies (PAb). The H5-polychonal antibody used to identify the H5 protein on the influenza virus A H5 and amplification of the signal shown on Figure 2.5 (Xie et al., 2014).

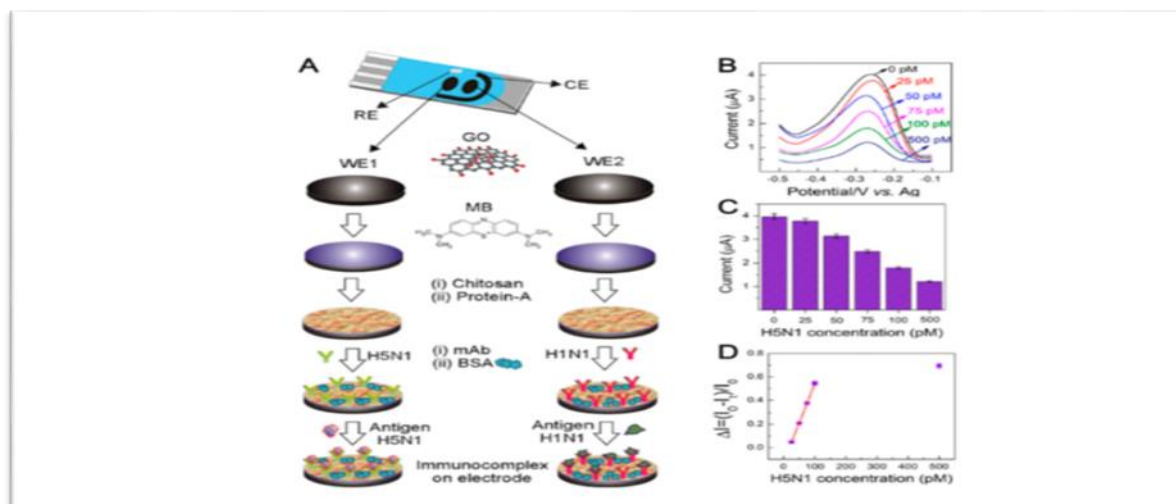


**Figure 2.5:** Schematic diagram of biosensor fabrication for the detection of H5N1 and H1N1 using antigen dual screen printed electrode image adopted from (T. Lee et al., 2016)

The GO-PAb-BSA biomaterials of nanohybrid could be applied to design the electrochemical immune biosensor (Immunosensor) to detect AIV H5N1. The H5N1 antibody is immobilized onto the gold electrode to capture the influenza virus A H5N1 at the viral and added the ferricyanide as the reduction and oxidation reporter and the signal was measured with cyclic voltammetry (CV) (Lee et al., 2018).

## 2.5 Optical Biosensor for Detection of H5N1

The Optical biosensor uses a specific light to detect the interaction, resonance, absorbance and reflectance between the bio recognition element and target of the AIV. Optical biosensor which is used to detect the AIV H5N1 has varieties of designed that depends on the types of techniques employed such as reflectance, surface plasmon resonance (SPR), fluorescent, and

luminescence and absorption sensors. The detection of optical biosensor either by analyte affects the optical properties (direct sensing with labeled free ) or detection with labeled or tagged to produce optical phenomena (Ronghui & Yanbin, 2016).

### **2.5.1 Surface plasmon resonance biosensor (SPR)**

SPR biosensor is designed with light source and this light exposed on the electrode surface which contain the target molecules, the probe modified substrate and biohybrid biomaterials, it activated the biomolecule near the electrode surface (sensor) and it produces oscillated and resonates of electron on the surface of electrode, this oscillation of produce movement of electron (Zeng, Baillargeat, Ho, & Yong, 2014).

SPR biosensor is an optical type of biosensor devices and its nondestructive method and sensitivity that can be measured in small changes of the light refractive index. The devices which contains light source, transduce (electrode, chip, microfluidics, film ...), prism and detectors. The SPR occur when the incident of light sources hits the transducer with their specific degree of angle. The analyze and the target molecules excitation and oscillation and produce the movements of electron and the detectors records such movements which proportional to the target concentration in the sample.

The SPR biosensor is an analytical device which is small in size, low cost, quick, friendly uses, selective and sensitive (Firdous, Anwar, & Rafya, 2018). The SPR biosensor is used in AIV gene hybridization, AIV detection and HA protein detection were to construct functional bio-probe such as antibody, aptamers and other biomaterials to enhance the performance and sensitivity of analytical devices (Anker et al., 2008).

### **2.5.2 Fluorescence based biosensor**

The fluorescence-based biosensor is the most known analytical device to detect AIV A H5N1 due to their highly selectivity and sensitivity which provides spectral characteristics during target and bio probe interaction. The fluorescence based biosensor requires labeling to produce fluorescence signal during binding of the target and bio probe (Strianese et al., 2012).

The Fluorescence based biosensor detection is based on the fluorescence signal on and off between the target binding to the bio probe fluorescent, such as fluorescent proteins, dye-labeled nucleic acid, fluorescent nanoparticles and when the bio probe was bound to the target the signal produce which it may be decrease or increase based on the design strategy to the detection of analyte (Lee et al., 2018).

One of the fluorescence-based biosensor influenza virus A H5N1 design is with aptamer, quantum dot and hydrogen. The quantum dot (QDs) used as for the fluorescence during aptamer bind with the target of influenza virus A H5N1. In another fluorescence biosensor for the detection of H5N1 is with the high luminescent Cadmium telluride (CdTe)/ Cadmium sulfide (CdS) and quantum dot (QDs). The CdTe/CdS Qd is synthesized and H5N1 antibody is conjugated with CdTe/CdS QD (Hoa, Thi, Thuy, & Vu, 2014). Recently the Fluorescence based biosensor design for the detection of H5N1 aptamers is with the molybdenum disulfide-QD (MoS<sub>2</sub>-QD) with magnetic nanoparticle(MNPs) shown on Figure 2.6 (Ahmed & Neethirajan, 2018).

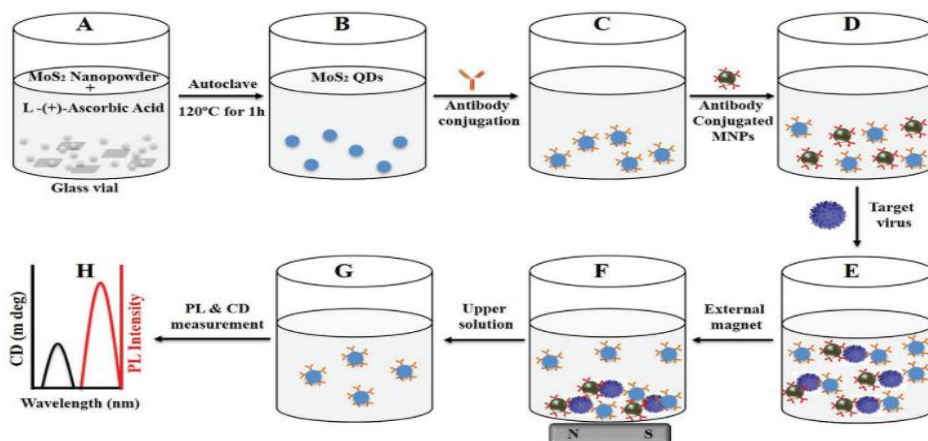


**Figure 2.6:** Schematic diagram of fluorescence-based biosensor design using MoS<sub>2</sub>-QD and MNPs using electrochemical spectroscopy (Ahmed & Neethirajan, 2018)

## 2.6 Electrochemical Measurements

### 2.6.1 Cyclic voltammetry (CV)

CV is the technique of electrochemical measurements that is used to investigate oxidation and reduction process between the analyte and bio receptors to provide the information and the data about the analyte and measures the current by varying the applied potential. The current produced in the reaction is measured at the WE and plotted as current(I) vs applied potential (E) (Elgrishi et al., 2018).

The cyclic voltammetry has two potential peaks; Cathode potential peak ( $E_{pc}$ ) and the anode potential peak ( $E_{pa}$ ). The  $E_{pc}$  is the maximum reduction potential and  $E_{pa}$  also the maximum anode potential shown on Figure 2.7. The capacitive current (charge current) developed between the electrolyte solution and electrode surface forms a depletion layer and it observed the minimum current which gradually increase the current to the faradic current.

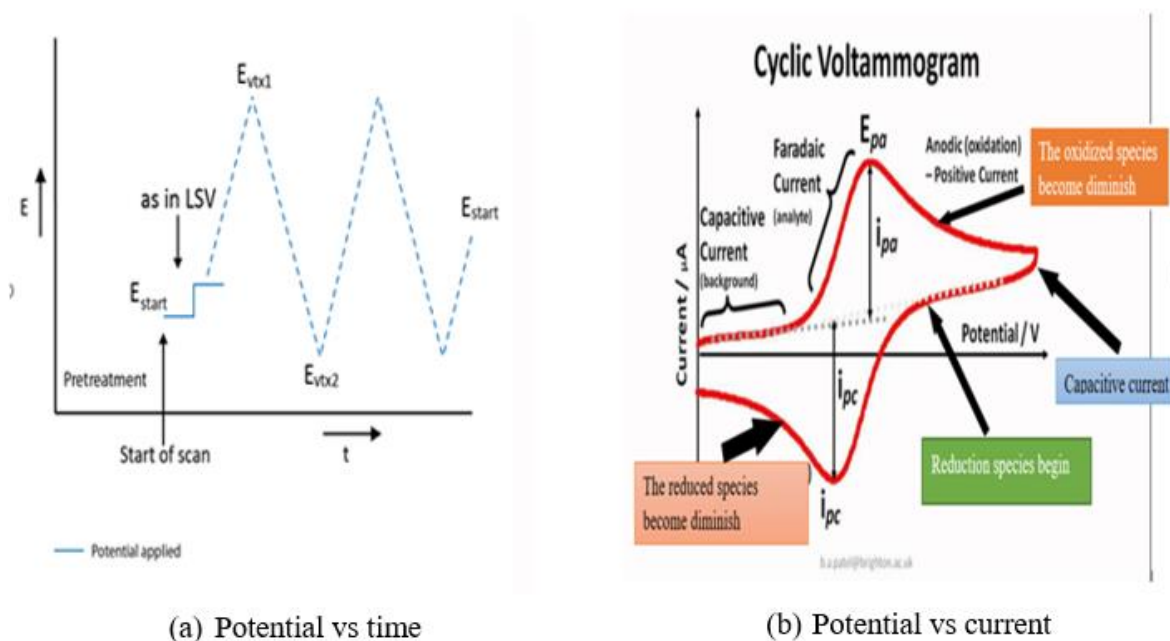


**Figure 2.7:** Schematic diagram of cyclic voltammetry

The current which is produced at the maximum cathode potential is called the maximum cathode current ( $i_{pc}$ ) and the maximum anode potential is anode maximum current ( $i_{pa}$ ). This current is faradic current which is produced on the working electrode in the movement of electron. The electrochemical cell contains electrolysis solution, analyte, target and three electrode system i.e. WE, RE, and CE. The potential is measured in WE and RE although the current is measured, WE and CE. During the oxidation and reduction processes, the cyclic voltammetry is measured and plotted the result of potential vs time or current as with potential.

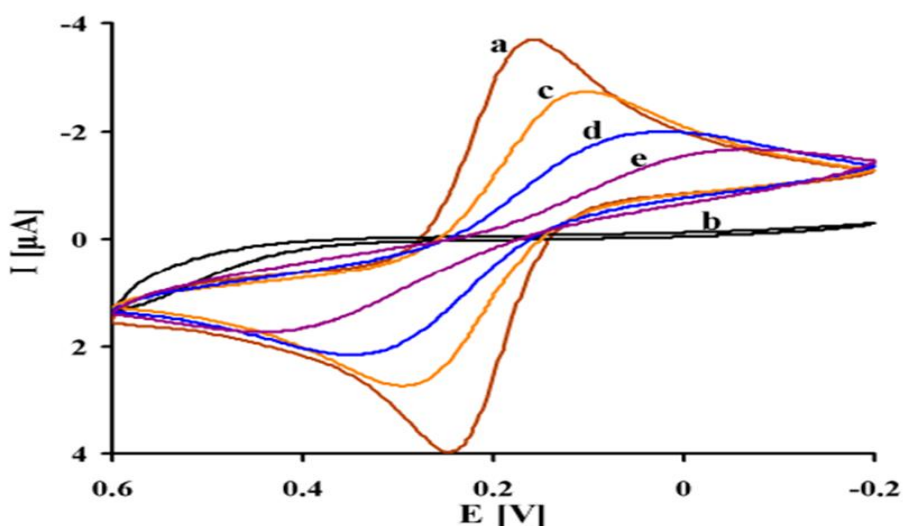


**Figure 2.8:** Immunosensor detection of AIV anti-hemagglutinin H5 using CV

The cyclic voltammetry graph on figure 2.8 , the scan range of potential from 0.6 to  $-0.2$  V with scan rate 0.1 V/s modified gold electrode : a) clean gold electrode, b) 1,6-hexanedithiol (HDT), c) colloidal gold particles(GCP) and 1,6 HDT, d) anti-hemagglutinin /GCP/1,6-HDT, e) Bovine serum albumin (BSA) /Fab'/GCP/1,6-HDT modified electrode measurement condition in 1 mM  $K_3[Fe(CN)_6]/K_4[Fe(CN)_6]$  as redox probe in 0.1 M PBS (pH 7.4) shown Figure 2.8 (Jarocka et al., 2014; Nidzworski et al.,

The solution contains oxidation reduction species which the voltage increase towards to the reduction potential peaks the cathode current peak increase and after this peaks the

concentration analyte become diminish and formed depletion layer and hence the oxidation potential increase. The reverse scan towards to the oxidation peaks and increase the anode current peaks and then the oxidation species analyte concentration consumed at the working electrode and the current begin decrease. The current never becomes zero because the capacitive current develop between the electrolysis solution and electrode. CV measurements provide the reverse and forward scan of a redox reaction current within in the given scan rate (Grieshaber et al., 2006).

The shape of the cyclic voltammetry “voltammogram” for a given electrochemical reaction depends on scan rate, electrode surface, catalyst concentration, the analyte concentration and depletion layer formed between the electrode surface and electrolysis solution (capacitive current) (Elgrishi et al., 2018).

### 2.6.2 Chronoamperometry (CA)

Chronoamperometry (CA) is another type of electrochemical measurement techniques which measures the current with time at constant applied DC potential. The measured current indicates the reduction and oxidation species process at the working electrode with time at constant and know potential shown on Figure 2.9 (Cavallini, 2015).

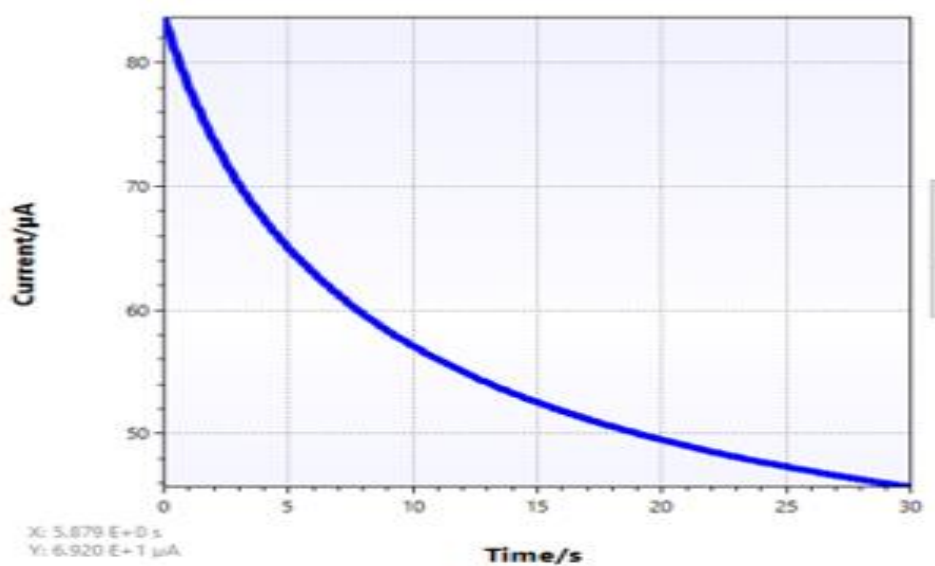


**Figure 2.9:** Schematic diagram of chronoamperometry graph

The peak current over the linear DC potential proportional (directly) to the concentration analyte in the sample. The amperometry techniques which are used to measure the current and concentration with constant interval time, can analyze the graph of the current with time to study the complete chemical reaction. The graph of chronoamperometry is obtained the known and constant potential applied into the cell and the current sampling in each interval of time and then plot the graph of chronoamperometry current with time (Grieshaber et al., 2006).

## **2.7 Biomaterials for Biosensor Design**

### **2.7.1 Polymers for improving sensitivity of electrode**

Polymer biomaterials have a fundamental application for biosensor designs and constructions due to their molecular structure. The polymer is highly bio compatible and it creates a suitable working environment for detection of analyte. The application of polymer biomaterials in the biosensor to support and enhancement of sensitivity, stability and reusability of the bio receptors, reduce time, prevent contaminate of the analyte, increase specificity of the bio receptors, increase the surface area, reduces other species redox the working electrodes and possibility of a continuous process (Geckeler & Muller, 1996).

Polymers have hydrophilicity and hydrophobicity as an electrical conductivity and hygroscopicity to attach the receptors at the electrode surface. It also consists of a varieties of amino acid residues and reaction sites including carboxyl, amino, phenol, and imidazole groups to immobilize which is favorable for the bio receptors. Polymers such as polyaniline, polypyrrole, polypyrrole–polyvinyl, poly(N-methylpyrrole), polyindole, polyphenylene diamine, others (Gerard, Chaubey, & Malhotra, 2002) and used in biosensors to immobilize antibodies, enzymes, DNA, aptamers, proteins, cells, organelles, and other bio recognition elements on the surface of electrodes to increase the stability, sensitivity, selectivity and reduce the interference of other chemical oxidation at the working electrode (D’Souza, 2001).

Nanomaterials have a unique properties for immobilization and their optical, large surface area, catalytic and stability properties offer a tremendous application for designing biosensor

devices. Biomaterials such as silk fibroin, sol-gel, chitosan and bio hybrid materials are commonly used for the immobilization of bio recognition element (Saxena & Das, 2016).

The micro/nano particles, including copper, silver, gold and palladium alloys such as iron–platinum, gold–copper, gold–silver and various allotropes of carbon such as carbon graphene, nanotubes, and fullerenes and semiconductors such as silicon, .... Other materials are also available for the detection of analyte with different shape rode by using multilayer designs (Cormode et al., 2018).

## **2.8 Biorecognition Elements**

Biorecognition is the brain of bio sensing devices. Biorecognition elements are immobilized on the electrodes, microfluidics, film, paper and other transducers to interact with specific analyte of a substance to determine and analyse the amount in the sample. The biorecognition elements are immobilized with nano/micro biomaterials to increase the stability and sensitivity on the transducers. The biorecognition element designs with the interest of specific analyte such as antibodies, enzymes, aptamers, DNA, cell, tissues, organelles, whole cells, microorganisms, etc. (Chamber et al., 2005).

### **2.8.1 Enzyme-based bio recognition elements**

Enzymes are proteins in nature, biological catalyst, that are required in small amount, to speed up the reaction. . Enzymes have an active site which binds to the specific analyte for oxidize and reduce to liberate the electron to quantify the analyte amount present in the bio sample (Zhao & Helong, 2018).

Electrochemical enzyme-based biosensors have been used for clinical, research and biotechnological application for monitoring and diagnosis. Specific enzyme immobilized on the transducers to detect specific analyte to monitor and diagnose the level of analyte. Enzymes have many application in biosensor designs by immobilization, encapsulation and matrix with other nano/micro particles and materials for increasing the selectivity and sensitivity of the electrodes to have accurate and reliable results (Zhao & Helong, 2018).

Enzyme-based bio-recognition includes glucose oxidase/glucose dehydrogenase, urease, hemoglobin and glucose oxidase, cholesterol oxidase, amino acid oxidase and other types

are available for designing biosensors for the specific analyte. Glucose oxidase is a common enzyme in the biosensor application to detect glucose in the blood. The glucose biosensor working based on the  $H_2O_2$  redox on the transduce shown Figure 2.10 (Zhao & Helong, 2018). The diagram shows the redox reaction of glucose with glucose oxidase in the biosensor transducer with the mediators to transfer electron.

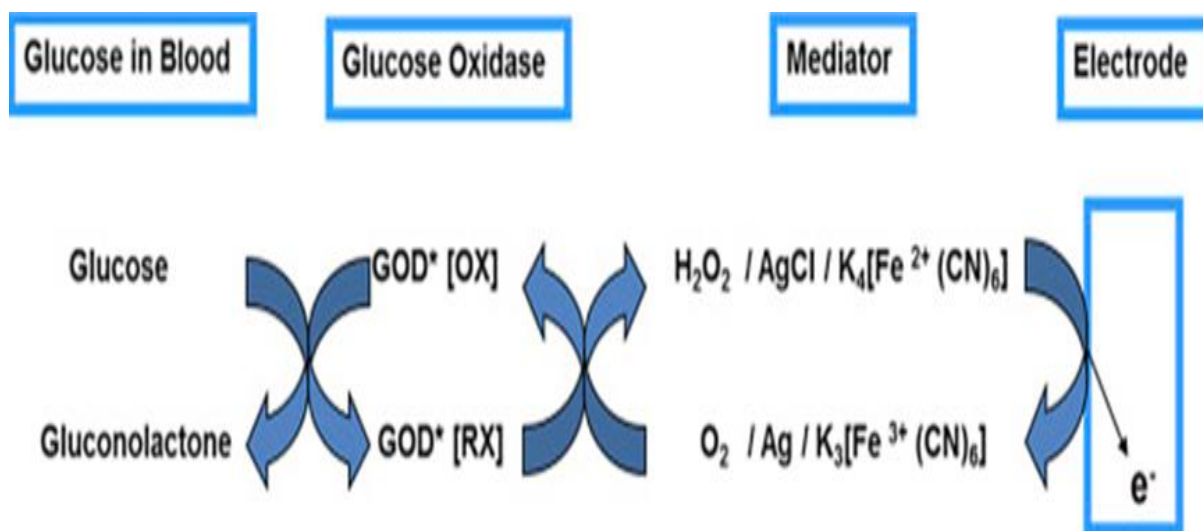


**Figure 2.10:** Schematic diagram of glucose biosensor (P. Tomar and Z. Hassep, 2019)

## 2.8.2 Antibody-based biorecognition elements

Antibodies are types of biorecognition elements which are specifically designed to bind a unique part of the target of antigens. Antibodies are specifically selected and designed for the specific target and the bio probe binds with the virus antibody shown on Figure 2.11. Antibodies are used in immunosensors, optical biosensors, impedance biosensors, conductance biosensors and other types of biosensors for the recognition of infectious diseases such as AIV H5N1 (P. Tomar and Z. Hassep, 2019).

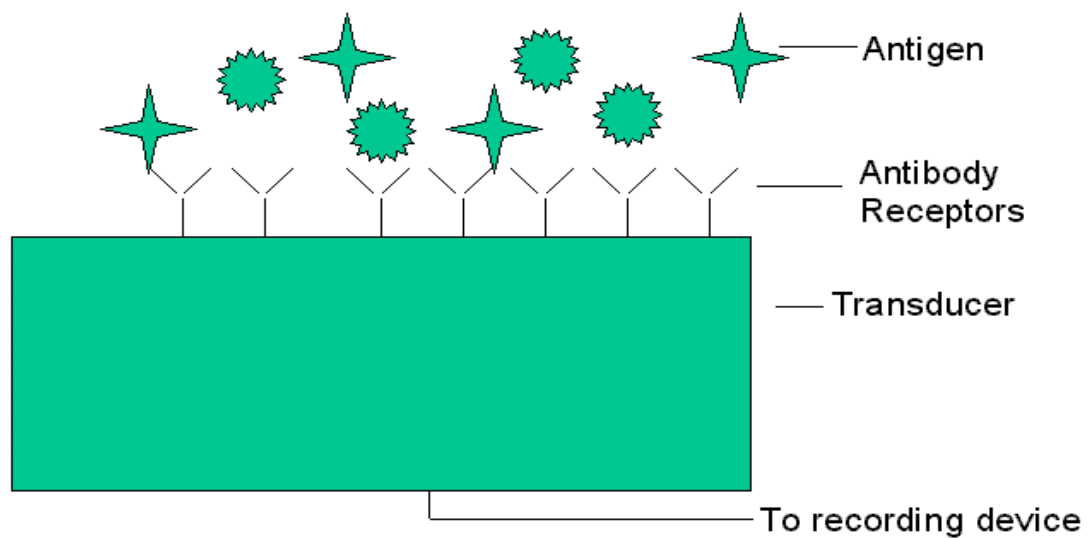


**Figure 2.11:** Schematic diagram of antibody-antigen interaction (Ashok Kumar, 2000).

Antibodies are immobilized on the transducer through the techniques of either adsorption, crosslinking or covalent methods. Antibodies are common bio receptors for biosensors and are produced by immunizing the antibody with antigen to produce measurable signals (Ronghui & Yanbin, 2016).

The biosensor recognition element is strongly depending on the sensitivity and selectivity that is immobilized on the electrode surface. Biosensors use antibodies for the biorecognition element because of their antibody-antigen binding and high specificity to detect the AIV H5N1. The antibodies show specificity of bio affinity for binding towards certain analyte to capture the antigen of the analyte. Antibodies can be monoclonal (MAb) which is an antibody produced from the single clonal and polyclonal (PAb), which is produced from multiple clones of B cells (Soler, 2016).

The AIV have subtypes based on neuraminidase (NA) N1 to N9 and hemagglutinin (HA) H1 to H16 proteins. H5 monoclonal antibodies (MAbs) is used to detect the AIV H5N1 the H5 hemagglutinin is specific to the target and recognize H5N1 virus and the N1 neuraminidase antibodies which is specific to the N1 to the target of H5N1 virus (Ho et al., 2009).

### **2.8.3 Aptamer based biorecognition elements**

Aptamers are peptides or oligonucleotide molecules that are specifically selected and designed to bind a specific target. The aptamers are used in biosensors as a biorecognition element for the identification of the target analyte in the sample. Aptamer biorecognition is the new approach for the design of biosensors in the detection of pathogenic disease and has good sensitivity, cheap synthesis, easier cell penetration, , small in size, stability and simplicity of chemical modification (Cheng et al., 2008).

The aptamers are alternative and potential to replace antibodies in the design of electrochemical and optical biosensors devices. Aptamers are RNA or Deoxyribonucleic acid (ssDNA) oligonucleotides which depend on electrostatic, hydrogen bonding and hydrophobic interactions rather than DNA base pairing Cytosine (C) bind to Guanine (G) and Adenine bind to (A) Thymine (T) for recognition to their target (Ronghui & Yanbin, 2016).

### **2.8.4 DNA based bio recognition element**

The DNA biosensor is designed and fabricated by immobilizing the oligonucleotides sequence on the DNA probe to identify the target DNA sequence. During the hybridization of DNA probe and target DNA sequence aligned each other based on the nitrogenous base sequence and it detects the oxidation peaks of guanine at specific potential and current produced in the reaction which determines the concentration of analyte (Zhu et al., 2009).

The DNA recognition element in influenza A virus H5N1 is also immobilized with other biomaterials for the stability, labeling and improving the sensitivity of the electrode like avidin biotin, methylene blue (MB), ferrocene (FC), etc. The DNA sequence which one of the DNA probe contains the single strand DNA (ssDNA) 5'-biotin-ATG AGT CTT CTA ACC GAG GTC GAA-3' and the target of Viral DNA 5' TTCGACCTCGGTTAGAAGACTCAT- 3' and the signal of current evaluated using cyclic voltammetry (Krejcová et al., 2014)

**Table 2.1:** Comparison of different types of influenza A Virus H5N1 biosensors

| <b>Name of Biosensor</b>                | <b>Bio Receptor</b>   | <b>Target</b> | <b>Hybrid biomaterial</b>   | <b>Electrode</b> | <b>Detection method</b>          | <b>Sensitivity</b>                | <b>Detection range</b> | <b>Ref.</b>             |
|---|-----------------------|---------------|-----------------------------|------------------|----------------------------------|-----------------------------------|------------------------|-------------------------|
| Immunosens                              | Antibody              | HA            | Gold nanoparticle           | Gold electrode   | CV                               | 2.2 pg/ml                         | 4–20 pg/ml             | (Jarocka, et al., 2014) |
|   | Antibody              | H5            | GO-PAb-BSA                  |                  | CV, DPV                          | 2–15                              | 2–15–2–8               | (Xie et al., 2014)      |
|   | Antibody              | HA            | Protein A                   | Glassy           | EIS                              | 2.1 pg/ml                         | 4–20 pg./ml            | (Jrocka et al., 2014)   |
| Impedance biosensor                     | Aptamer               | Virus         | M. bead and AuNP            | SPE              | Impedance CV.                    | 8×10 <sup>-4</sup> HAU/<br>200 µl | 0.001–1 HAU            | (Fu et al., 2014)       |
| Immunosens or colorimetric immunosensor | Aptameranti body pair | Viral protein | gold nanoparticle           |                  | CV, DPV                          | 100 fM                            | 100 fM–10 pM           | (F., Kim, & Lee, 2015)  |
|   | Antibody              |               | HRP-encapsulate d liposomes | microplate       | Naked eye observation absorbance | 0.04 ng/mL                        | 0.1 to 4.0 ng/m        | (Cuiying et al., 2019)  |
| QCM aptasensor                          | Aptamer               | Virus         | polymeric hydrogel          | Gold electrode   | QCM signal in.                   | 0.0128 HAU                        | 30 min                 | (R. Wang & Li, 2013)    |

|                        |                 |         |                      |                  |                   |                           |                                   |                             |
|------------------------|-----------------|---------|----------------------|------------------|-------------------|---------------------------|-----------------------------------|-----------------------------|
| Geno sensor            | Oligonucleotide | H5 & N1 | Ferrocene and B      | Gold electrode   | SWV               | -                         | 18-21 nM                          | (Grabowska et al., 2013)    |
| Geno sensor            | Oligonucleotide | DNA     | Epoxy-amine          | Gold electrode   | CV, SWV, DPV      | 0.87 PM DNA<br>73 pM- RNA | PM range                          | (Malecka et al., 2015)      |
| Fluorescence biosensor | Antibody        | H5N1    | CdTe/CdS             | Chromatophores   | CV, DPV           | Peak at 525 nm)           | low as 3 ng $\mu$ l <sup>-1</sup> | (Hoa et al., 2014)          |
| Optical biosensor      | Antibody        | H5N1    | MoS2 QDs             | CD               | external magnetic | 7.35 pg/mL                | -                                 | (Ahmed & Neethirajan, 2018) |
| Geno sensor            | Oligonucleotide | DNA     | MWCNTs-CoPC/PAM      | carbon electrode | DPV               | 0.01 ng/mL                | -                                 | (Lee et al., 2018)          |
| Immunosensor           | Antibody        | H5N1    | MB-GO and Chitosan   | CSPE             | DPV, CA           | 1 minutes                 | -                                 | (Murugan et al., 2016)      |
| Geno sensor            | oligonucleotids | DNA     | MWNTs-CoPc and PAMAM | GCE              | DPV               | 1.0 pg/ml                 | 0.01 - 500 ng/ml                  | (Zhu, et al., 2009)         |

## **2.9 Techniques of Bio Receptor Immobilization**

The immobilization of bioreceptors has become rapidly growth for the surface modification of electrode in biosensor design. Immobilization is the technique that attaches specific bio recognition on electrode surface to make more stable and sensitive. This technique- is not only used in biosensor application but also used in medical diagnostic, therapy, industrial process, and food industry and biomaterial detection. The immobilization method is used in biosensor designs due to its excellent functional properties such as increasing sensitivity, reliability, ph and temperature stable, cost-effectiveness, reusability and optimality (Hiep & Kim, 2017).

The basic principle of bioreceptor immobilization systems are the method of attachment and the matrix or encapsulation. The first enzyme immobilization was designed by us,ng the *Aspergillus oryzae* aminoacylase immobilization and the resolution of “D Lamino acids” racemic synthetic (Beatriz et al., 2007).

The immobilization techniques have many methods on the interest of specific analyte, working principle of biosensor design and types application. Herewith listed some methods of immobilization techniques of bio recognition elements on the sold electrode surface , This methods are entrapment, crosslinking, adsorption and covalence shown on Figure 2.12 (Hiep & Kim, 2017).

### **2.9.1 Entrapment**

Entrapment is the method conducted the immobilization technique by attaching or “covering” the bio recognition element into a matrix film which primarily consisted of support materials. The entrapment techniques of immobilization is indirectly attached to the transducers surface but entrapment within a biomaterials polymeric network and which allows merely the traverse of bio sample or substrate and products but preserves or retain the bio receptors hence diffusion is constrained (Hsueh & Liu, 2013).

The Entrapment bio receptors immobilization process is conducted through mixing into a polymer and biomaterials and then followed polymerization of bio receptors solution by

reaction of chemicals or changing experimental conditions. This method improves the stability, minimize the bio receptorsdenaturation, leach and optimize microenvironment to have optimal stability however, this method has a drawback. It cannot diffuse deep in to the electrode surface into the bio receptor active sites (Hiep & Kim, 2017).

### 2.9.2 Adsorption

Adsorption bio receptors immobilization technique is the easiest method physical immobilization at the surface of sold carrier and the mechanism by the of week bond electrostatic attraction, hydrophobic and hydrogen bond. The adsorption method with encapsulation or matrix entrapment to the support on the transducers surface with, generally week reaction and non-destructive for bio receptors activity (Sassolas, et al., 2012).

### 2.9.3 Covalent

Covalent immobilization techniques is coupling bio receptors to the polymeric support chemically with specific biomolecule functional group. The covalent coupling have achieved high stability and required large amounts of bio receptors and the covalent immobilization of bio receptors occupy the same active site (Sassolas et al., 2012).

### 2.9.4 Crosslinking

The Crosslinking is a technique used in bioreceptors immobilization and it's a common approach for design of biosensors. The bio component of a cross-linking with Tri (ethylene glycol) dimethacrylate, glutaraldehyde and other bi functional agents. (Sassolas et al., 2012).

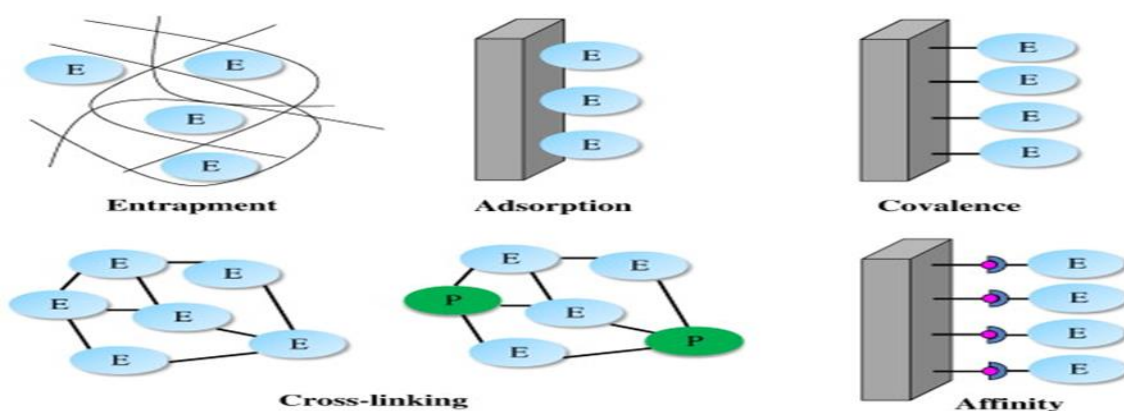


**Figure 2.12:** Schematic immobilization techniques (Sassolas, et.al., 2012)

The bio receptors cross-linked with each with polymers, biomaterials and other functional inert protein like silk fibroin, this method is the simplest and achieve strong chemical bond binding between bio-recognition element and surface of transducers (Hiep & Kim, 2017; Sassolas et al., 2012).

## **2.10 Silk Cocoons**

Silks are natural proteins produced from silk cocoons of *Bombyx mori* (T.Adali & Uncu, 2016). The hydrophobic B-sheet arrangements grant them robust physical, mechanical toughness and strength. Silks are the best biomaterials due to their molecular arrangements allowing to engineered and modify the electrode surface for the biosensor application with biological and chemical functionalities and they stable the bio receptors or immobilization with incorporated with its active site for the improvements of selectivity and sensitivity the electrodes (Shan et al., 2018).

Silk fibroins are compose of naturally proteins (Cao et at. 2013). Silk fibroin low immunogenicity and biocompatibility due to their chemical and physical properties achieved by alternating the polyelectrolyte deposition on the electrode surface for the immobilization of enzyme (Shen, et al., 2015).

Fibroin is used for bio receptor immobilized on the biosensor electrode surface for the determinations of analyte. The analyte concentration determines from the redox of the analyte and bio receptor at the transducer surface and it is used for rapidly, sensitively and reduces interference of oxidize or reduces of other analyte to analyze various bio-samples and it consists of a variety of amino acid residues and has reaction sites such as amino, carboxyl, phenol, and imidazole groups to immobilize the bio receptors for the surface increases, which is favorable for bio receptors immobilization (Zhang, 1998).

### **2.10.1 Silk Properties**

The silk is considered as outstanding biomaterial because of its great biocompatibility, flexibility, low thrombogenic, biodegradation, high tensile strength, elasticity, and good degree of tough- ness that supports bio receptors attachment, support and proliferation (T. Luongl et al., 2015).

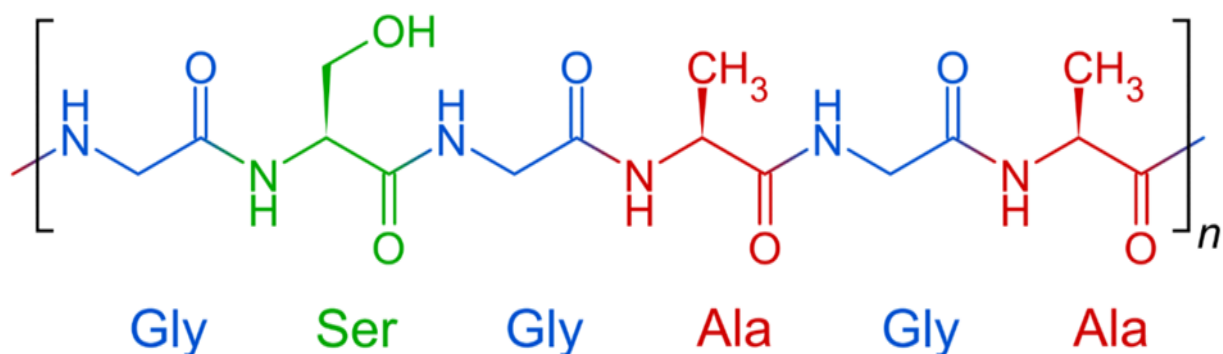


**Figure 2.13:** Structure of SF (U. L. Abia, 2018)

The silk is a biomaterial which is a biocompatible, biodegradable and due to its chemical, physical and mechanical properties is used for the immobilization of bio receptors. The silk consists of fibroin and sericin proteins. The sericin is removed by the degumming process and the remaining fibroin is used for the immobilization of bio receptors. The fibroin is composed of parallel beta-sheet arrangement or structure of amino acid with serine (12%), alanine (30%) and acid glycine (43%) and it contains fat, wax and mineral salt was shown on Figure 2.13.

The composition of silk fibroin makes for the immobilization of bio receptors thermodynamically stable, remarkable mechanical tensile strength proteins (Nikhom, et al., 2012). U.S FDA approved this biomaterial for medical uses and for designing of biosensor diagnostic equipment It is also used in scaffolds, tissue engineering and drug delivery systems (W. Zhang et al., 2017).

## 2.11 Reduction and Oxidation Species

### 2.11.1 Potassium ferricyanide (K<sub>3</sub> [Fe (CN) 6])

Cyclic voltammetry is an electroanalytical procedure to study the behavior of electroactive species, and monitors oxidation/reduction chemical reactions and current produced at the working electrode. The voltammogram provides fundamental information about the redox species reaction (Niranjana et al., 2009).

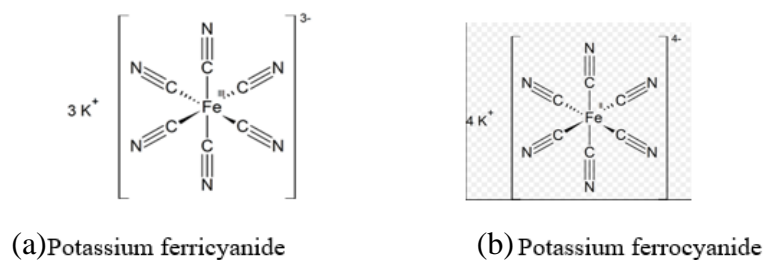


**Figure 2.14:** Structure of potassium ferricyanide

Potassium ferricyanide chemical formula  $K_3[Fe(CN)_6]$  is an oxidized agent used for the investigation of oxidation and reduction peaks at cyclic voltammetry. Two forms one which in oxidized for form  $K_3[Fe(CN)_6]$  and reduced form  $K_4[Fe(CN)_6]$  was shown on Figure 2.14 (a) and (b) respectively (Pandurangachar et al., 2010).

Oxidation equation:



Reduction equation:



The main difference of the two forms using in cyclic voltammetry measurement is the signal that observed at the first graph direction and using  $K_4[Fe(CN)_6]$  it undergoes the oxidation reaction and the scanning increasing towards to positive potentials and observed the oxidation signal graph and after the reverse to the second half the scanning direction the signal of reduction observed from the potassium ferricyanide  $K_3[Fe(CN)_6]$  (Pandurangachar et al., 2010). Using  $K_3[Fe(CN)_6]$  undergo the reduction and with increasing the positive potential scanning the at the first half cycle not observed the oxidation of graph at the anodic and observed the signal at the cathode half cycle of the reduction signal. This reagent is used for the indirect measurement of H5N1 in the electrochemical detection method (Pandurangachar et al., 2010).

## CHAPTER 3

### MATERIALS AND METHODS

#### 3.1 Materials

*Bombyx Mori* (*B. mori*) cocoons obtained from villages of North Cyprus, sodium carbonate ( $\text{Na}_2\text{CO}_3$ ), potassium ferric cyanide ( $\text{K}_4[\text{Fe}(\text{CN})_6]$ ), calcium chloride ( $\text{CaCl}_2$ ), and ethanol ( $\text{C}_2\text{H}_5\text{OH}$ , 98%), sodium chloride ( $\text{NaCl}$ ), potassium chloride ( $\text{KCl}$ ), disodium phosphate ( $\text{Na}_2\text{HPO}_4, 2\text{H}_2\text{O}$ ), potassium dihydrogen phosphate ( $\text{KH}_2\text{PO}_4$ ), and hydrochloric acid ( $\text{HCl}$ ), monoclonal Anti-C10orf F54 antibody produced in mouse and inactivated H5N1 antigen were used in this study.



**Figure 3.1:** Chemicals and materials

#### 3.1.1 PalmSens4 Blv, potentiostat

PalmSens4 potentiostat, Netherland is an electrochemical analysis device that is used to measure the electrochemical analysis of cyclic voltammetry and chronoamperometry to provide biological information of analyte present in the sample. The device consists three electrodes system with labeled cable, screen printed electrode holder, cell and software PSTarces 5.5 shown on Figure 3.2.

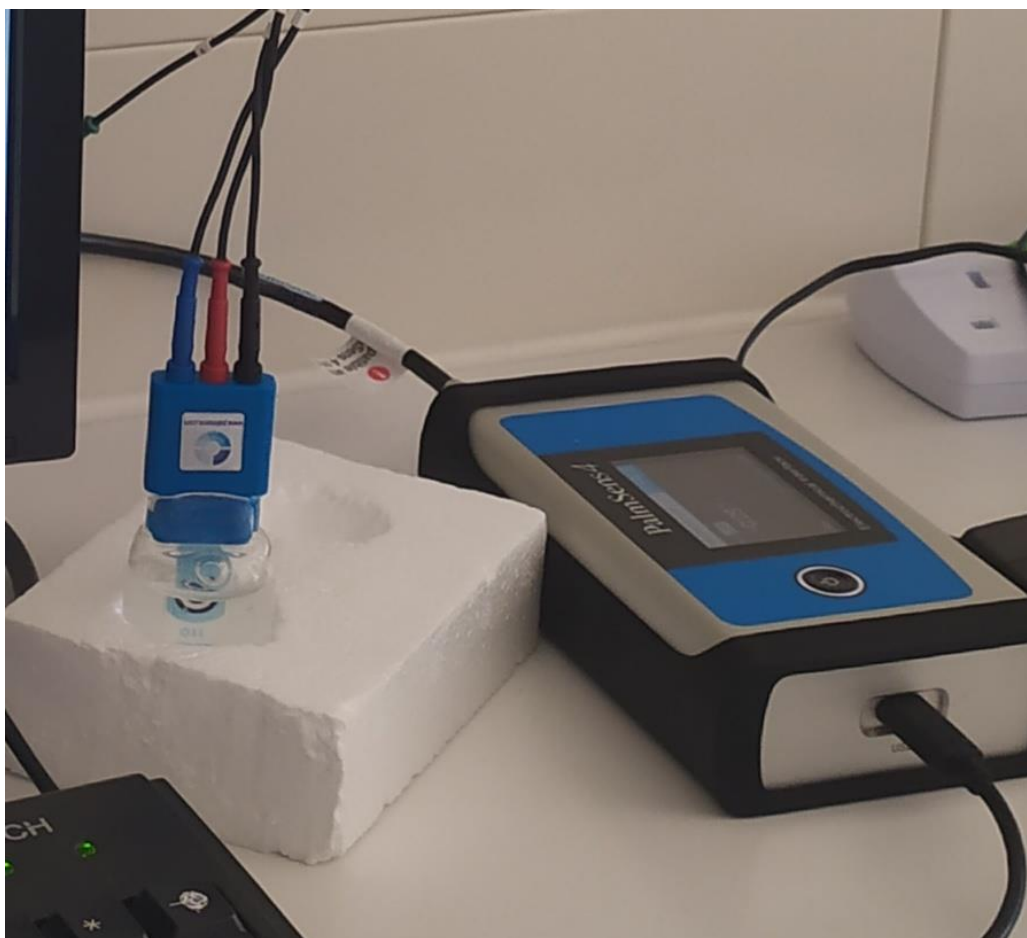


**Figure 3.2:** Electrochemical instrument PalmSens4 Blv

### **3.1.2 Screen printed electrode (SPE)**

Screen printed electrode is used due to its good conductivity, suitable for the experiment, sensitivity and simple to measurement of electrochemical reaction. This electrode is designed with compact of three electrodes which are RE, WE and CE shown on Figure 3.3. The chemical reduction and oxidation reactions take place on the working electrode which the desirable current is measured on it.

The reference electrode is used to provide the potential across the working electrode and make stable between the working electrodes. The auxiliary/counter electrode low resistance and the current flow through this wire else round other electrodes which the current needs

low resistance flow into the cell. The counter electrode is used as current supply between the working electrodes.



**Figure 3.3:** Screen printed electrode

## **3.2 Methods**

### **3.2.1 Purification of silk fibroin**

#### **3.2.1.1 Cleaning process**

The silk is natural abundant protein, nontoxic purify and is obtained from silkworms and it produces the final product of silk fibroin protein through the scientific silk fibroin preparation steps. The cocoons are cheap and they can be purchased from local markets. The surface of the silk cocoons may have unwanted insects and materials like pupa, dust, impurities, and other foreign particles that may affect the result of the experiment so, these parts must be cleaned before cutting into pieces for the next degumming process shown on Figure 3.4.



(a) Silk cocoons



(b) Cut into pieces

**Figure 3.4:** Silk cocoons and cutting into pieces

### 3.2.1.2 Degumming process

Silk degumming is the process of eliminating the glue protein and sticky substance called sericin which is a glue/gum bond together the silk fiber which have an effect on material characteristics of silk fibroin was shown in Figure 3.5.

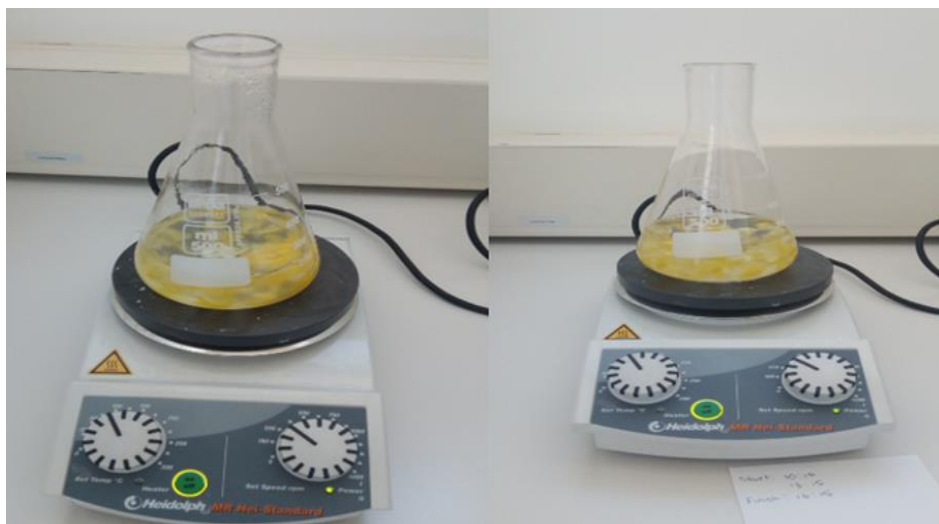


**Figure 3.5:** Degumming of silk cocoons with 0.1M  $\text{Na}_2\text{CO}_3$  solution

The most common method in degumming is to remove and eliminate the sericin by sodium carbonate. The sericin protein which is the glue-like substance cover or coat the fibroin which can be removed by the thermochemical treatment of the cocoons, which is also known as degumming (Melke et al., 2016).

For the preparation of the sodium carbonate solution; weighed 12grams of sodium carbonate and mixed with 200ml deionized water and then mixed with using the magnetic stirrer to dissolve in homogeneously. Weighed 2-grams of cut silk cocoons and inserted into the flask and then added 200ml of sodium carbonate solution into the flask.

Using electro-spurned magnetic stirrer with 75°C for three hours and three rounds. The sodium carbonate solution was changed at each round for three times. and the silk was washed with deionized water more than 3 times in each round up to the yellow color disappear and the residue of deionized water clear enough each. After the degumming process for three hours and three rounds, unbounded the fibers into too small as much as possible for easily dissolution takes place then put into a small petri dish overnight to dry the fiber. The next step was dissolution.

### **3.2.1.3 Dissolution process**

The silk of cocoon *B.moxi* mainly two protein components, sericin is the water soluble substance that hold the silk fiber together and the fibroin is the water insoluble protein components which accounts for cocoons 70% . The glue and sticky substance was removed by the degumming process.

The dried silk fiber mixed with together the strong electrolyte solution. The dissolution process was done by measured in the ratio of in the ration of CaCl<sub>2</sub>: C<sub>2</sub>H<sub>5</sub>OH: nH<sub>2</sub>O (Calcium chloride (27.79gram), ethanol (29.13ml), deionized water (36ml)) at 75<sup>oc</sup> with continuous stirring until the total dissolution. By altering the W/V (weight of the fiber to the volume of electrolyte solution) different aqueous silk fibroin concentrations can be obtained and the dried fibers mix together then the silk fibers changed into solution.

### 3.2.1.4 Dialysis process

Dialysis is the process by which salt is removed from a liquid silk fibroin protein solution, and the final steps for the purification of a pure silk fibroin solution. The silk fibroin solution is poured into a dialysis tube and then used in larger beakers that are totally immersed in the dialysis tube and filled with deionized water.

The dialysis process was done for 48 hours with the deionized water being changed every three hours. After 48 hours of dialysis, the pure silk fibroin solution was extracted from the dialysate by using a large syringe and then poured into a bottle, as shown in Figure 3.6.



**Figure 3.6:** Purification method of pure SF protein

### 3.2.1 Preparation of phosphate buffer saline solution (PBS)

Phosphate buffer saline solution (PBS) helps to maintain a stable and constant pH. The ion concentration and osmolality of the solution commonly matches those of the human body (isotone). It is isotonic and nontoxic to the cells. It is used to dilute substance for the preparation of 1L of 10mM PBS solution.

**Table 3.1:** Contents of PBS

| Chemicals                        | Concentration g/L | Concentrations Mmole/L |
|----------------------------------|-------------------|------------------------|
| NaCl                             | 8                 | 137mM                  |
| KCl                              | 0.2               | 2.7mM                  |
| Na <sub>2</sub> HPO <sub>4</sub> | 1.44              | 10mM                   |
| KH <sub>2</sub> PO <sub>4</sub>  | 0.24              | 2mM                    |

Start with 800ml of distilled water and added all the chemicals listed on the table and added distilled water to a total of volume of 1L shown on Table 3.1. Dispensed the solution into aliquots and sterilized by autoclave (20 min, 121° c, liquid cycle) and stored at room temperature

### 3.2.2 Preparation of silk fibroin micro particles

Nanoparticles have played an enormously importance in the construction and designing of electrochemical biosensors. The micro particles increase the surface area which the oxidation-reduction takes place, reduce the capacitive current, increase the sensitivity and selective performance of a biosensor. Figure 3.7 was shown the extraction of micro particles of SF.

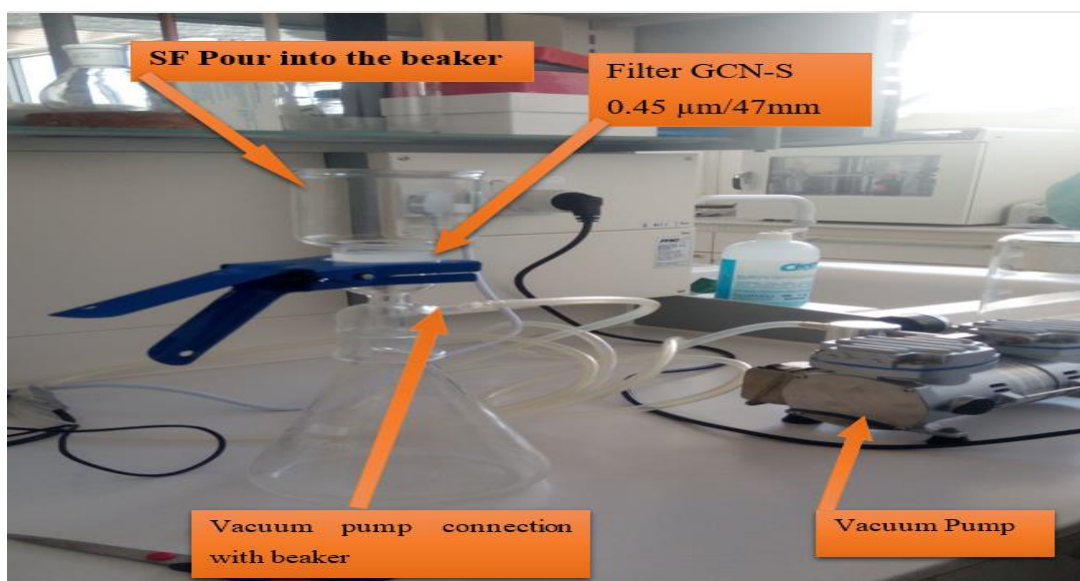


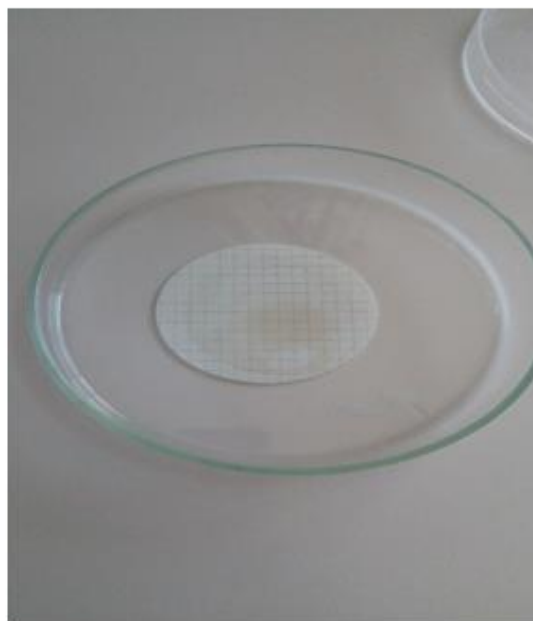
**Figure 3.7:** Extraction method of SF micro particles

The silk fibroin was obtained from the silk cocoons through the silk purification steps in silk degumming with sodium carbonate, dissolution with an electrolyte solution and dialysis process. The micro particles of silk fibroin were extracted from the pure silk fibroin solution using the vacuum pump and special filters. Micro particles of silk fibroin were purified through the following steps.

- 1) The vacuum pump connected with vacuum chambers, at the top of the funnel put the type of filter GCN-S 0.45 $\mu\text{m}$ /47mm, poured the pure SF solution into the beakers tubes, turned on the vacuum pump at 400mmHg or 53.329Kpa and then waited until the solution parts totally drained out.
- 2) The SF micro particles were left at the top of the filter and let off the vacuum pump.
- 3) The SF micro particles then carefully were collected from the surface of the filter and mixed with phosphate buffer solution (PH = 7.0) with a magnetic stirrer at 250 rpm shown on Figure 3.8.



(a) Magnetic stirrer mixing SNP



(b) Filter GCN-S 0.45 $\mu$ m/47mm

**Figure 3.8:** SF micro particles mixing with PBS solution and filter

### 3.2.3 Connection of the screen-printed electrode

The compact screen-printed electrode mounting on the device of voltammetry cell kit which holds the analyte was used. The screen-printed electrodes have been designed for a single use only. The design consists of the three electrode wires on the surface and with connectors and screen printed slotted card.

The slotted card have USB connector which make electrical connection between the Palmsens4 devices with the electrolyte and analyte. To connect the SPE with slotted card plugin the carbon electrode in the USB slotted features and the at the top of the connectors three hole with color labeled to connect with palmsens4 devices wires i.e. working, reference and counter electrode shown on Figure 3.9.

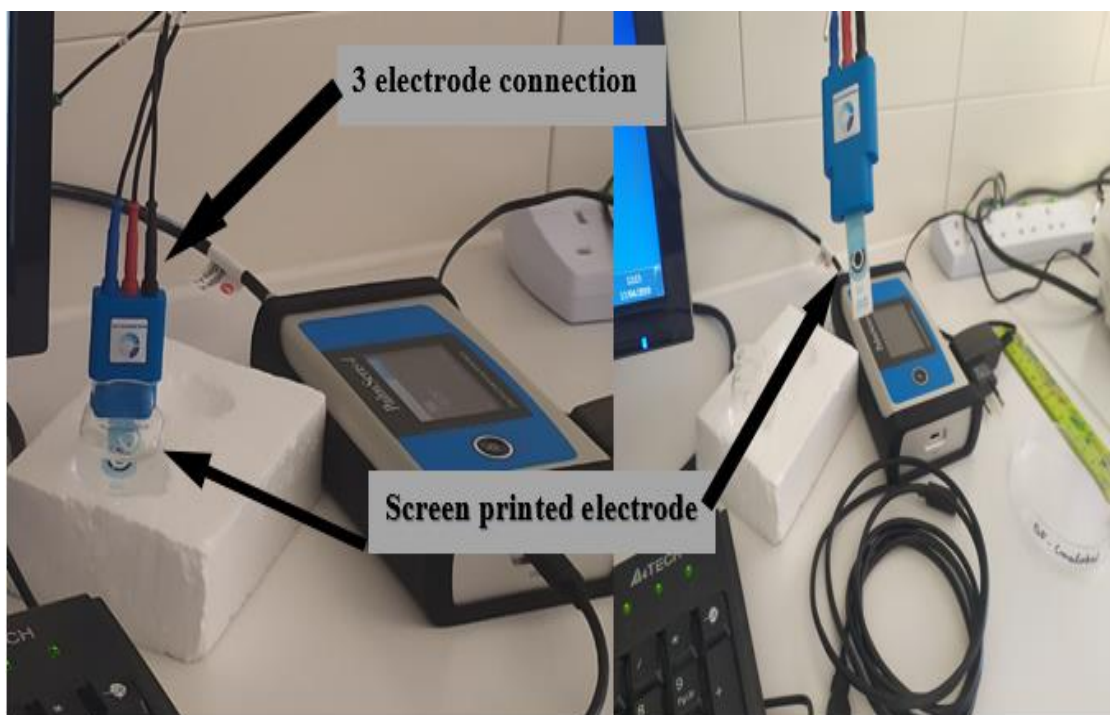


**Figure 3.9:** Mounting screen-printed electrode on the cell kit

### 3.2.4 Construction of H5N1 biosensor on the screen-printed electrode

The immobilization of H5N1 antibody conducted through the following techniques to detect the antigen of H5N1 using electrochemical measurement techniques with cyclic voltammetry and chronoamperometry. Prepared 0.4243gram of 0.385ml SF solution and SF/x-link film. The density of silk fibroin solution was 1.10g/ml. Prepared sterilized, cleaned dried 10 petri dish shown on Figure 5.10 and labeled with:

1. Unused SPE (C4, A4, C5)
2. SF film was immobilized with 6 drops (385 $\mu$ l) (A1, A2,A3,A5, C3)
3. Immobilized SF/x-linked A drop (C1,C2)
4. Dry overnight

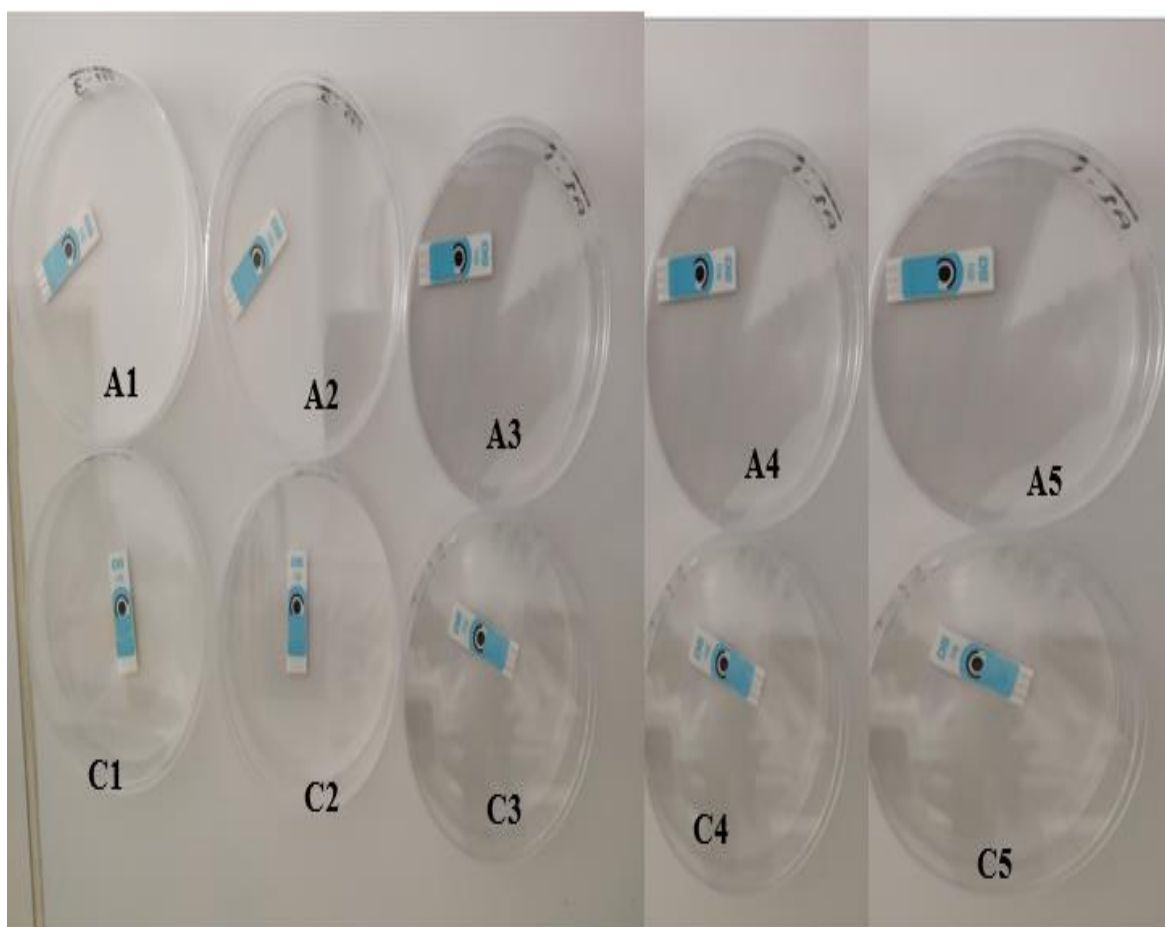


**Figure 3.10:** SPE electrodes for the construction of H5N1 biosensor

The techniques achieved with layer by layer disposition of silk fibroin film, SF/x-linked film with antibody of H5N1 respectively. A SPE consists of the three electrode (RE, WE, and CE) and SF immobilized with H5N1 antibody on the SPE in order to improve and detect impedance of conductivity of the electrode.

The central reading zone of those electrodes are at their center where we modified SF film and SF/x-linked film for detecting the antigen of H5N1 from the analyte through the techniques of cyclic voltammetry and chronoamperometry.

### 3.2.5 Preparation antibody of H5N1

Monoclonal Anti-C-10orf54 antibody produced in mouse clone ORF.4 was used in the designing of this biosensor. The antibody immobilized on to the screen-printed electrode after cross-linked with SF. The screen-printed electrodes left to dry an overnight and 25  $\mu$ l of antibody was put on to the electrodes. The monoclonal antibody concentration was 1.0 mg/mL. The solution was diluted with 10Mm PBS solution before used. The antibody solution was prepared by using 10 $\mu$ l of H5N1 antibody and 40 $\mu$ l of 10mM PBS. After preparation of this antibody solution, 25 $\mu$ l of antibody solution was used for each screen-printed electrode on Figure 3.11 (A1, A5, C1). The electrodes were left for couple of hours for drying.

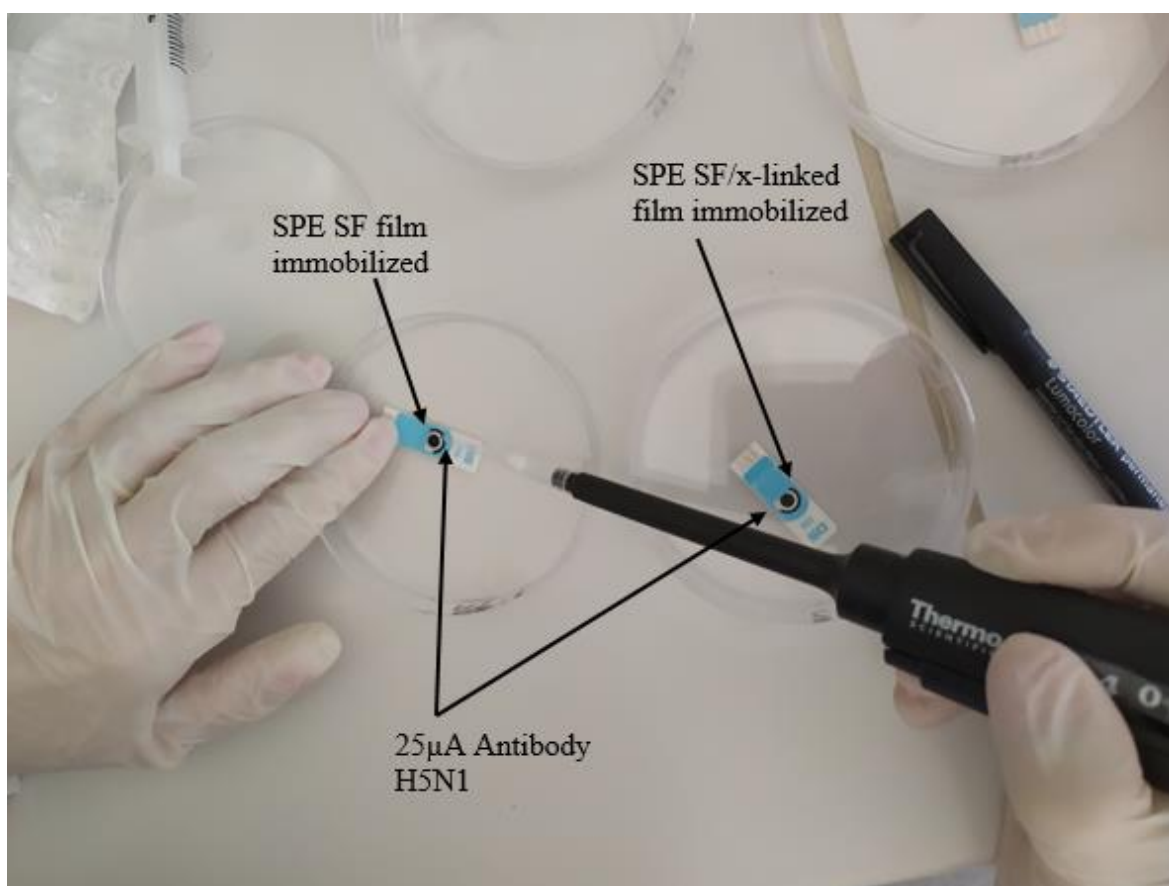


**Figure 3.11:** Immobilization of H5N1 on to the SPE

### 3.2.6 Preparation of H5N1 inactivated antigen

H5N1 inactivated antigen ( A/Ck/Scot/59 (H5N1) inactivated antigen, APHA Scientific, UK) was used in this study. Before use, 1ml of the antigen was reconstituted with 1ml sterilized distilled water. The excessive antigen was stored at 2-8°C for up to one week until use. In order to obtain the accurate concentration of antigen, we added one more ml distilled water to the solution. We had a 2ml H5N1 antigen solution at the end. We used 400  $\mu$ l of specimen from that solution which involved 150  $\mu$ l H5N1. The measurements took place in a special glass chalet of Palm Sens potentiostats. The glass chalet can take in 17.5 ml solution. So, we preferred to put 16.6 ml PBS (ph:7.4) and 400  $\mu$ l of antigen solution before measurements. The methods shown on Figure 3.12, measurements of characterization of CV and CA for PBS solution, PBS solution with SF film, SF/x-linked , antibody and inactive antigen of H5N1 and Figure 3.13, indicted methods of detection of H5N1.

### 3.2.7 Method 1: Characterization of CV and CA

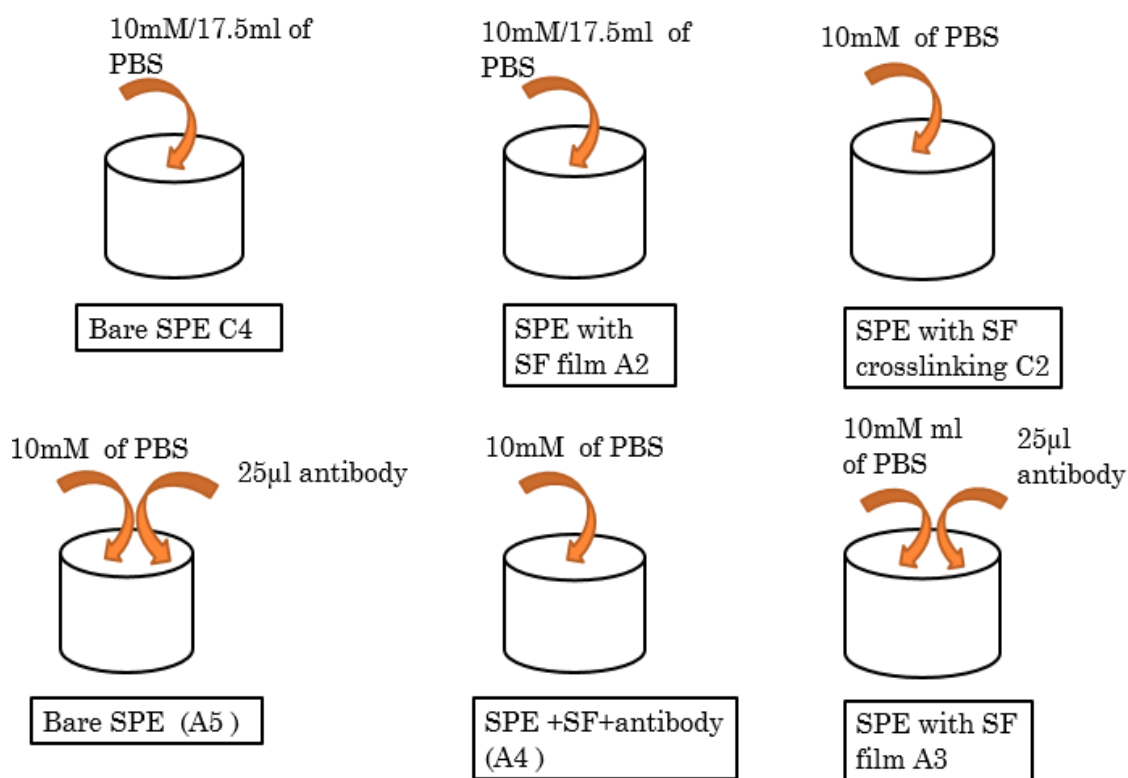


**Figure 3.12:** Characterization using CV and CA

### 3.2.8 Method 2: Detection of H5N1 using CV and CA

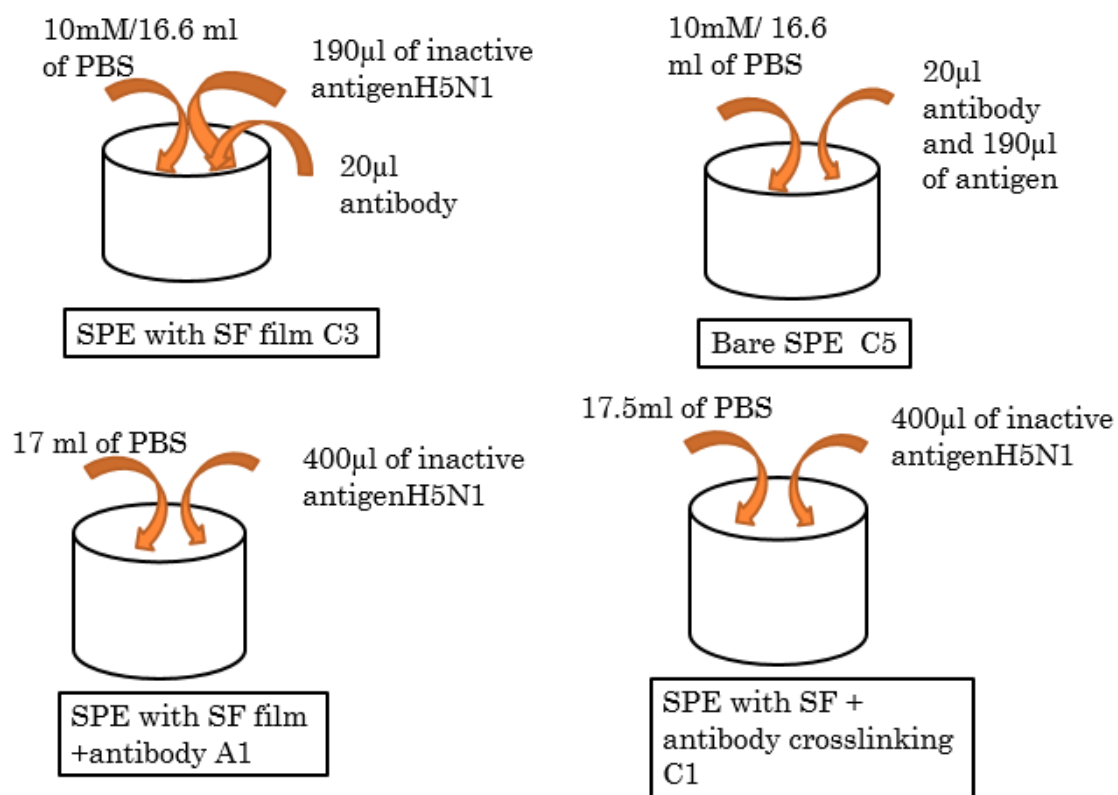


**Figure 3.13:** Detection of H5N1 using CV and CA

### 3.2.9 Setup Devices

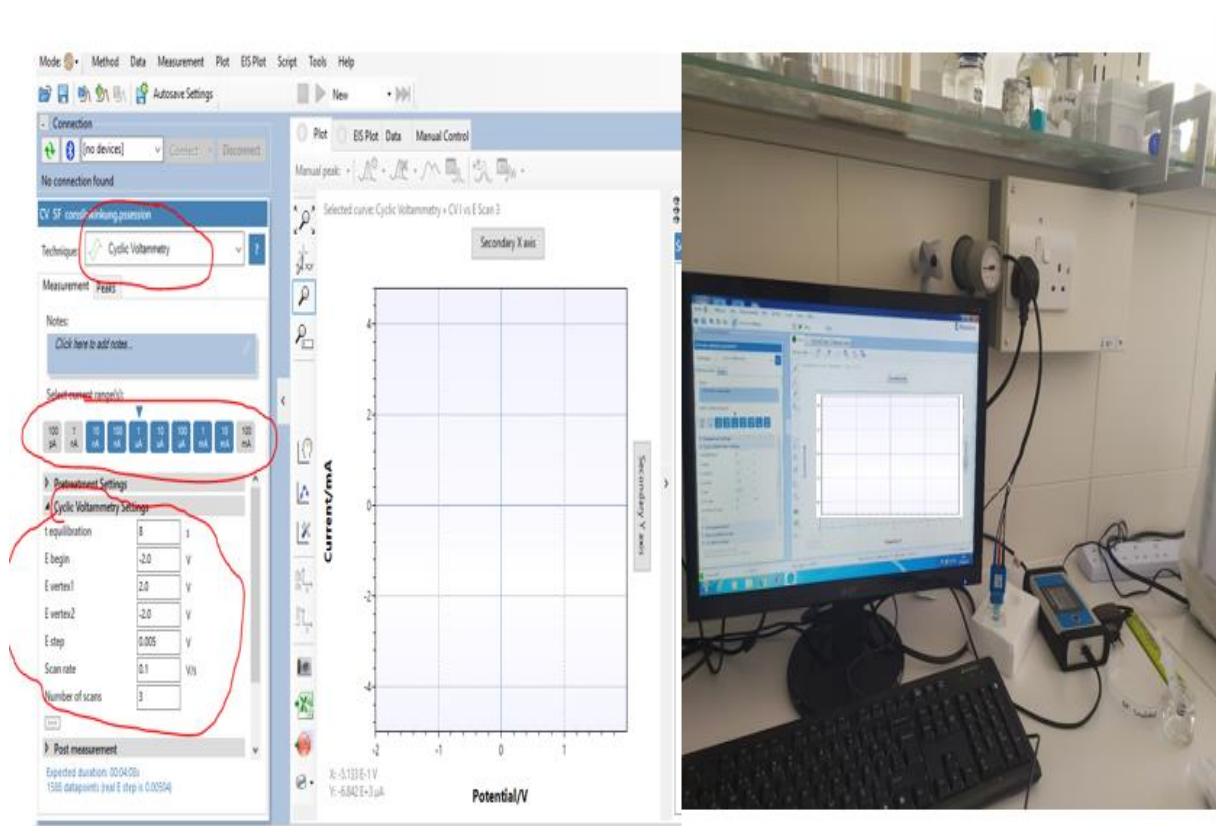


Figure 3.14: Plam Sens4 and configuration of software PSTrace 5.5

### 3.2.10 Electrochemical measurements

The electrochemical measurement techniques were achieved by using Palm Sens4, potentiostat–Netherlands. The SPE were configuration applied to the slotted jack with color labeled arrangement. Cyclic voltammetry (CV), chronoamperometry (CA) measurements were achieved in the presence 10mM PBS (pH 7.4) with using coated and uncoated screen printed electrode to control and detect the of H5N1 antigen. The CV scan cycled potential from -0.4 V to 0.7 V with a scan rate of 0.1 V/s shown on Figure 3.14. The chronoamperometry procedures, constant DC potential of 1.4v and with sampling t interval 0.1 seconds were used.

## **CHAPTER 4**

### **RESULTS AND DISCUSSION**

#### **4.1 Cyclic Voltammetry and Chronoamperometry Analysis**

Cyclic voltammetry is an electrochemical analysis method to provide a biological information from the unknown sample. Cyclic voltammetry techniques supply selected potential  $V_1$  and  $V_2$  to measure the current produced from the reaction. The cyclic voltammetry is a cyclic to scan the forward and reverse reaction to determine the current at which in the cathode and anode peaks with respective of the potential.

Chronoamperometry measurement was obtained by applying constant DC potential. The current sampled in each time of interval to record the current at the working electrode. During the measurement of the current with time, the current gradually decreases due to the redox species diminished with time and at a time the oxidation and reduction appeared current show a spike with high faradic current.

The current produced in the reaction directly proportional to the amount of unknown analyte in the given sample. In this method the current had the faradic and capacitive current parts. The faradic current produced the movement of electron during the selected potential applied to the electrolyte solution and the capacitive current produced when the electrolyte solution and the electrode create a charge between them and it develops the barriers and that depletion layer acting as capacitive.

In this experiment, uncoated SPEs, SF film, SF/x-linked film coated and SF coated SPEs which have been immobilized with antibody of H5N1 were measured by using CV.

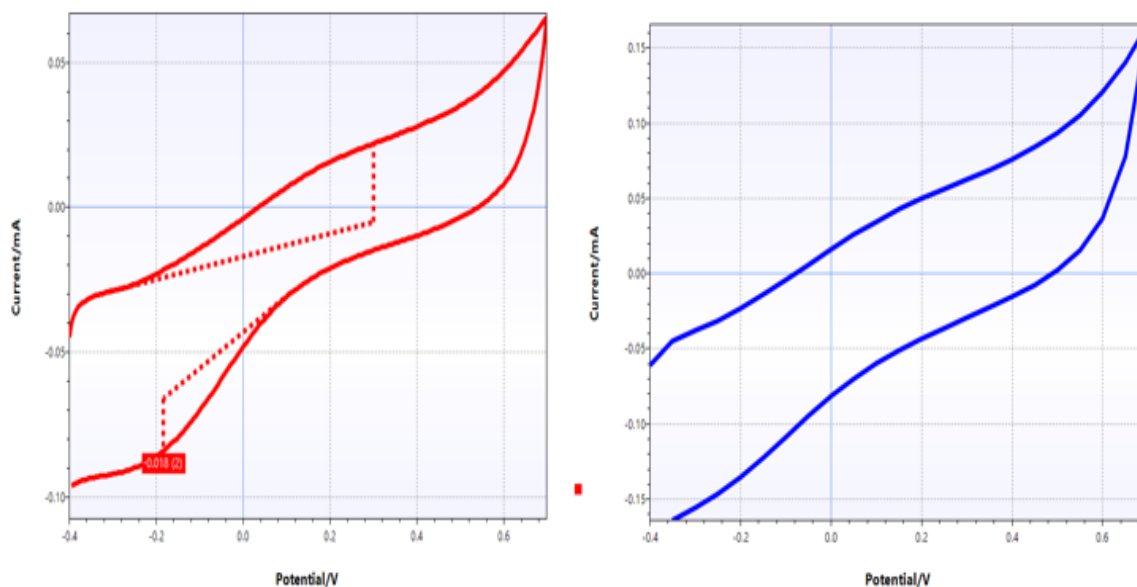
##### **4.1.1 Characterization using platinum as a working electrode**

Platinum wire were used as WE and CE to measure the characteristics of PBS solution and silk fibroin solution in each procedure. The platinum wire is less resistance to conduct the current to the solution. The current supplied across with the working and counter electrode

to measure the response of the solution and the produced current at the working electrode observed by CV and CA electrochemical measurement techniques. These methods are used for the characterization of the PBS buffer solution and silk fibroin solution. The behavioral response of each sample at the oxidation and reduction peaks with respect to supply potential are analyzed.

Figure 4.1 (b) shows the CV graph of the PBS buffer solution. The buffer solution has very small electrons due to that may have small or may have no reduction and oxidation peaks observed in the experiment. During applied a potential the movements of electrons produced have been detected by and transferred into the system to display the graph. The graph shown on the Figure 4.1 (b) has no peaks of oxidation and reduction. At Figure 4.1 (a) the PBS buffer solution with SF were the reduction and oxidation peaks that have been observed. This indicated that, the silk fibroin improves the sensitivity of the platinum wire and transfer the electrons produced during in the reduction and oxidation reactions. The peaks of at the anode and cathode potential were observed at ( $E_{pa} = 0.3v$  and  $E_{pc} = -0.183v$ ) and the current of peaks at the anode and the cathode was observed at  $I_{pa} = 0.269\mu A$  and  $I_{pc} = -0.793\mu A$  respectively shown on Table 4.1.

The chronoamperometry analysis at Figure 4.2 indicated that, the current produced in the working electrode and decayed with time. The buffer solution produced less current and decayed with time at Figure 4.2 (lower line) whereas, the buffer solution with silk fibroin shown at Figure 4.2 (upper line) almost produced high current at the working electrode and decayed with time. This indicated that, the silk fibroin improves the sensitivity of platinum wire electrode, because of the tyrosine amino acid present on the backbone of the polypeptide has oxidizing properly.



(a) CV analysis of SF PBS buffer solution

(b) CV analysis of PBS solution

**Figure 4.1:** Characterization of PBS buffer and Sf (3% w/v) solutions with platinum electrode

**Table 4.1:** Peaks data of CV silk fibroin analysis

| Peak               | Potential/V | Height/ $\mu$ A |
|--------------------|-------------|-----------------|
| PBS + silk fibroin |             |                 |
| Oxidation scan     | 0.29996     | 26.9382         |
| Reduction scan     | -0.18348    | -17.9344        |

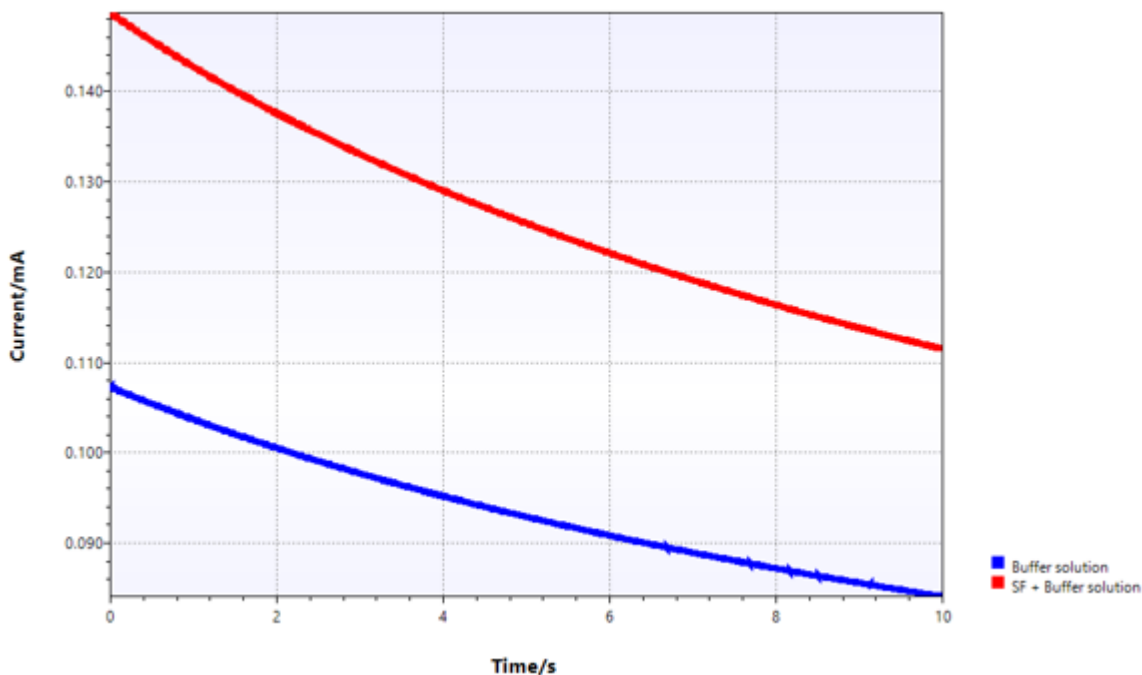


**Figure 4.2:** Chronoamperometry analysis of PBS buffer and SF solutions

#### 4.1.2 Characterization using screen printed electrode

Disposable single screen-printed electrode (SPE) contains three electrodes (wires) inside the printed design. This wires central circular carbon (Black) as a working electrode, crescent shaped carbon as a counter, and silver color as a reference electrode. This compacted screen printed electrode is easily used for the experiment.

The characterization of PBS solution using SPE is shown on the Figure 4.3 (a). The cyclic voltammetry graph indicate that, SPE has better sensitivity than the platinum wire and it measured the reduction and oxidation peaks properly. The potential peaks of anode and cathode were measured as  $E_{pa}$  0.04 and  $E_{pc}$  -0.15v respectively. The current peaks were produced with respective potentials at  $I_{pa}$  0.074 $\mu$ A and  $I_{pc}$  -0.11 $\mu$ A respectively.

The SF micro improved the sensitivity and increased conductivity of the screen printed electrode as shown on Figure 4.3 (c). The micro particles of silk fibroin increased the surface area and the electron transfer during the reduction and oxidation peaks was increased. This phenomenon has been detected by the cyclic voltammetry measurement when compared

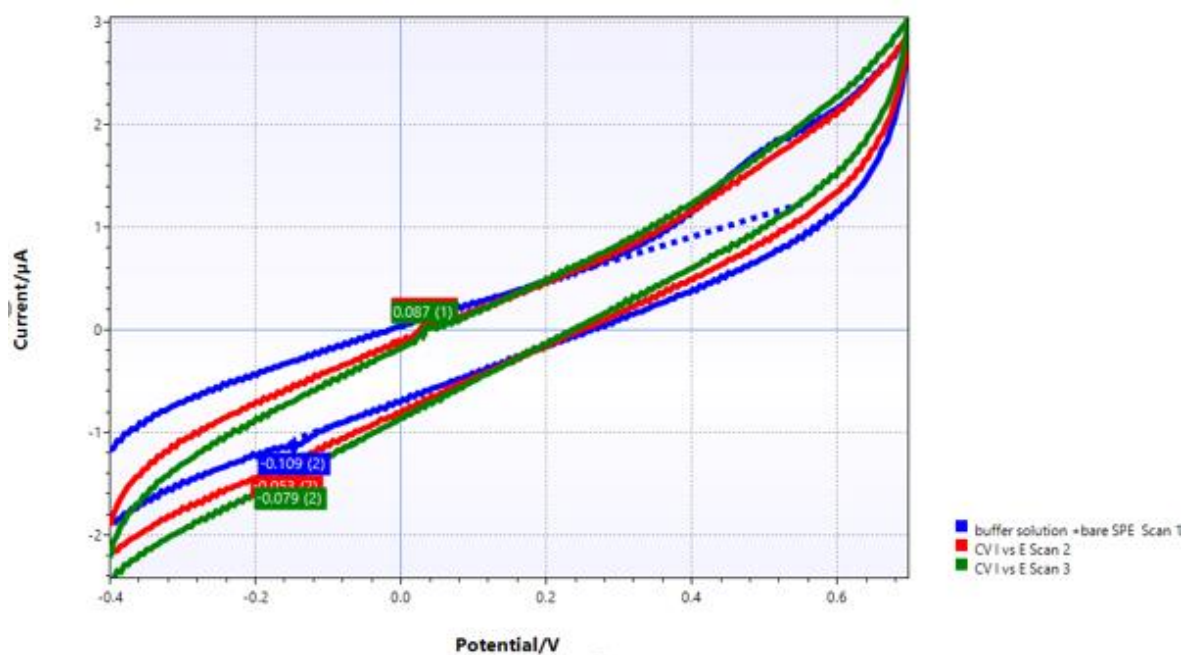
with the PBS buffer solution. The peaks of cathode and anode potentials were  $E_{pa}$  0.028 and  $E_{pc}$  -0.304v. The peaks for the current at anode and cathode were observed  $I_{pa}$  0.075  $\mu$ A and  $I_{pc}$  -7.99  $\mu$ A.

By using the screen printed electrode, the characterization of SF film coated SPE is shown on Figure 4.3 (d). The cyclic voltammetry graph showed that the anode and potential peaks were  $E_{pa}$  0.4258v and the current produced on the anode  $I_{pa}$  was 21.399  $\mu$ A.

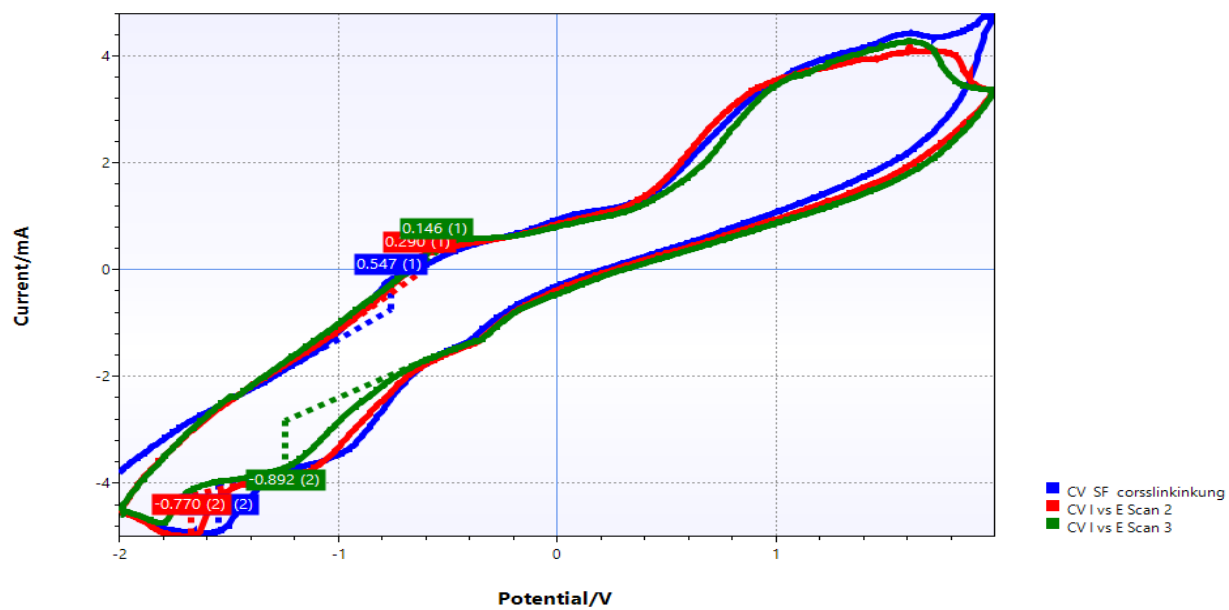
At the same time the SF/x-linked film coated SPE characterization also conducted at (b). The peaks of Potential  $E_{pa}$  -0.76v and  $E_{pc}$  -1.547v and the current peaks  $I_{pa}$  547.075 $\mu$ A and  $I_{pc}$  - 885.740  $\mu$ A shown on Table 4.2.

The chronoamperometry analysis show on Figure 4.4 (a) PBS buffer solution, (b) silk fibroin micro particles, (d) SF film and (c) SF/x-linked film coated. The SF film and SF/x-linked film coated SPE indicated the current was smoothly decay during the process.

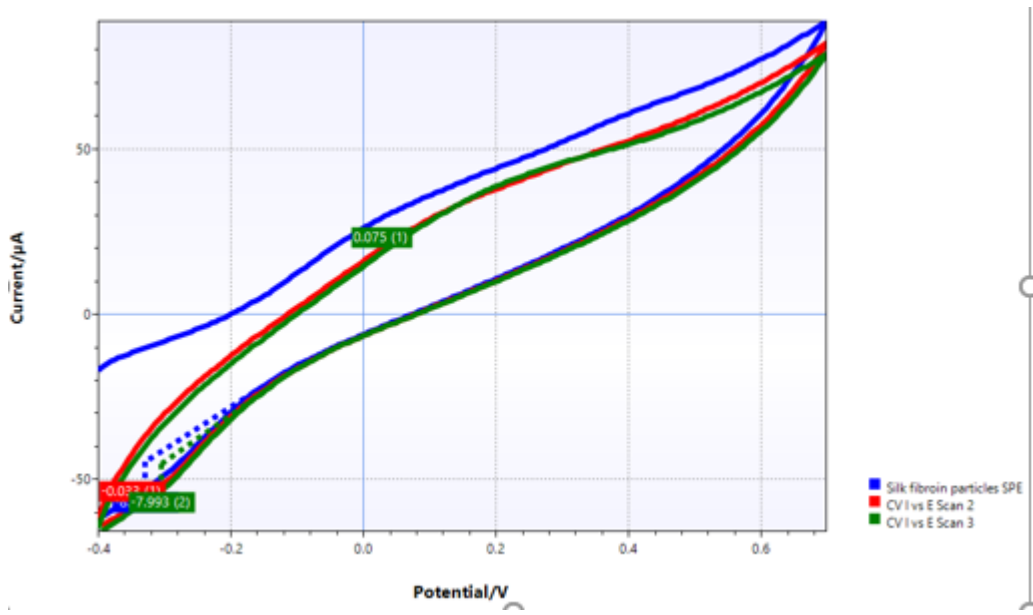
The cyclic voltammetry and chronoamperometry analysis of SF film and SF/x-linked film coated SPE showed good sensitivity and conductivity. Peaks for the modification of screen-printed electrode. The peaks achieved in silk fibroin crosslinking anode current was 547.075 $\mu$ A and cathode current was 891.900  $\mu$ A and at the same time SF film coated SPE achieved the peaks at 21.399  $\mu$ A. The peaks of current observed in this characterization increased and SF/x-linked is a good candidate for the modification of screen-printed electrode.



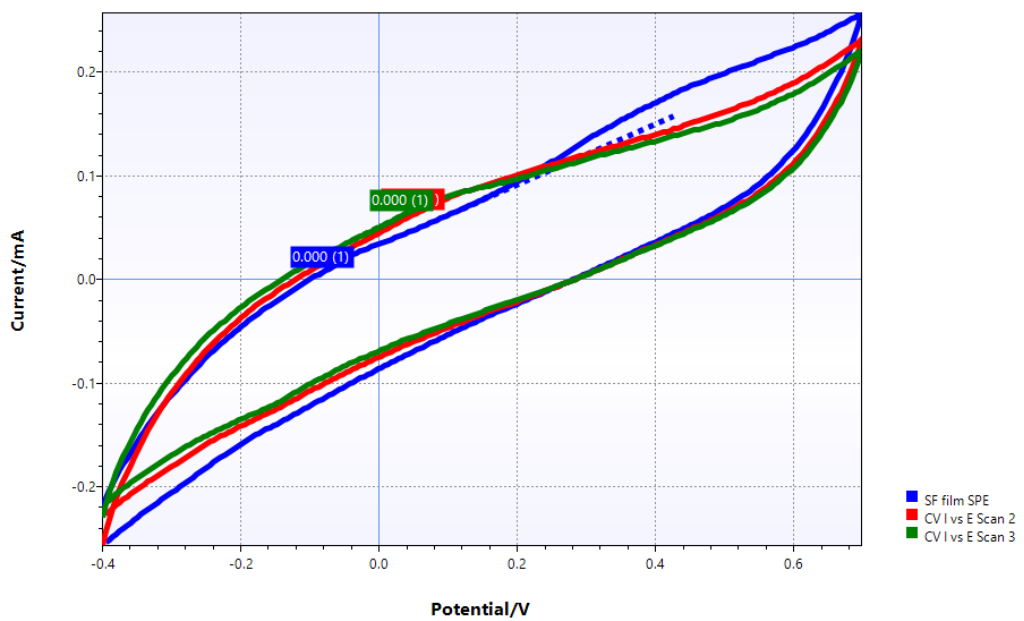
(a) CV response of SPE in PBS solution



(b) CV response SF/x-linked film coated SPE in PBS buffer solution



(c) CV response of SPE SF micro particles in PBS solution

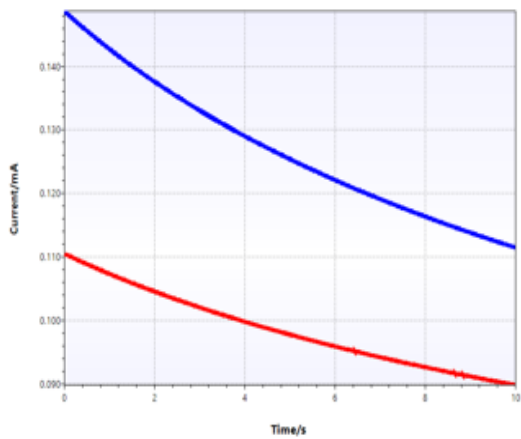


(d) CV response SF film coated SPE in PBS buffer solution

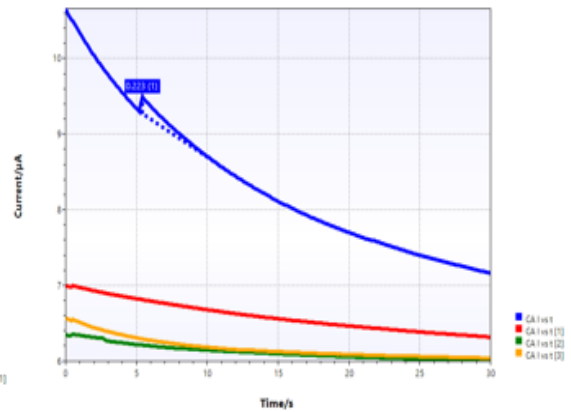
**Figure 4.3:** Cyclic voltammetry characterization

**Table 4.2:** Peaks data of cyclic voltammetry using SPE

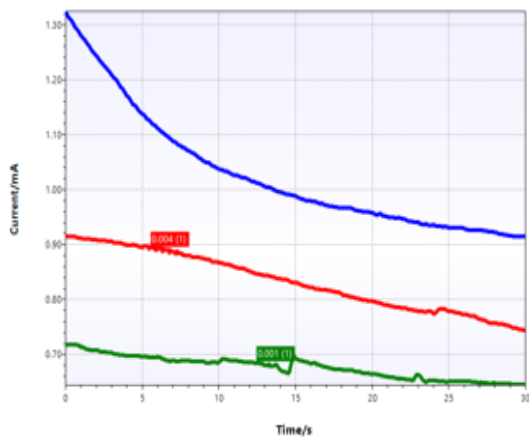
| Peak                        | Potential/<br>V | Height/ $\mu$<br>A | Area/ $\mu$ A<br>V | Width/<br>V | Y<br>Offset/ $\mu$<br>A | Max<br>slope/ $\mu$ A/<br>V | Min<br>slope/ $\mu$ A/<br>V | Sum/ $\mu$ A/<br>V |
|-----------------------------|-----------------|--------------------|--------------------|-------------|-------------------------|-----------------------------|-----------------------------|--------------------|
| PBS solution                |                 |                    |                    |             |                         |                             |                             |                    |
| 1                           | 0.03809         | 0.07456            | NaN                | NaN         | 0.10851                 | 3.99278                     | 2.36471                     | 6.35749            |
| 2                           | -0.14816        | -0.10905           | NaN                | NaN         | -1.06819                | -2.61915                    | -4.40027                    | 7.01943            |
| SF micro particles          |                 |                    |                    |             |                         |                             |                             |                    |
| 1                           | 0.02801         | 0.07490            | NaN                | NaN         | 18.6479                 | 145.272                     | 142.365                     | 287.637            |
| 2                           | -0.30434        | -7.99300           | NaN                | NaN         | -45.3174                | -155.219                    | -217.899                    | 373.119            |
| SF film coated SPE          |                 |                    |                    |             |                         |                             |                             |                    |
| 1                           | 0.42582         | 21.3993            | NaN                | NaN         | 158.243                 | 427.986                     | 297.208                     | 725.194            |
| CV I vs E Scan 2            |                 |                    |                    |             |                         |                             |                             |                    |
| 1                           | 0.04816         | 0.27933            | NaN                | NaN         | 62.1842                 | 355.930                     | 350.064                     | 705.994            |
| CV I vs E Scan 3            |                 |                    |                    |             |                         |                             |                             |                    |
| 1                           | 0.03309         | 0.12948            | NaN                | NaN         | 61.4757                 | 342.417                     | 326.537                     | 668.955            |
| SF/x-linked film coated SPE |                 |                    |                    |             |                         |                             |                             |                    |
| 1                           | -0.76129        | 547.075            | NaN                | NaN         | -738.168                | 5310.55                     | 2531.21                     | 7841.76            |
| 2                           | -1.54684        | -885.740           | NaN                | NaN         | -4018.62                | -819.319                    | -7172.67                    | 7991.99            |
| CV I vs E Scan 2            |                 |                    |                    |             |                         |                             |                             |                    |
| 1                           | -0.62535        | 290.111            | NaN                | NaN         | -53.9637                | 4737.44                     | 2971.93                     | 7709.37            |
| 2                           | -1.67270        | -770.410           | NaN                | NaN         | -4218.78                | -732.635                    | -12769.4                    | 13502.1            |
| CV I vs E Scan 3            |                 |                    |                    |             |                         |                             |                             |                    |
| 1                           | -0.54981        | 145.619            | NaN                | NaN         | 330.283                 | 4136.76                     | 2903.29                     | 7040.04            |
| 2                           | -1.24473        | -891.900           | NaN                | NaN         | -2818.36                | -1761.86                    | -4616.86                    | 6378.71            |



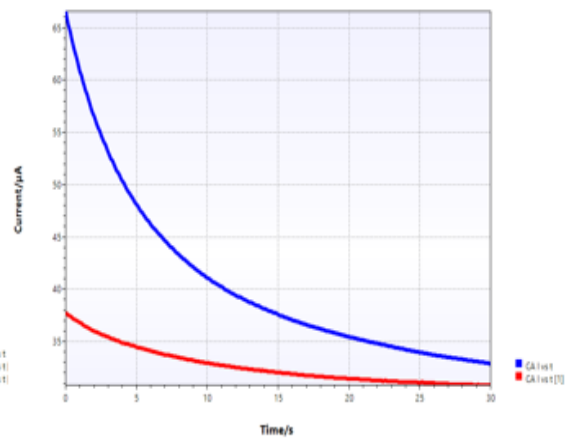
(a) CA graphs of PBS



(b) CA graphs of SF micro particles



(c) CA graphs of SF/x-linked coated SPE



(d) CA graphs of SF film coated SPE

**Figure 4.4:** Chronoamperometry characterization by using SPE

#### 4.1.3 CV analysis of the monoclonal antibody immobilized SF film coated SPE in PBS solution with and without H5N1 antigen

The monoclonal antibody immobilized SF film coated SPE was used for CV analysis is shown on Figure 4.5. The peaks of anode potentials observed at Epa 0.672, without peak of cathode potential. The current peak anode and cathode were at Ipa 116.84  $\mu$ A.

In the second trial 25 $\mu$ l of antibody added in the 16.75ml of PBS. The responses of CV measurements are shown at Figure 6.6. The cyclic voltammetry recorded the anode and cathode peaks as shown on Table 4.4. The CV indicated that, shortages of electron follows in the cell has by observing less current production the cell. This indicated that, immobilization of monoclonal antibody on the surface of film improved the conductivity and sensitivity of the SPE as shown on Figure 4.5.

In the third trial, SF film coated SPE was used and 10  $\mu$ l monoclonal antibody were added the solution of PBS buffer (116.99ml). The cyclic voltammetry response is shown on Figure 4.7. As shown on Table 4.5, the CV analysis indicated that antibodies within the PBS solution has in order to calibrate and characterize the experiment design SPE has been studied to detect as antigen H5N1 in the PBS solution.

#### 4.1.4 Antibody immobilized SF/x-linked film on SPE

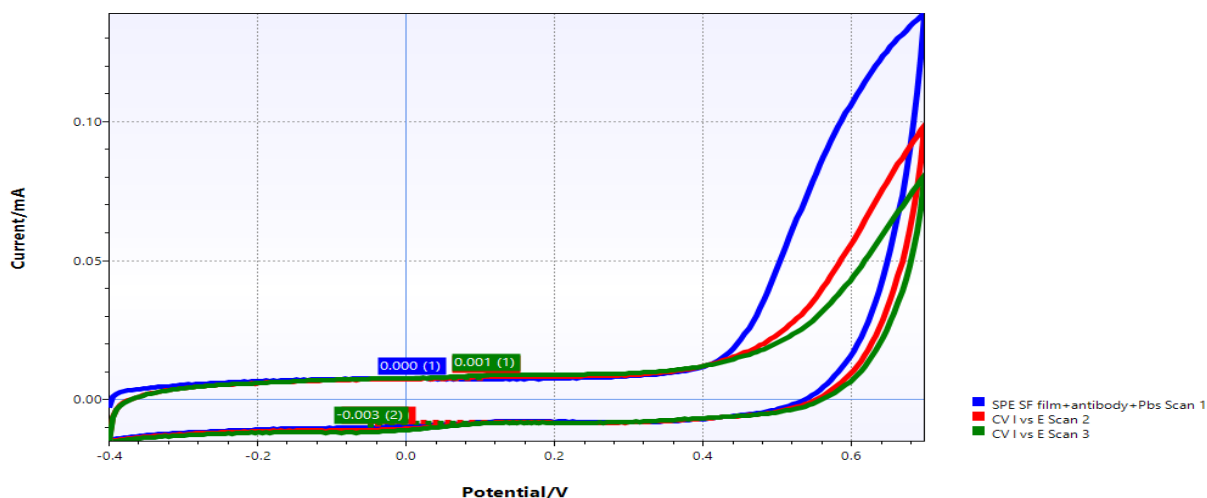


**Figure 4.5:** CV analysis of SPE coated monoclonal antibody immobilized SF film

**Table 4.3:** Data of Figure 4.5

| Peak                            | Potential/V | Height/ $\mu$ A | Area/ $\mu$ A $\cdot$ V | Width/V | Y Offset/ $\mu$ A | Max slope/ $\mu$ A/V | Min slope/ $\mu$ A/V | Sum/ $\mu$ A/V |
|---------------------------------|-------------|-----------------|-------------------------|---------|-------------------|----------------------|----------------------|----------------|
| SPE SF film+antibody+Pbs Scan 1 |             |                 |                         |         |                   |                      |                      |                |
| 1                               | 0.00793     | 0.05868         | NaN                     | NaN     | 7.56001           | -                    | 3.40282E+38          | 6.80565E+38    |
| 2                               | 0.67254     | 116.849         | NaN                     | NaN     | 15.9436           | 668.916              | -1745.24             | 2414.15        |
| CV I vs E Scan 2                |             |                 |                         |         |                   |                      |                      |                |
| 1                               | 0.10863     | 0.47654         | NaN                     | NaN     | 7.77445           | 11.4236              | 4.52643              | 15.9500        |
| 2                               | -0.03738    | -2.87402        | NaN                     | NaN     | -8.05538          | -1.83593             | -26.2155             | 28.0515        |
| CV I vs E Scan 3                |             |                 |                         |         |                   |                      |                      |                |
| 1                               | 0.10863     | 0.89586         | NaN                     | NaN     | 8.04702           | 15.8850              | 2.16950              | 18.0545        |
| 2                               | -0.04746    | -3.25439        | NaN                     | NaN     | -8.40311          | 5.44646              | -31.1642             | 36.6107        |

#### 4.1.5 Unused SPE with 25 $\mu$ l antibody with the PBS solution

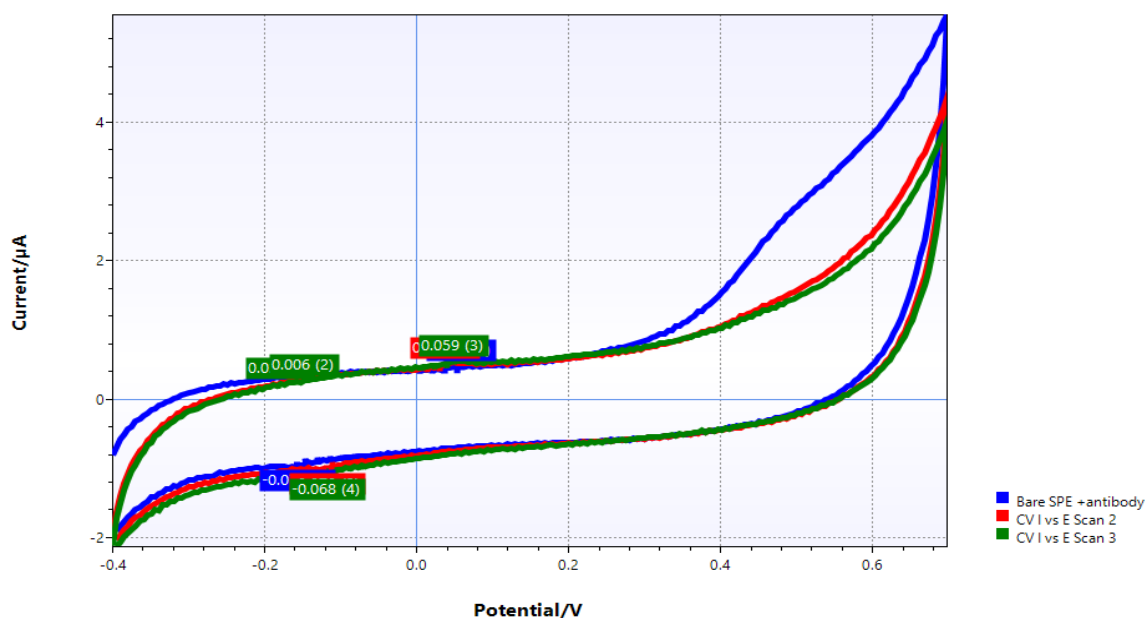


**Figure 4.6:** CV voltammogram for unused SPE with 25 $\mu$ l of antibody with PBS solution

**Table 4.4:** CV analysis date SPE with 25 $\mu$ l of antibody within the PBS as a solution

| Peak                 | Potential/<br>V | Height/ $\mu$<br>A | Area/ $\mu$ A<br>V | Width/<br>V | Y<br>Offset/ $\mu$<br>A | Max<br>slope/ $\mu$ A/<br>V | Min<br>slope/ $\mu$ A/<br>V | Sum/ $\mu$ A/<br>V |
|----------------------|-----------------|--------------------|--------------------|-------------|-------------------------|-----------------------------|-----------------------------|--------------------|
| Unused SPE +antibody |                 |                    |                    |             |                         |                             |                             |                    |
| 1                    | 0.05824         | 0.06473            | NaN                | NaN         | 0.42036                 | 1.61324                     | 0.08833                     | 1.70157            |
| 2                    | -0.15824        | -0.07868           | NaN                | NaN         | -0.90206                | -1.20737                    | -2.36887                    | 3.57624            |
| CV I vs E Scan 2     |                 |                    |                    |             |                         |                             |                             |                    |
| 1                    | 0.03809         | 0.04965            | NaN                | NaN         | 0.45886                 | 1.36057                     | 0.83732                     | 2.19789            |
| 2                    | -0.11801        | -0.07006           | NaN                | NaN         | -0.95936                | -1.07006                    | -3.06495                    | 4.13501            |
| CV I vs E Scan 3     |                 |                    |                    |             |                         |                             |                             |                    |
| 1                    | -0.17840        | 0.02250            | NaN                | NaN         | 0.19254                 | -3.40E+38                   | 3.40E+38                    | 6.81E+38           |
| 2                    | -0.14816        | 0.00632            | NaN                | NaN         | 0.26352                 | -3.40E+38                   | 3.40E+38                    | 6.81E+38           |
| 3                    | 0.04816         | 0.05859            | NaN                | NaN         | 0.49294                 | 2.24219                     | 1.25607                     | 3.49827            |
| 4                    | -0.11801        | -0.06844           | NaN                | NaN         | -1.04486                | -1.63309                    | -3.04343                    | 4.67651            |

#### 4.1.6 SF film coated SPE and 25 $\mu$ l antibody within the PBS solution

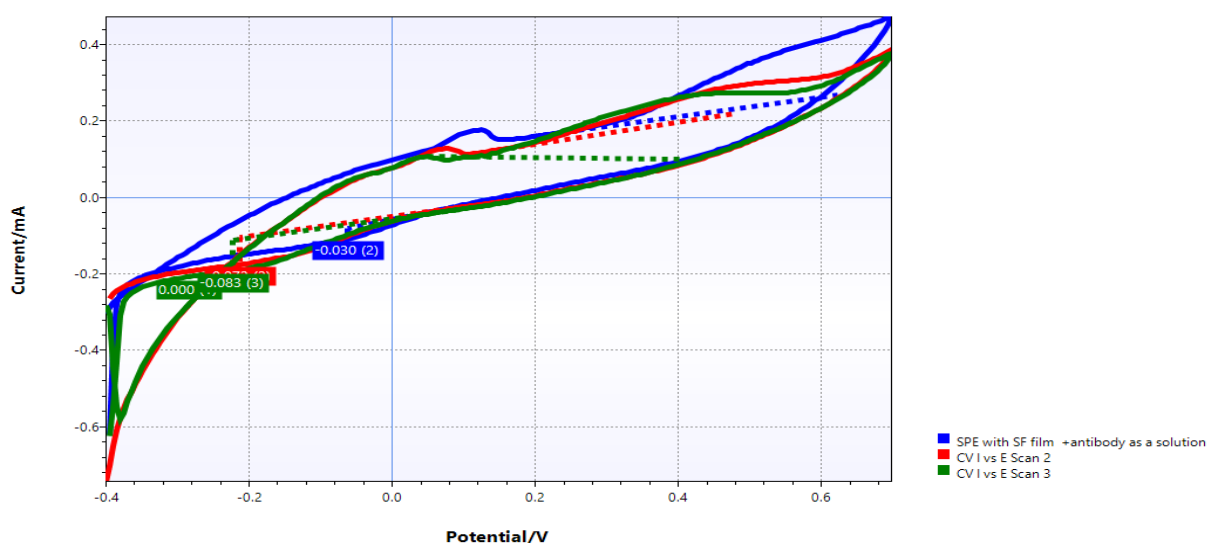


**Figure 4.7:** CV voltammogram of SF film coated SPE and 25 $\mu$ l antibody within a PBS solution

**Table 4.5:** CV SF film coated SPE and 25 $\mu$ l antibody within a PBS solution

| Pea k                                    | Potential/V | Height/ $\mu$ A | Area/ $\mu$ A V | Width/V | Y Offset/ $\mu$ A | Max slope/ $\mu$ A/V | Min slope/ $\mu$ A/V | Sum/ $\mu$ A/V |
|--|-------------|-----------------|-----------------|---------|-------------------|----------------------|----------------------|----------------|
| SPE with SF film +antibody as a solution |             |                 |                 |         |                   |                      |                      |                |
| 1  | 0.62223     | 157.507         | NaN             | NaN     | 267.211           | 936.018              | -2820.81             | 3756.83        |
| 2  | -0.06262    | -30.4728        | NaN             | NaN     | -79.5082          | -390.539             | -654.107             | 1044.65        |
| CV I vs E Scan 2                         |             |                 |                 |         |                   |                      |                      |                |
| 1  | 0.47621     | 71.3500         | NaN             | NaN     | 219.720           | 633.236              | 304.964              | 938.200        |
| 2  | -0.21363    | -71.8088        | NaN             | NaN     | -104.400          | 1484.00              | -2153.85             | 3637.85        |
| CV I vs E Scan 3                         |             |                 |                 |         |                   |                      |                      |                |
| 2  | 0.40566     | 163.776         | NaN             | NaN     | 100.014           | 948.872              | -2055.55             | 3004.42        |
| 3  | -0.22371    | -82.7561        | NaN             | NaN     | -112.259          | 1546.37              | -2055.55             | 3601.92        |

## 4.2 Potassium Ferricyanide

The sensitivity silk nanoparticles conducted with one of the redox species of 2.5mM potassium ferric cyanide and three scan with electrochemical analysis devices of plamsens4. The cyclic voltammetry of the first scan observed at potential anodic oxidation peaks (E<sub>pa</sub>) 0.32012v and anodic current peak (i<sub>pa</sub>) or height 9.41550 $\mu$ A. The reduction peaks observed at potential cathode peak (E<sub>pc</sub>) -0.19856v and the cathode current peak (I<sub>pc</sub>) -7.93988 $\mu$  A shown on Figure 4.8.

The second scan anodic potential E<sub>pa</sub> 0.28988v and anodic current i<sub>pa</sub> 3.42031 $\mu$ A and cathode potential E<sub>pc</sub> -0.22897v and cathode current i<sub>pc</sub> 9.36560 $\mu$ A. The third scan anodic potential E<sub>pa</sub> 0.27481v and anodic current i<sub>pa</sub> 2.67929 $\mu$ A and cathode potential E<sub>pc</sub> -0.21363v and cathode current i<sub>pc</sub> -9.65135 $\mu$ A. The redox species clearly show the peaks and the cyclic of the graph because the species have more electrons than the PBs solution shown on Figure 4.8.

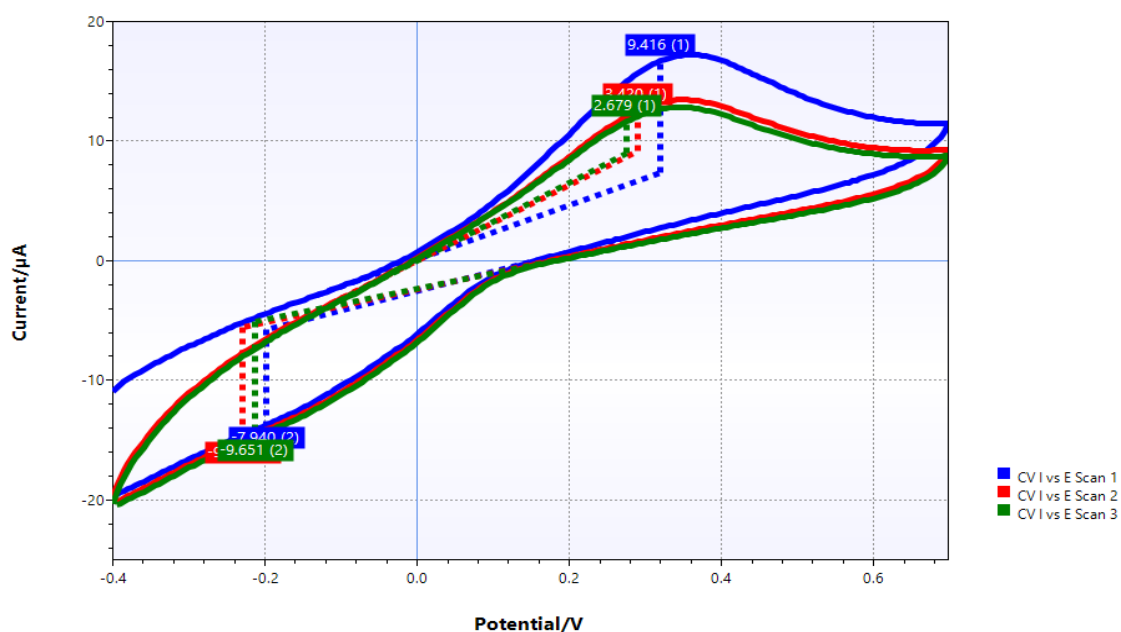


**Figure 4.8:** CV analysis of potassium ferric cyanide

**Table 4.6:** Peaks data of Figure 4.8

| Peak             | Potential /V | Height/ $\mu$ A | Area/ $\mu$ A<br>V | Width/V | Y Offset / $\mu$ A | Max slope / $\mu$ A/V | Min slope / $\mu$ A/V | Sum/ $\mu$ A/<br>V |
|------------------|--------------|-----------------|--------------------|---------|--------------------|-----------------------|-----------------------|--------------------|
| CV I vs E Scan 1 |              |                 |                    |         |                    |                       |                       |                    |
| 1                | 0.32012      | 9.41550         | NaN                | NaN     | 7.33850            | 61.5297               | -71.8355              | 133.365            |
| 2                | -0.19856     | -7.93988        | NaN                | NaN     | -5.78712           | 61.5297               | -71.8355              | 133.365            |
| CV I vs E Scan 2 |              |                 |                    |         |                    |                       |                       |                    |
| 1                | 0.28988      | 3.42031         | NaN                | NaN     | 9.17129            | 49.1649               | 31.9851               | 81.1500            |
| 2                | -0.22879     | -9.36560        | NaN                | NaN     | -5.55730           | 49.1649               | -63.9913              | 113.156            |
| CV I vs E Scan 3 |              |                 |                    |         |                    |                       |                       |                    |
| 1                | 0.27481      | 2.67929         | NaN                | NaN     | 8.96151            | 46.6395               | 33.0926               | 79.7321            |
| 2                | -0.21363     | -9.65135        | NaN                | NaN     | -5.09795           | 46.6395               | -62.0463              | 108.686            |

### 4.3 Antibody- Antigen Concentration

In this experiment the monoclonal antibody of H5N1 (Monoclonal Anti-C 10orf 54 antibody produced in mouse clone ORF.4, Sigma-Aldrch USA) immobilized on the silk fibroin cross linked screen printed electrode. The antibody is a bio receptor element immobilized in specifically to the H5N1 which is designed to bind a unique part of target of antigen H5N1

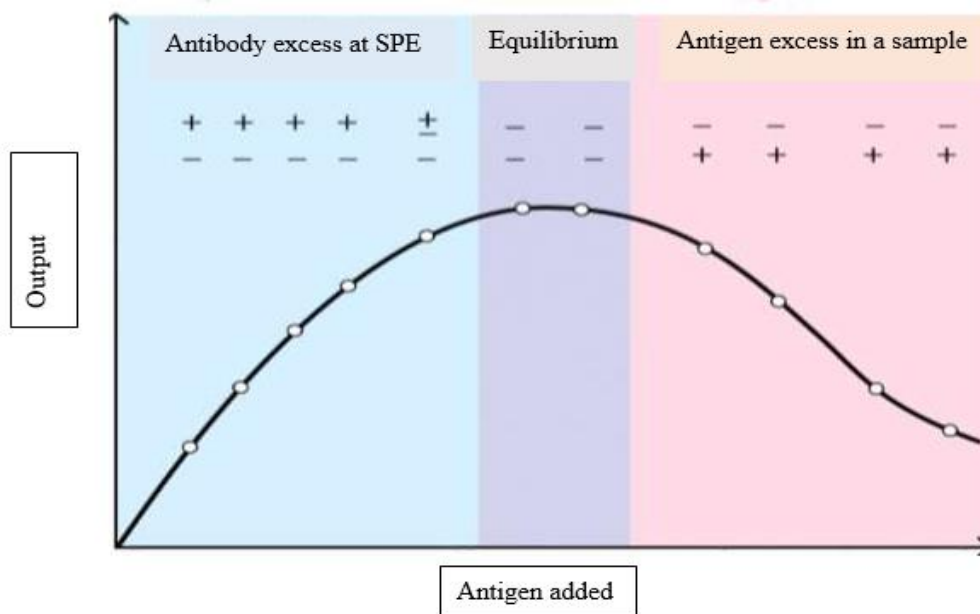


**Figure 4.9:** Antibody –antigen concentration

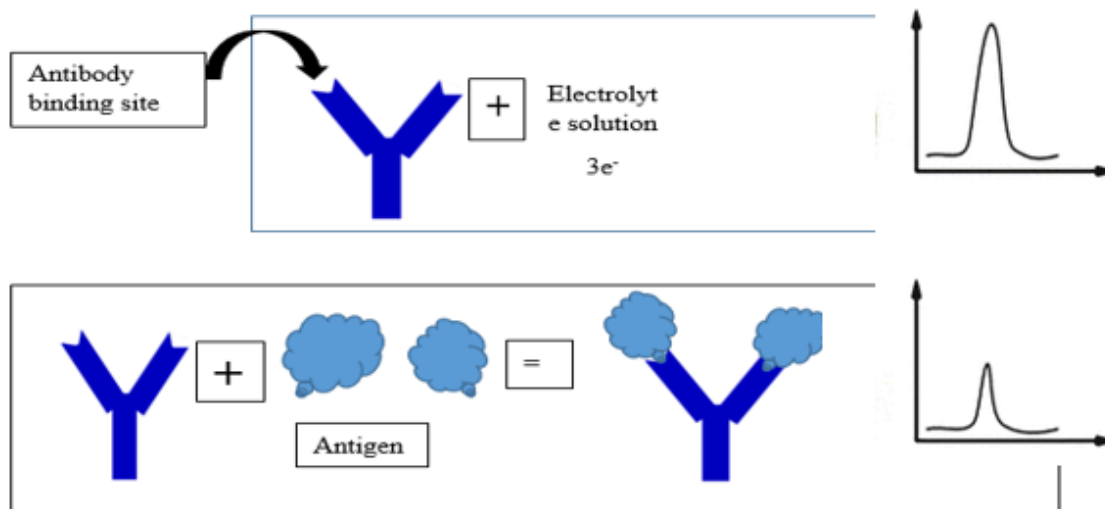
The screen-printed electrode or the bio probe which was cross-linked with SF was immobilized to the antibody of H5N1 as a film and the antigen of H5N1 was added to phosphate buffer solution to detect H5N1. During this process the concentration or the amount of the antigen or antibody affected the result of detection in the experiment.

Figure 4.9 shows the three regions happened in the experiment and it procedured the output based on the phenomena observed in the graph. The antigen and antibody produced peaks current during at equilibrium which all the antibody in the screen-printed electrode binds to the antigen present in the analyte. At this stage the cyclic voltammetry was recorded it showed the potential and current peaks.

#### **4.4 Antibody –Antigen Interaction**

The antibody and antigen interaction are very specific that lead to the detection of antigen in the given sample. The antibody analogues structure with antigen which lock and key designed. The antibody has a Y shape at it tips and variable region which called the fragment

antigen binding site for the recognition of the antigen. In this experiment the antibody immobilized on the screen-printed electrode with silk fibroin solution shown on Figure 4.10..



**Figure 4.10:** Show the interaction of antigen and antibody before and after the antigen added in the electrolyte solution.

During the interaction of antibody and antigen, the antigen fit to the binding site of the antibody which produce the desired output for the determination of the H5N1 in the sample. This interaction affects the movements of electron from the electrolysis solution to the electrode surface. The reference took before the antigen added in the electrolyte solution and then added the antigen to observe the interaction of the antibody and antigen.

#### 4.5 Detection of H5N1 by Screen Printed Electrode

The detection of H5N1 shown Figure 4.11 with PSE coated SF film and antibody as solutions added was shown at method2 on Figure 3.13. The detection observed the anode peak potential -0.128v and the cathode potential peak Epc 0.0632v. The anode peak and cathode peaks current were 0.76 and -7.28 $\mu$ A respectively as shown on Table 4.7. By using unused SPE with inactivated antigen and antibody of H5N1 used as a solution were shown method2 on Figure 3.13. The CV profile indicated that peaks of anode and cathode potential 0.24v and -0.31V shown Table 4.8. The peaks current of anode and cathode 45.708 $\mu$ A and -32.105 $\mu$ A respectively shown on Figure 4.12. The third type of detection using SPE coated

with SF film and antibody immobilized and the inactive antigen of H5N1 added on the PBS solution. The CV voltammograph indicated that the Peaks of potential anode and cathode - 0.083v and 0.173v respectively shown on Table 4.9. The peaks current of anode and cathode 0.157 $\mu$ A and -9.104 $\mu$ A respectively shown on Figure 4.13.

By using SF/x-linked film Figure 4.14, the potential peaks of anode and cathode were observed at Epa 0.003v and Epc at -0.299v and the output current produced with respective potential peaks were Ipa 5.626 $\mu$ A and Ipc -0.8578 $\mu$ A shown Table 4.10. The peaks current produced with the peaks of potential (a potential that produced high current) during the redox reaction is directly proportional to the amount of inactive antigen present in the sample in both experimental protocols.

The chronoamperometry profiles indicated on Figure 4.15 SF film coated and at Figure 4.16 SPE coated with SF/x-linked immobilized antibody of H5N1 that produced the current on the working electrode was (SPE) decayed with time and it showed spike at a time. This spike indicated that, this process during formation of antigen-antibody the maximum current was produced where the electrode recorded within that time. This current indicated the concentration or amount of antigen present in the sample during chronoamperometry determination.

The recombination or formation of antigen- antibody affects the movement of electrons from the center of reduction and oxidation reaction. The current produced in cyclic voltammetry procedures of silk fibroin film Ipa 21.399 $\mu$ A and SF/x-linked film were Ipa 547.075 $\mu$ A and Ipc -888.740 $\mu$ A. The current produced in the presence of antigen antibody of silk fibroin film Ipa 4.951 $\mu$ A and Ipc -1.91  $\mu$ A and SF/x-linked film Ipa 5.626  $\mu$ A and Ipc -0.857  $\mu$ A.

In this experiment, we concluded that the current produced without antigen- antibody larger than the current produced with antigen-antibody b/c in the antigen-antibody formation affects the movement of electron from the redox center into the electrode surface and this phenomenon reduced the amount of current produced in the cell.

#### 4.5.1 SPE with immobilized SF film antigen and antibody as a solution

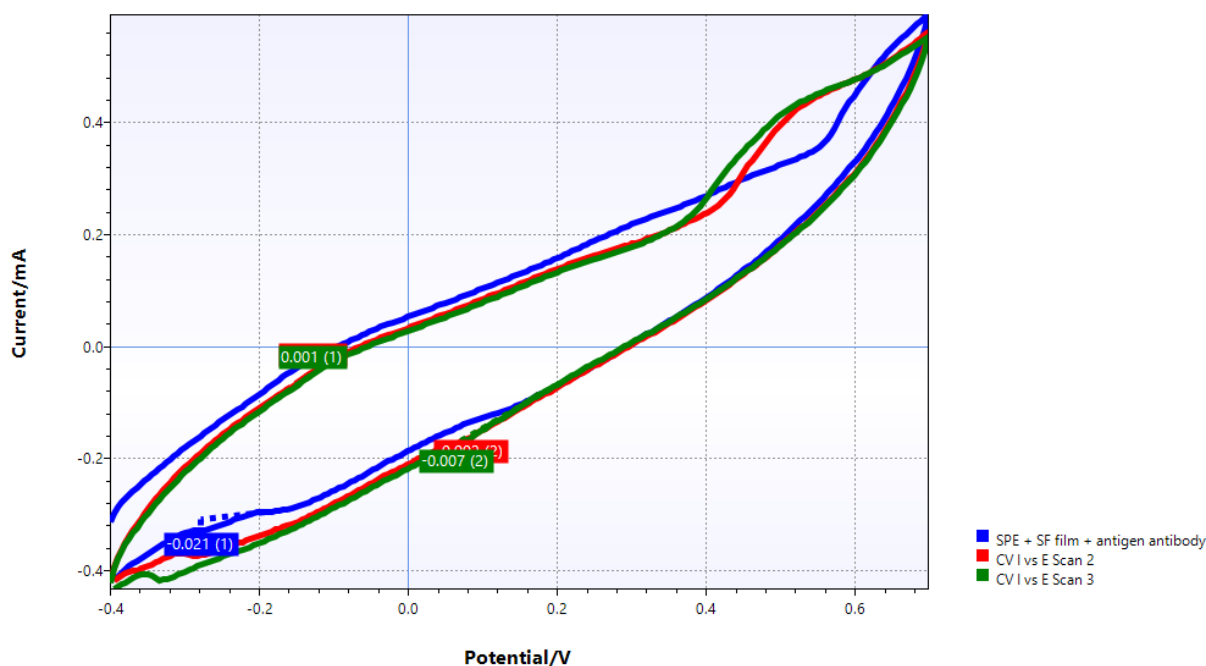


**Figure 4.11:** CV voltammogram SPE with SF film antigen and antibody as a solution

**Table 4.7:** Peaks date of CV with SPE SF film antigen and antibody as a solution

| Pea k  | Potential/V | Height/ $\mu$ A | Area/ $\mu$ A V | Width/V | Y Offset/ $\mu$ A | Max slope/ $\mu$ A/V | Min slope/ $\mu$ A/V | Sum/ $\mu$ A/V |
|--|-------------|-----------------|-----------------|---------|-------------------|----------------------|----------------------|----------------|
| SPE + SF film + antigen antibody as a solution |             |                 |                 |         |                   |                      |                      |                |
| 1  | -0.27910    | -20.5495        | NaN             | NaN     | -307.727          | -293.321             | -559.171             | 852.493        |
| CV I vs E Scan 2                               |             |                 |                 |         |                   |                      |                      |                |
| 1  | -0.12809    | 1.96883         | NaN             | NaN     | -45.2062          | 932.305              | 878.495              | 1810.80        |
| 2  | 0.08340     | -1.64185        | NaN             | NaN     | -159.842          | -755.639             | -784.012             | 1539.65        |
| CV I vs E Scan 3                               |             |                 |                 |         |                   |                      |                      |                |
| 1  | -0.12809    | 0.76702         | NaN             | NaN     | -49.1733          | 946.663              | 917.267              | 1863.93        |
| 2  | 0.06332     | -7.28383        | NaN             | NaN     | -172.887          | -778.814             | -867.934             | 1646.75        |

#### 4.5.2 Measurements of unused SPE in antigen, antibody and PBS solution

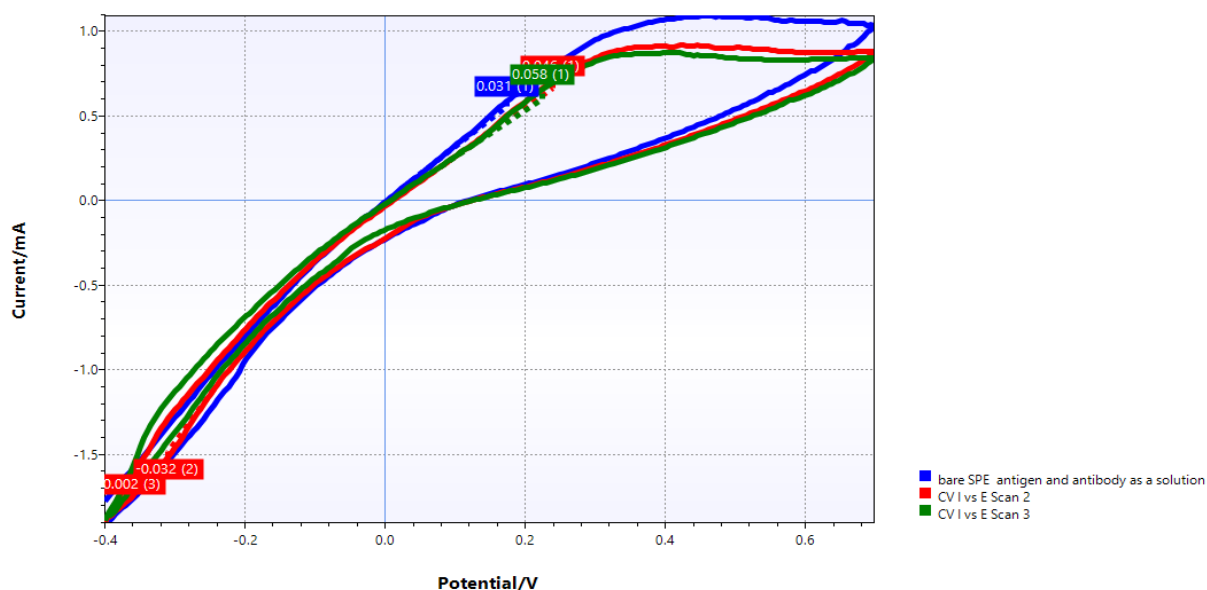


**Figure 4.12:** CV Voltammograph for unused SPE in antigen, antibody and PBS solution

**Table 4.8:** Peaks data of unused SPE in antigen, antibody and PBS as a solution

| Pea k   | Potential/V | Height/ $\mu$ A | Area/ $\mu$ A | Width/V | Y Offset/ $\mu$ A | Max slope/ $\mu$ A/V | Min slope/ $\mu$ A/V | Sum/ $\mu$ A/V |
|---|-------------|-----------------|---------------|---------|-------------------|----------------------|----------------------|----------------|
| Unused SPE antigen and antibody as a solution |             |                 |               |         |                   |                      |                      |                |
| 1   | 0.17410     | 31.0199         | NaN           | NaN     | 558.079           | 3680.67              | 3217.32              | 6897.99        |
| CV I vs E Scan 2                              |             |                 |               |         |                   |                      |                      |                |
| 1   | 0.23949     | 45.7087         | NaN           | NaN     | 663.708           | 3543.87              | 2838.68              | 6382.55        |
| 2   | -0.30934    | -32.1051        | NaN           | NaN     | -1484.12          | -5828.41             | -6630.64             | 12459.1        |
| 3   | -0.36473    | -1.59247        | NaN           | NaN     | -1761.36          | -3.40E+38            | 3.40E+38             | 6.81E+38       |
| CV I vs E Scan 3                              |             |                 |               |         |                   |                      |                      |                |
| 1   | 0.22442     | 57.7310         | NaN           | NaN     | 599.806           | 3598.22              | 2746.09              | 6344.31        |

### 4.5.3 Antibody immobilized SF film coated SPE in antigen and PBS solution

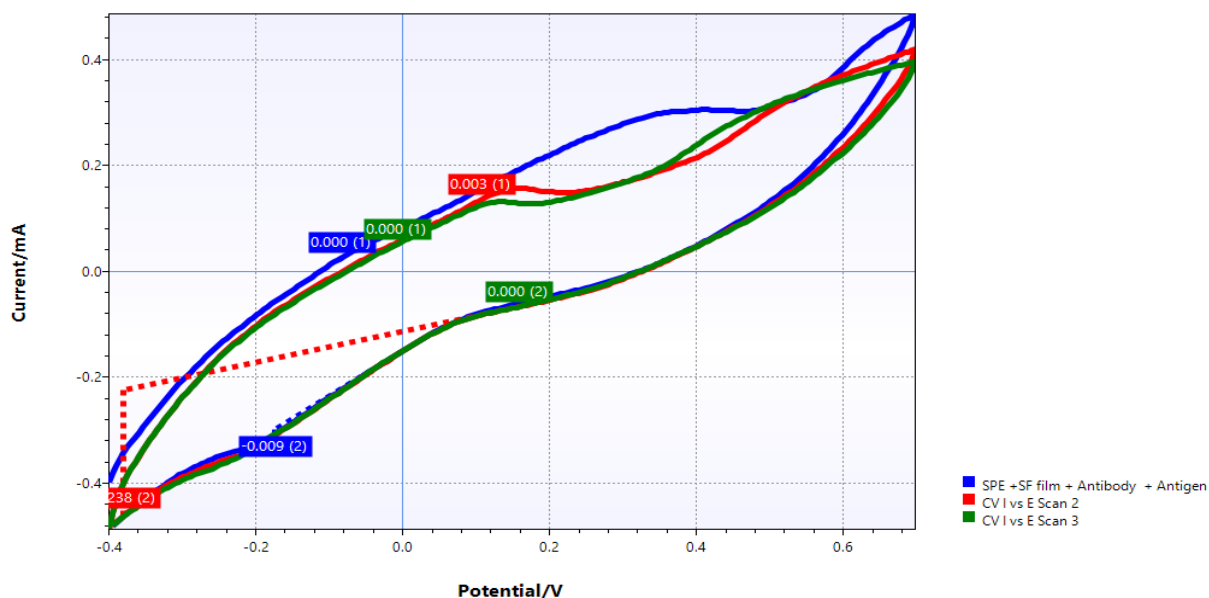


**Figure 4.13:** CV recorded detection of H5N1 antigen using SF film

**Table 4.9:** Peaks date of CV using silk SF film with SPE

| Pea k  | Potential/V | Height/ $\mu$ A | Area/ $\mu$ A V | Width/V | Y Offset/ $\mu$ A | Max slope/ $\mu$ A/V | Min slope/ $\mu$ A/V | Sum/ $\mu$ A/V |
|--|-------------|-----------------|-----------------|---------|-------------------|----------------------|----------------------|----------------|
| SF film coated SPE and immobilized 25 $\mu$ l Antibody + 400 $\mu$ l Antigen |             |                 |                 |         |                   |                      |                      |                |
| 1  | -0.08277    | 0.15711         | NaN             | NaN     | 26.3959           | -3.40E+38            | 3.40E+38             | 6.81E+38       |
| 2  | -0.17340    | -9.10375        | NaN             | NaN     | -297.906          | -868.364             | -964.614             | 1832.98        |
| 1  | 0.10863     | 3.48578         | NaN             | NaN     | 133.579           | 762.913              | 683.175              | 1446.09        |
| 2  | -0.37981    | -237.582        | NaN             | NaN     | -224.077          | 2380.75              | -2497.71             | 4878.46        |
| 1  | -0.00723    | 0.18398         | NaN             | NaN     | 51.7273           | -3.40E+38            | 3.40E+38             | 6.81E+38       |
| 2  | 0.15895     | -0.38568        | NaN             | NaN     | -66.0117          | -3.40E+38            | 3.40E+38             | 6.81E+38       |

#### 4.5.4 SPE with immobilized SF/x-linked film antibody and antigen

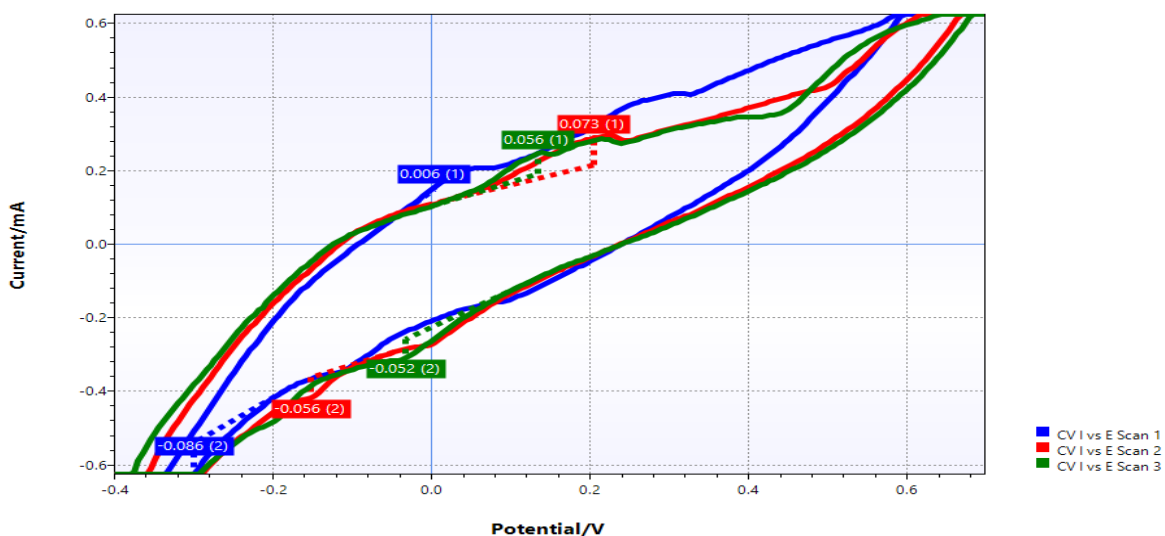


**Figure 4.14:** CV recorded detection of H5N1 using SF/x-linked film

**Table 4.10:** Peaks data CV recorded using SF/x-linked film with SPE

| Pea k            | Potential/V | Height/ $\mu$ A | Area/ $\mu$ A V | Width/V | Y Offset/ $\mu$ A | Max slope/ $\mu$ A/V | Min slope/ $\mu$ A/V | Sum/ $\mu$ A/V |
|------------------|-------------|-----------------|-----------------|---------|-------------------|----------------------|----------------------|----------------|
| CV I vs E Scan 1 |             |                 |                 |         |                   |                      |                      |                |
| 1                | 0.00285     | 5.62629         | NaN             | NaN     | 149.697           | 1752.36              | 1551.29              | 3303.65        |
| 2                | -0.29926    | -85.7833        | NaN             | NaN     | -539.217          | 3220.41              | -2691.36             | 5911.77        |
| CV I vs E Scan 2 |             |                 |                 |         |                   |                      |                      |                |
| 1                | 0.20426     | 72.7557         | NaN             | NaN     | 216.144           | 1177.18              | 586.057              | 1763.24        |
| 2                | -0.15324    | -56.1010        | NaN             | NaN     | -362.046          | -748.129             | -1866.24             | 2614.37        |
| CV I vs E Scan 3 |             |                 |                 |         |                   |                      |                      |                |
| 1                | 0.13379     | 56.1632         | NaN             | NaN     | 191.266           | 1423.01              | 695.289              | 2118.30        |
| 2                | -0.03238    | -52.1564        | NaN             | NaN     | -257.205          | -1081.66             | -1564.31             | 2645.97        |

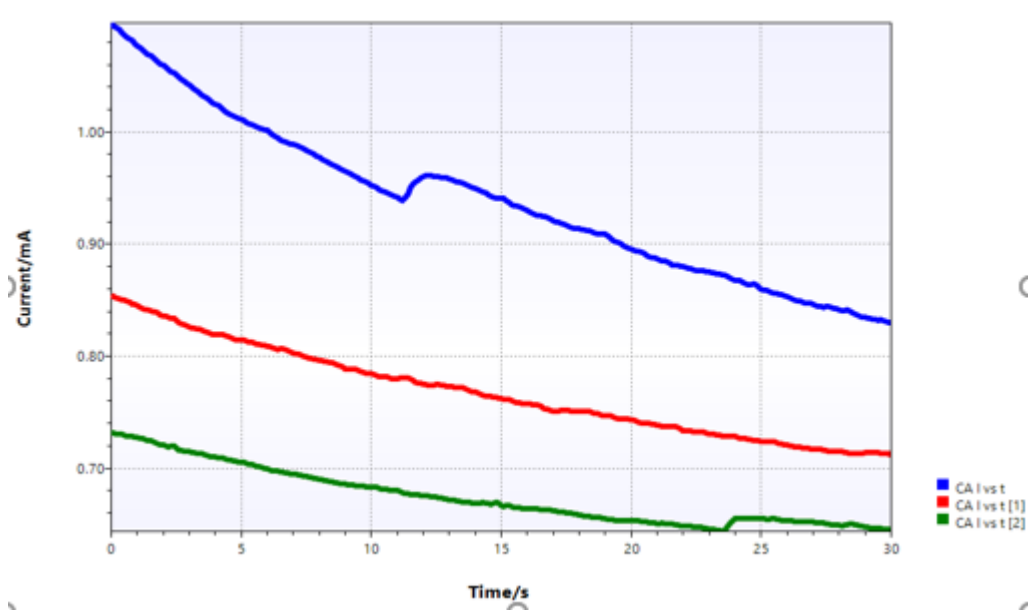


**Figure 4.15:** Chronoamperometry detection of H5N1 using of SF film with SPE

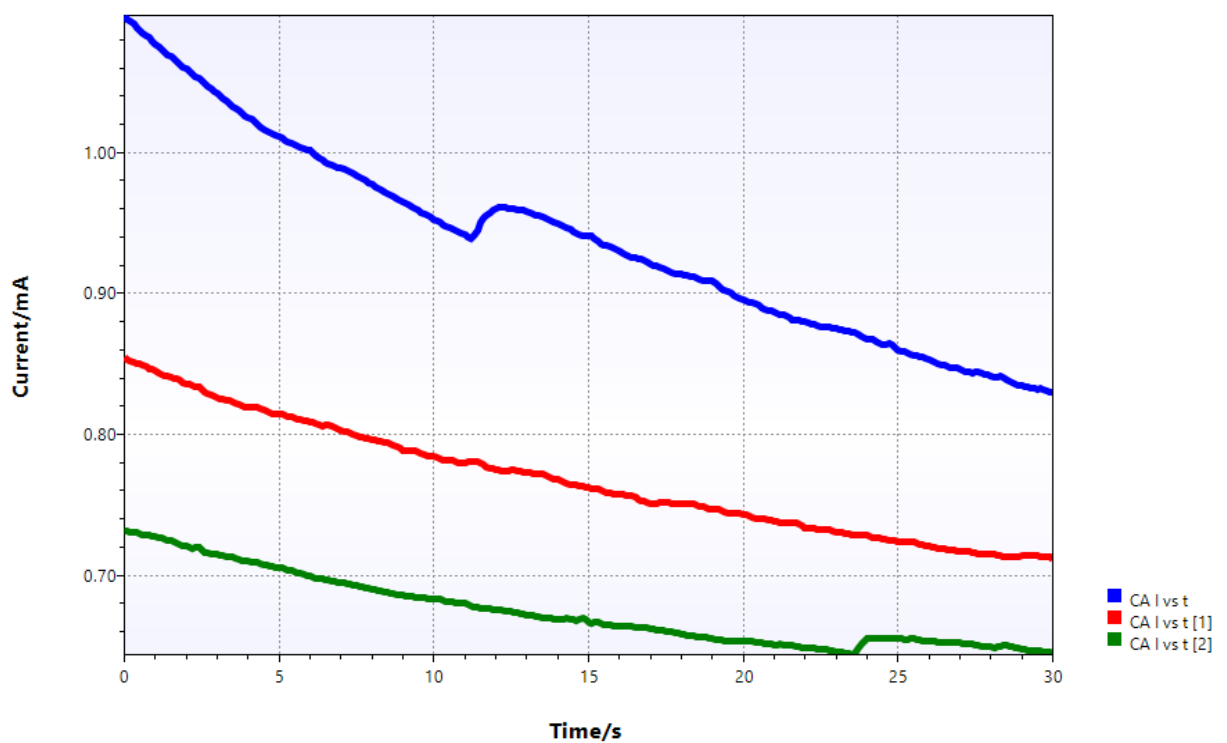


**Figure 4.16 :** Chronoamperometry detection of H5N1 using SF/x-linked film coated SPE

## 4.6 Findings

The findings of characterization and detection of inactivated H5N1 antigen in the electrochemical measurement of the cyclic voltammetry and chronoamperometry were involved as the following points.

Layer by layer SF film and SF / x-linking film

- SF/x-linked film and SF film were performed good conductivity and sensitivity for the modification of biosensors applications.
- Improve sensitivity and conductivity of SPE
- Achieved variation of potential and current peaks at anode and cathode
- The current produced without antigen- antibody larger than the current produced with antigen-antibody
- Antigen-antibody formation affected the movement of electron from the redox center into the electrode surface and this phenomenon reduced the amount of current produced in the cell.

**Table 4.11:** Results of characterization and detection H5N1 antigen using SF film

| Peak  | Potential/<br>V | Height/ $\mu$<br>A | Area/ $\mu$ A<br>V | Width/<br>V | Y<br>Offset/ $\mu$<br>A | Max<br>slope/ $\mu$ A/<br>V | Min<br>slope/ $\mu$ A/<br>V | Sum/ $\mu$ A/<br>V |
|---|-----------------|--------------------|--------------------|-------------|-------------------------|-----------------------------|-----------------------------|--------------------|
| Unused SPE, PBS solution (17.5ml)                             |                 |                    |                    |             |                         |                             |                             |                    |
| 1   | 0.03809         | 0.07456            | NaN                | NaN         | 0.10851                 | 3.99278                     | 2.36471                     | 6.35749            |
| 2   | 0.55676         | 0.74863            | NaN                | NaN         | 1.24353                 | 8.26732                     | -32.0979                    | 40.3652            |
| Unused SPE = antibody (25 $\mu$ l) + PBS (17.5ml)             |                 |                    |                    |             |                         |                             |                             |                    |
| 1   | 0.05824         | 0.06473            | NaN                | NaN         | 0.42036                 | 1.61324                     | 0.08833                     | 1.70157            |
| 2   | -0.15824        | -0.07868           | NaN                | NaN         | -0.90206                | -1.20737                    | -2.36887                    | 3.57624            |
| Unused SPE = antibody + antigen as a solution added, 17ml PBS |                 |                    |                    |             |                         |                             |                             |                    |
| 1   | 0.23949         | 45.7087            | NaN                | NaN         | 663.708                 | 3543.87                     | 2838.68                     | 6382.55            |
| 2   | -0.30934        | -32.1051           | NaN                | NaN         | -1484.12                | -5828.41                    | -6630.64                    | 12459.1            |
| SPE +SF film + antibody immobilized , PBS (17.5ml)            |                 |                    |                    |             |                         |                             |                             |                    |
| 1   | 0.00793         | 0.05868            | NaN                | NaN         | 7.56001                 | -3.40E+38                   | 3.40E+38                    | 6.81E+38           |
| 2   | 0.10863         | 0.47654            | NaN                | NaN         | 7.77445                 | 11.4236                     | 4.52643                     | 15.9500            |
| SPE +SF film + Antibody Immobilized = antigen+ PBS            |                 |                    |                    |             |                         |                             |                             |                    |
| 1   | -0.08277        | 0.15711            | NaN                | NaN         | 26.3959                 | -3.40E+38                   | 3.40E+38                    | 6.81E+38           |
| 2   | -0.17340        | -9.10375           | NaN                | NaN         | -297.906                | -868.364                    | -964.614                    | 1832.98            |

**Table 4.11** : Results of characterization and detection H5N1 antigen using SF/x-linked

| Peak   | Potential/<br>V | Height/ $\mu$<br>A | Area/ $\mu$ A<br>V | Width/<br>V | Y<br>Offset/ $\mu$<br>A | Max<br>slope/ $\mu$ A/<br>V | Min<br>slope/ $\mu$ A/<br>V | Sum/ $\mu$ A/<br>V |
|--|-----------------|--------------------|--------------------|-------------|-------------------------|-----------------------------|-----------------------------|--------------------|
| Unused SPE, PBS (17.5ml)   |                 |                    |                    |             |                         |                             |                             |                    |
| 1  | 0.03809         | 0.07456            | NaN                | NaN         | 0.10851                 | 3.99278                     | 2.36471                     | 6.35749            |
| 2  | 0.55676         | 0.74863            | NaN                | NaN         | 1.24353                 | 8.26732                     | -32.0979                    | 40.3652            |
| Unused SPE = antibody (25 $\mu$ l) + PBS (17.5ml)  |                 |                    |                    |             |                         |                             |                             |                    |
| 1  | 0.05824         | 0.06473            | NaN                | NaN         | 0.42036                 | 1.61324                     | 0.08833                     | 1.70157            |
| 2  | -0.15824        | -0.07868           | NaN                | NaN         | -0.90206                | -1.20737                    | -2.36887                    | 3.57624            |
| Unused SPE = antibody (20 $\mu$ l) + antigen (190 $\mu$ l) as a solution added, PBS (17ml) |                 |                    |                    |             |                         |                             |                             |                    |
| 1  | 0.23949         | 45.7087            | NaN                | NaN         | 663.708                 | 3543.87                     | 2838.68                     | 6382.55            |
| 2  | -0.30934        | -32.1051           | NaN                | NaN         | -1484.12                | -5828.41                    | -6630.64                    | 12459.1            |
| SF/x-linked film coated SPE + 50 $\mu$ l antibody , 400 $\mu$ l antigen+ PBS (17.5ml)      |                 |                    |                    |             |                         |                             |                             |                    |
| 1  | 0.00285         | 5.62600            | NaN                | NaN         | 149.697                 | 1752.36                     | 1551.29                     | 3303.65            |
| 2  | -0.29926        | -85.7830           | NaN                | NaN         | -539.217                | 3220.41                     | -2691.36                    | 5911.77            |

#### 4.7 Comparison to the Other Studies

Comparing my thesis to other electrochemical biosensor d with cost effectiveness, techniques of design and performance. The most popular designed of H5N1 electrochemical biosensor was using sDNA immobilized on the electrode surface with multiwall carbon nanotube and polymers. This designed biosensor is expensive and longtime design of techniques. The challenges of H5N1 DNA biosensor, the viral genome of H5N1 viruses formed from different virus of two parents and it mutate the viral genome. Single strand DNA electrochemical biosensor used hybridization of nitrogenous bases and it faces long time viral isolation, separation, load, miss pairing and it leads redox peaks based on the bond which created between the bases.

The second types of H5N1 biosensor designed was using antibody on SPE modified with gold-graphene nanocomposites and polymers. The electrode and the materials used for the antibody immobilization and the magnitude produced from the mediator of Cadmium telluride (CdTe) quantum with graphene oxide, H5-polychonal antibody and bovine serum albumin. The third design of fluorescence biosensor for the detection of H5N1 with the high luminescent Cadmium telluride (CdTe)/ Cadmium sulfide (CdS) and quantum dot (QDs)

The biomaterials and micro/nano particles used to designed DNA antibody is expensive and the second generation of designed which needed the mediator to transfer electron from the center of redox into the electrode surface. Design of a novel H5N1 electrochemical biosensor used a local available biomaterials silk cocoons which low price, simple techniques of design, materials locally available and it improves the sensitivity and conductivity of screen printed electrode. The detection that performed layer-by-layer deposition of SF film and SF/x-linked film.

## CHAPTER 5

### CONCLUSION

#### 5.1 Conclusion

On global scale, AIV H5N1 is a pathogenic disease and highly mortality rate in animal and human which causes devastating outbreak and a major global health, social and economic problem. The prevention of outbreak of AIV is limited and inadequate diagnostic biosensors tools because of inappropriate to field work, time consuming, poor access and high cost for the medical care. Design of novel H5N1 biosensor device provides sensitive and selective results for early detection and prevention of AIV H5N1 diseases which allows ultrasensitive, rapid detection, point of care, inexpensive and efficient device.

The silk locally available biomaterial, inexpensive and good biocompatibility which purified through degumming, dissolution and dialysis process for the immobilization of antibody H5N1 on the SPE. The layer – by –layer design of SPE; improves the stability, sensitivity and conductivity of the H5N1 biosensor design. The immobilization of antibody achieved on the SF film and SF/x-linked film coated SPE support the attachment and stability. Cyclic voltammetry and chronoamperometry characterization indicated that, SF film and SF / x-linking film are proposed as good candidates for the detection of H5N1 with the proposed design.

The detection of AIV H5N1 on the SPE based on the formation of antibody-antigen complex at the screen printed electrode which contains immobilized H5N1 biosensor SF/x-linked film and inactive antigen of H5N1 in cell which affects the movements or accessibility of ions (electrons) from redox centers towards into the embedded electrode sensing layers which observed in the graph of CV and CA. The detection of SF film and SF/x-linked film without antigen-antibody was  $I_{pc}$  21.399  $\mu$ A and 545.075 $\mu$ A and without 4.951 $\mu$ A and 5.626  $\mu$ A of the anodic peaks current respectively. The output of current produced in the experiment is directly proportion to the concentration of H5N1 presents in the sample

## REFERENCE

- Ahmed, S. R., & Neethirajan, S. (2018). Chiral MoS<sub>2</sub> Quantum Dots: Dual-Mode Detection Approaches for Avian Influenza Viruses. *Global Challenges*, 1700071, 1700071. <https://doi.org/10.1002/gch2.201700071>
- Anker, J. N., Hall, W. P., Lyandres, O., Shah, N. C., Zhao, J., & Duyne, R. P. Van. (2008). Biosensing with plasmonic nanosensors Recent. *Nature Materials*, 7(June), 8–10. <https://doi.org/10.1038/nmat2162>
- Beatriz Brena , Paula González-Pombo, and F. B.-V. (2007). *Immobilization of Enzymes: A Literature Survey*. <https://doi.org/10.1007/978-1-59745-053-9>
- Buoziš, J., Ahmed, S. R., Chand, R., Nagy, É., & Neethirajan, S. (2018). Direct immunosensing of avian influenza A virus in whole blood using hybrid nanocomposites, 1–26.
- Cao, T. T., Wang, Y. J., & Zhang, Y. Q. (2013). Effect of Strongly Alkaline Electrolyzed Water on Silk Degumming and the Physical Properties of the Fibroin Fiber. *PLoS ONE*, 8(6). <https://doi.org/10.1371/journal.pone.0065654>
- Cavallini, A. (2015). Amperometric test strips for point of care biosensors : an overview, (March), 1–5. Retrieved from <http://qloudlab.com/wp-content/uploads/2015/04/amperometric-test-strips-for-point-of-care-biosensors-an-overview.pdf>
- Cernavodeanu, P. (2001). Nouvelles recherches sur l’histoire de la Dobroudja. *Revue Roumaine D`Histoire*, 13(3), 1974. [https://doi.org/10.1016/S0956-5663\(01\)00115-4](https://doi.org/10.1016/S0956-5663(01)00115-4)
- Cheng, C., Dong, J., Yao, L., Chen, A., Jia, R., Huan, L., ... Zhang, Z. (2008). Potent inhibition of human influenza H5N1 virus by oligonucleotides derived by SELEX. *Biochemical and Biophysical Research Communications*, 366(3), 670–674. <https://doi.org/10.1016/j.bbrc.2007.11.183>
- Cormode, D. P., Gao, L., & Koo, H. (2018). Emerging Biomedical Applications of

- Enzyme-Like Catalytic Nanomaterials. *Trends in Biotechnology*, 36(1), 15–29.  
<https://doi.org/10.1016/j.tibtech.2017.09.006>
- Cuiying, L., Yajuan, G., Zhaoa, M., Suna, M., Luob, F., Guoa, L., ... Chen, G. (2019). Highly sensitive colorimetric immunosensor for influenza virus H5N1 based on enzyme-encapsulated liposome, 21. <https://doi.org/Analytica Chimica Acta 963> (2017) 112e118
- D'Souza, S. F. (2001). Immobilization and stabilization of biomaterials for biosensor applications. *Applied Biochemistry and Biotechnology - Part A Enzyme Engineering and Biotechnology*, 96(1–3), 225–238. <https://doi.org/10.1385/ABAB:96:1-3:225>
- Diseas-, I., Farrar, J., Diseases, T., Chi, H., City, M., Han, A. M., ... Kong, H. (2013). Avian Influenza A (H5N1) Infection in Humans, 1374–1385.
- Dziąbowska, K., Czaczyk, E., & Nidzworski, D. (2018). Detection Methods of Human and Animal Influenza Virus-Current Trends. *Biosensors*, 8(4), 1–24.  
<https://doi.org/10.3390/bios8040094>
- Elgrishi, N., Rountree, K. J., McCarthy, B. D., Rountree, E. S., Eisenhart, T. T., & Dempsey, J. L. (2018). A Practical Beginner's Guide to Cyclic Voltammetry. *Journal of Chemical Education*, 95(2), 197–206. <https://doi.org/10.1021/acs.jchemed.7b00361>
- F., S. D., Kim, S., & Lee, H. J. (2015). Amperometric bioaffinity sensing platform for avian influenza virus proteins with aptamer modified gold nanoparticles on carbon chips. *Biosensors and Bioelectronics*, 72, 355–361.  
<https://doi.org/10.1016/j.bios.2015.05.020>
- Firdous, S., Anwar, S., & Rafya, R. (2018). Development of surface plasmon resonance (SPR) biosensors for use in the diagnostics of malignant and infectious diseases. *Laser Physics Letters*, 15(6), 18–23. <https://doi.org/10.1088/1612-202X/aab43f>
- Fu, Y., Callaway, Z., Lum, J., Wang, R., Lin, J., & Li, Y. (2014). Exploiting enzyme catalysis in ultra-low ion strength media for impedance biosensing of avian influenza

- virus using a bare interdigitated electrode. *Analytical Chemistry*, 86(4), 1965–1971.  
<https://doi.org/10.1021/ac402550f>
- Fujiyoshi, Y., Kume, N. P., Sakata, K., & Sato, S. B. (2012). Fine structure of influenza A virus observed by electron cryo-microscopy Yoshinori. *Encyclopedia of Biophysics*, 1(2), 573–573. [https://doi.org/10.1007/978-3-642-16712-6\\_101138](https://doi.org/10.1007/978-3-642-16712-6_101138)
- Geckeler, K. E., & Muller, B. (1996). Polymer Materials in Biosensors. *Cell*, 220(83), 255–263. <https://doi.org/10.1007/BF01139752>
- Gerard, M., Chaubey, A., & Malhotra, B. D. (2002). Application of conducting polymers to biosensors. *Biosensors and Bioelectronics*, 17(5), 345–359.  
[https://doi.org/10.1016/S0956-5663\(01\)00312-8](https://doi.org/10.1016/S0956-5663(01)00312-8)
- Goloubeva, O. G., Govorkova, E. A., Bush, K., Webster, R. G., & Leneva, I. A. (2002). Comparison of Efficacies of RWJ-270201, Zanamivir, and Oseltamivir against H5N1, H9N2, and Other Avian Influenza Viruses. *Antimicrobial Agents and Chemotherapy*, 45(10), 2723–2732. <https://doi.org/10.1128/aac.45.10.2723-2732.2001>
- Grabowska, I., Malecka, K., Jarocka, U., Radecki, J., & Radecka, H. (2014). Electrochemical biosensors for detection of avian influenza virus - current status and future trends. *Acta Biochimica Polonica*, 61(3), 471–478.
- Grabowska, I., Malecka, K., Stachyra, A., Góra-Sochacka, A., Sirko, A., Zagórski-Ostoja, W., ... Radecki, J. (2013). Single electrode genosensor for simultaneous determination of sequences encoding hemagglutinin and neuraminidase of avian influenza virus type H5N1. *Analytical Chemistry*, 85(21), 10167–10173.  
<https://doi.org/10.1021/ac401547h>
- Grieshaber, D., MacKenzie, R., Voros, J., & Reimhult, E. (2006). Electrochemical Biosensors - Sensor Principles and Architectures. *Kunststoffe International*, 96(7), 48–50. <https://doi.org/10.3390/s80314000>
- Hiep Nguyen, H., & Kim, M. (2017). An Overview of Techniques in Enzyme

Immobilization. *Appl. Sci. Converg. Technol*, 26(6), 157–163.

<https://doi.org/10.5757/ASCT.2017.26.6.157>

Ho, H. T., Qian, H. L., He, F., Meng, T., Szyporta, M., Prabhu, N., ... Kwang, J. (2009). Rapid detection of H5N1 subtype influenza viruses by antigen capture enzyme-linked immunosorbent assay using H5- And N1-specific monoclonal antibodies. *Clinical and Vaccine Immunology*, 16(5), 726–732. <https://doi.org/10.1128/CVI.00465-08>

Hoa, N., Thi, U., Thuy, D., & Vu, T. H. (2014). Fluorescence biosensor based on CdTe quantum dots for specific detection of H5N1 avian influenza virus My IOPscience Fluorescence biosensor based on CdTe quantum dots for specific detection of H5N1 avian influenza virus View the table of contents for this, (September 2012). <https://doi.org/10.1088/2043-6262/3/3/035014>

HSUEH, C.-J. (ALAN), & Liu, C.-C. (2013). Development of electrochemical biosensors for potential liver disease detections of alt&ast and application of ionic liquid into biosensing-modified electrodes. *Department of Chemical Engineering CASE WESTERN RESERVE UNIVERSITY*.

Jarocka, U., Sawicka, R., Góra-Sochacka, A., Sirko, A., Zagórski-Ostoja, W., Radecki, J., & Radecka, H. (2014a). An immunosensor based on antibody binding fragments attached to gold nanoparticles for the detection of peptides derived from avian influenza hemagglutinin H5. *Sensors (Switzerland)*, 14(9), 15714–15728. <https://doi.org/10.3390/s140915714>

Jarocka, U., Sawicka, R., Góra-Sochacka, A., Sirko, A., Zagórski-Ostoja, W., Radecki, J., & Radecka, H. (2014b). Electrochemical immunosensor for detection of antibodies against influenza A virus H5N1 in hen serum. *Biosensors and Bioelectronics*, 55, 301–306. <https://doi.org/10.1016/j.bios.2013.12.030>

Krejcová, L., Hynek, D., Michalek, P., Milosavljevic, Kopel, P., Zitka, Kizek, R. (2014). Electrochemical sensors and biosensors for influenza detection - literature survey 2012-2013. *International Journal of Electrochemical Science*, 9(7), 3440–3448.

- Lee, T., Ahn, J. H., Park, S. Y., Kim, G. H., Kim, J., Kim, T. H., ... Lee, M. H. (2018). Recent Advances in AIV Biosensors Composed of Nanobio Hybrid Material. *Micromachines (Basel)*, 9(12), 1–17. <https://doi.org/10.3390/mi9120651>
- Malecka, K., Stachyra, A., Góra-Sochacka, A., Sirko, A., Zagórski-Ostoja, W., Dehaen, W., ... Radecki, J. (2015). New redox-active layer create via epoxy-amine reaction - The base of genosensor for the detection of specific DNA and RNA sequences of avian influenza virus H5N1. *Biosensors and Bioelectronics*, 65, 427–434. <https://doi.org/10.1016/j.bios.2014.10.069>
- Mehrotra, P. (2016). Biosensors and their applications - A review. *Journal of Oral Biology and Craniofacial Research*, 6(2), 153–159. <https://doi.org/10.1016/j.jobcr.2015.12.002>
- Melke, J., Midha, S., Ghosh, S., Ito, K., & Hofmann, S. (2016). Silk fibroin as biomaterial for bone tissue engineering. *Acta Biomaterialia*, 31, 1–16. <https://doi.org/10.1016/j.actbio.2015.09.005>
- Moreno, A., Lelli, D., Brocchi, E., Sozzi, E., Vinco, L. J., Grilli, G., & Cordioli, P. (2013). Monoclonal antibody-based ELISA for detection of antibodies against H5 avian influenza viruses. *Journal of Virological Methods*, 187(2), 424–430. <https://doi.org/10.1016/j.jviromet.2012.11.006>
- Murugan V., Robert H., S. N. (2016). Dual immunosensor based on methylene blue-electroadsorbed graphene oxide for rapid detection of the influenza A virus antigen. *Talanta*, 155, 250–257. <https://doi.org/10.1016/j.talanta.2016.04.047>
- Naksupan, N., Saelim, U., Pornarin, T., & Niwat, A. (2012). Toxicity Testing and Wound Healing Efficacy of Fibroin Gel in, 1–6. <https://doi.org/1st Mae Fah Luang University International Conference>
- Nelson, E. E., & Guyer, A. E. (2012). Cellular networks involved in the influenza virus life cycle, 1(3), 233–245. <https://doi.org/10.1016/j.dcn.2011.01.002>.The

- Neumann, G., Noda, T., & Kawaoka, Y. (2009). Emergence and pandemic potential of swine-origin H1N1 influenza virus. *Nature*, 459(7249), 931–939.  
<https://doi.org/10.1038/nature08157>
- Nidzworski, D., Pranszke, P., Grudniewska, M., Król, E., & Gromadzka, B. (2014). Universal biosensor for detection of influenza virus. *Biosensors and Bioelectronics*, 59, 239–242. <https://doi.org/10.1016/j.bios.2014.03.050>
- P. Chambers James, A. B. P., Leann, L. M., Weis3, A., & James, J. V. (2005). Biosensor Recognition Elements, 1–12. Retrieved from [www.cimb.org](http://www.cimb.org)
- Peiris, J. S. M., De Jong, M. D., & Guan, Y. (2007). Avian influenza virus (H5N1): A threat to human health. *Clinical Microbiology Reviews*, 20(2), 243–267.  
<https://doi.org/10.1128/CMR.00037-06>
- Regea, G. (2017). Review on Influenza Virus and its Prevention and Control, 4(Table 1), 1–6.
- Ronghui, W., & Yanbin, L. (2016). Biosensors for Rapid Detection of Avian Influenza. *Web of Science*. Retrieved from <http://dx.doi.org/10.5772/64353>
- Samji, T. (2008). Influenza A: Understanding the Viral Life Cycle, 82, 2008.
- Sassolas, A., Blum, L. J., & Leca-Bouvier, B. D. (2012). Immobilization strategies to develop enzymatic biosensors. *Biotechnology Advances*, 30(3), 489–511.  
<https://doi.org/10.1016/j.biotechadv.2011.09.003>
- Shan, D., Gerhard, E., Zhang, C., Tierney, J. W., Xie, D., Liu, Z., & Yang, J. (2018). Polymeric biomaterials for biophotonic applications. *Bioactive Materials*, 3(4), 434–445. <https://doi.org/10.1016/j.bioactmat.2018.07.001>
- Shen, G., Hu, X., Guan, G., & Wang, L. (2015). Surface modification and characterisation of silk fibroin fabric produced by the layer-by-layer self-assembly of multilayer alginate/regenerated silk fibroin. *PLoS ONE*, 10(4), 1–19.  
<https://doi.org/10.1371/journal.pone.0124811>

- Soler, M. (2016). *Nanoplasmonic Biosensors for Clinical Diagnosis at the Point of Care*.
- Steinhoff, M. (2007). Influenza: Virus and Disease, *Epidemics Epidemics and pandemics. Johns Hopkins Bloomberg School of Public Health*, 67(6), 14–21.
- Strianese, M., Staiano, M., Ruggiero, G., Labella, T., Pellecchia, C., & Auria, S. D. (2012). Fluorescence-Based Biosensors, 875(2). <https://doi.org/10.1007/978-1-61779-806-1>
- Tepeli, Y., & Ülkü, A. (2018). Electrochemical biosensors for influenza virus a detection: The potential of adaptation of these devices to POC systems. *Sensors and Actuators, B: Chemical*, 254, 377–384. <https://doi.org/10.1016/j.snb.2017.07.126>
- Thu-Hien Luong<sup>1</sup>, Dang<sup>1</sup>, T.-N. N., Oanh Pham Thi Ngoc, Dinh-Thuy, T.-H., Nguyen, T.-H. N., Toi, V. Van, ... Son, H. Le. (2015). Investigation of the Silk Fiber Extraction Process from the Vietnam Natural Bombyx Mori Silkworm Cocoon. *IFMBE Proceedings*, 46(June). <https://doi.org/10.1007/978-3-319-11776-8>
- Wang, R., & Li, Y. (2013). Hydrogel based QCM aptasensor for detection of avian influenza virus. *Biosensors and Bioelectronics*, 42(1), 148–155. <https://doi.org/10.1016/j.bios.2012.10.038>
- Wang, S. B., & Tang, D. Y. (2008). Electrochemical immune-biosensor for immunoglobulin G based bioelectrocatalytic reaction on micro-comb electrodes. *Bioprocess and Biosystems Engineering*, 31(5), 385–392. <https://doi.org/10.1007/s00449-007-0173-5>
- Wang, W. S., Kuo, W. T., Huang, H. Y., & Luo, C. H. (2010). Wide dynamic range CMOS potentiostat for amperometric chemical sensor. *Sensors*, 10(3), 1782–1797. <https://doi.org/10.3390/s100301782>
- Wong, C. L., Chua, M., Mittman, H., Choo, L. X., Lim, H. Q., & Olivo, M. (2017). A phase-intensity surface plasmon resonance biosensor for avian influenza a (H5N1) detection. *Sensors (Switzerland)*, 17(10), 1–9. <https://doi.org/10.3390/s17102363>

- Xie, Z., Huang, J., Luo, S., Xie, Z., Xie, L., Liu, J., ... Fan, Q. (2014). Ultrasensitive electrochemical immunoassay for avian influenza subtype H5 using nanocomposite. *PLoS ONE*, 9(4), 96–99. <https://doi.org/10.1371/journal.pone.0094685>
- Yang, J. M., Kim, K. R., & Kim, C. S. (2018). Biosensor for Rapid and Sensitive Detection of Influenza Virus. *Biotechnology and Bioprocess Engineering*, 23(4), 371–382. <https://doi.org/10.1007/s12257-018-0220-x>
- Yoo, E. H., & Lee, S. Y. (2010). Glucose biosensors: An overview of use in clinical practice. *Sensors*, 10(5), 4558–4576. <https://doi.org/10.3390/s100504558>
- Zeng, S., Baillargeat, D., Ho, H. P., & Yong, K. T. (2014). Nanomaterials enhanced surface plasmon resonance for biological and chemical sensing applications. *Chemical Society Reviews*, 43(10), 3426–3452. <https://doi.org/10.1039/c3cs60479a>
- Zhang, W., Chen, L., Chen, J., Wang, L., Gui, X., Ran, J., ... Zou, X. (2017). Silk Fibroin Biomaterial Shows Safe and Effective Wound Healing in Animal Models and a Randomized Controlled Clinical Trial. *Advanced Healthcare Materials*, 6(10), 1–16. <https://doi.org/10.1002/adhm.201700121>
- Zhang, Y. Q. (1998). Natural silk fibroin as a support for enzyme immobilization. *Biotechnology Advances*, 16(5–6), 961–971. [https://doi.org/10.1016/S0734-9750\(98\)00012-3](https://doi.org/10.1016/S0734-9750(98)00012-3)
- Zhao, Z., & Helong, J. (2018). Enzyme-based Electrochemical Biosensors. *Intech Open*, 2, 64. <https://doi.org/10.5772/32009>
- Zhu, X., Ai, S., Chen, Q., Yin, H., & Xu, J. (2009). Label-free electrochemical detection of Avian Influenza Virus genotype utilizing multi-walled carbon nanotubes-cobalt phthalocyanine-PAMAM nanocomposite modified glassy carbon electrode. *Electrochemistry Communications*, 11(7), 1543–1546. <https://doi.org/10.1016/j.elecom.2009.05.055>